



2021

$^{40}\text{Ar}/^{39}\text{Ar}$ geochronology of the Cooe Dolerite, NW Tasmania, and notes on its mineralogy and petrology

Authors: J. L. Everard, E. Matchan, R.S. Bottrill, C.J. Jackman, A. V. Brown and H. Zwingmann

Date: 01/12/2021
Email: info@mrt.tas.gov.au
Website: www.mrt.tas.gov.au

REPORT No: TR26



Geological Survey
Technical Report 26





Mineral Resources Tasmania
Department of State Growth

Geological Survey Technical Report 26:

$^{40}\text{Ar}/^{39}\text{Ar}$ geochronology of the Cooee Dolerite, NW Tasmania, and notes on its mineralogy and petrology

by J. L. Everard, E. Matchan, R.S. Bottrill, C.J. Jackman, A.V. Brown and H. Zwingmann

Cover: Peperitic dolerite-mudstone contact, near west end of West Beach, Burnie (407608mE, 5455521mN).
Photo- C.J. Jackman.

While every care has been taken in the preparation of this report, no warranty is given as to the correctness of the information and no liability is accepted for any statement or opinion or for any error or omission. No reader should act or fail to act on the basis of any material contained herein. Readers should consult professional advisers. As a result the Crown in Right of the State of Tasmania and its employees, contractors and agents expressly disclaim all and any liability (including all liability from or attributable to any negligent or wrongful act or omission) to any persons whatsoever in respect of anything done or omitted to be done by any such person in reliance whether in whole or in part upon any of the material in this report. Crown Copyright reserved.

$^{40}\text{Ar}/^{39}\text{Ar}$ geochronology of the Cooe Dolerite, NW Tasmania, and notes on its mineralogy and petrology

by J. L. Everard¹, E. Matchan², R.S. Bottrill¹, C.J. Jackman¹, A. V. Brown^{1*} and H. Zwingmann³

¹ Geological Survey Branch, Mineral Resources Tasmania (*retired)

² School of Geography, Earth and Atmospheric Sciences, University of Melbourne

³ CSIRO Division of Petroleum Resources & Centre of Excellence in Mass Spectrometry, School of Applied Geology, Curtin University, WA (present address: Division of Earth and Planetary Science, Kyoto University, Japan)

CONTENTS

1.0 Introduction.....	5
2.0 Field Relations	5
3.0 Sampling and sample preparation.....	5
4.0 Petrography	5
5.0 X-ray diffraction.....	10
6.0 Mineral chemistry	10
6.1 Biotite	17
6.2 Amphibole	17
6.3 Clinopyroxene	20
6.4 Feldspars.....	20
6.5 Prehnite	20
6.8 Grossular	20
6.9 Chlorite	21
6.10 Muscovite	22
6.11 Titanite.....	22
6.12 Apatite	22
6.13 Ilmenite.....	22
6.14 Zircon	22
7.0 Metamorphism	22
8.0 Geochemistry	23
9.0 Magnetic susceptibility and oxidation state.....	23
10 Geochronology.....	27
10.1 Previous work.....	27
11.0 K/Ar	27
12.0 $^{40}\text{Ar}/^{39}\text{Ar}$: analytical procedure.....	27
13.0 $^{40}\text{Ar}/^{39}\text{Ar}$: Geochronological results	28
14.0 Discussion	28
15.0 Conclusion	29
16.0 Acknowledgements.....	29
17.0 References.....	30

FIGURES

Figure 1. Proterozoic geology of NW Tasmania	6
Figure 2. Cooee Dolerite sample locations	7
Figure 3. Detail of Cooee Dolerite sample locations.....	7
Figure 4. Lower contact of small sill of Cooee Dolerite.....	8
Figure 5. Detail of peperitic dolerite-mudstone contact	8
Figure 6. Peperitic interfingering of Oonah Formation mudstone and Cooee Dolerite.....	9
Figure 7. Sawn hand specimen of $^{40}\text{Ar}/^{39}\text{Ar}$ dated sample (C112167A).....	9
Figure 8. Photomicrograph of sample C112164A	11
Figure 9. Photomicrograph of sample C112168A	12
Figure 10. Photomicrograph of dated sample C112167A	13
Figure 11. Photomicrograph of sample C112165	14
Figure 12. Photomicrograph of sample R012627	15
Figure 13. Photomicrograph of sample R016519.....	16
Figure 14. Plot of scanning electron microscope (SEM) analyses of biotite.....	18
Figure 15. Plot of scanning electron microscope (SEM) analyses of amphibole	19
Figure 16. Plot of scanning electron microscope (SEM) analyses of clinopyroxene	21
Figure 17. Plot of scanning electron microscope (SEM) analyses of chlorite	22
Figure 18. Plot of major elements against Mg# for Cooee Dolerite.....	24
Figure 19. Plot of trace elements for Cooee Dolerite	25
Figure 20. Chondrite-normalised rare-earth element plots for the Cooee Dolerite	27
Figure 21. $^{40}\text{Ar}/^{39}\text{Ar}$ age spectra (plotted using Ludwig 2012) for biotite aliquots	29

APPENDIX 1

Table 1. Sample location and treatment.....	33
Table 2. Whole rock (XRF) analyses	34
Table 3. Summary of petrography	36
Table 4. XRD Analysis Report.....	37
Table 5. Biotite analyses	38
Table 6. Amphibole (kaersutite) analyses	40
Table 7. Clinopyroxene analyses	41
Table 8. Feldspar analyses	42
Table 9. Prehnite analyses.....	43
Table 10. Clinozoisite analyses.....	44
Table 11. Pumpellyite analyses.....	45
Table 12. Grossular analyses.....	46
Table 13. Chlorite analyses	47
Table 14. Chlorite-biotite mixtures.....	48
Table 15. Muscovite (sericite) analyses	49
Table 16. Titanite analyses.....	50
Table 17. Apatite analyses.....	51
Table 18. Ilmenite analyses.....	52
Table 19. Zircon analysis	52
Table 20. Probable mixtures	53
Table 21. Rare earth element (REE), Hf, Ta and Th analyses.....	53
Table 22. Isotopic analyses	54
Table 23. K/Ar results	54
Table 24. ARGUSVI $^{40}\text{Ar}/^{39}\text{Ar}$ laser step-heating analytical results for BR1 biotite (C112167A).....	55
Table 24a. ARGUSVI $^{40}\text{Ar}/^{39}\text{Ar}$ data and blank values for laser step-heating analysis.....	56

Abstract

The Cooee Dolerite comprises several thick (≤ 300 m) subconcordant sheet-like intrusions and narrow offshoots, of alkali basalt composition, emplaced into a quartzwacke turbidite sequence assigned to the Oonah Formation. Coarse-grained zones are probably crystal-enriched orthocumulates. Primary minerals were plagioclase (now altered), clinopyroxene (titaniferous augite), olivine (now altered), Ti-biotite, and minor potash feldspar, ilmenite and apatite. Large euhedral prisms of amphibole (kaersutite) are also present in more fractionated samples, which may have been crystallised from late intercumulus liquid displaced from the orthocumulates. The groundmass is a fine-grained aggregate of mainly metamorphic minerals including albite, chlorite, clinozoisite, prehnite, pumpellyite, secondary biotite, titanite, minor sericite and rare grossular, characteristic of the prehnite-pumpellyite facies.

A biotite separate yielded a well-defined $^{40}\text{Ar}/^{39}\text{Ar}$ age of 733.8 ± 0.4 Ma (2σ), based on identical weighted means of the high temperature heating steps for two aliquots. This Neoproterozoic (Tonian) age is interpreted as that of the crystallisation of the dolerite, and is fully compatible with, but more precise than, previous K/Ar (biotite) and U-Pb (apatite) age determinations.

As the Cooee Dolerite locally displays peperitic contacts indicating intrusion into wet, unconsolidated sediments, the age is also considered to define the depositional age of the Oonah Formation locally, and by correlation to approximate it elsewhere in Tasmania. Thus the conclusions of Mulder et al. (2018), in particular that the Oonah Formation is coeval with the basal Togari Group (Forest Conglomerate and Quartzite) and lower Ahrberg Group (Donaldson Formation), are corroborated.

1.0 Introduction

The term Cooee Dolerite was introduced by Spry (1957) for “small bodies” of dolerite “that outcrop sporadically along the coast from Blythe Heads to Crayfish Creek” but “have their greatest concentration between Burnie and Cooee Point.” However, Brown (1989, p. 62 - 68) and Crawford and Berry (1992) showed that the northeast-trending dykes that intrude the Rocky Cape Group, west of the Arthur Lineament, are petrologically distinct from the intrusions east of the Lineament, near Burnie and Cooee. Subsequently the former group has been informally referred to as the Rocky Cape Dyke Swarm (Crawford and Berry, 1992) and more recently formalised as the Tayatea Dyke Swarm (Everard et al., 2007), whereas the term Cooee Dolerite has been restricted to the intrusions on and near the foreshore between Parsonage Point at Burnie and Red Rock Point at Cooee. These intrude a quartzwacke turbidite sequence previously known as the Burnie Formation (Spry, 1957; Gee, 1977) but now correlated with the Oonah Formation, a lithologically similar unit originally defined near Zeehan (Spry, 1958; see also Brown, 1986) but widespread in western and northern Tasmania (Figure 1).

2.0 Field Relations

The most detailed published mapping (at ~1:5,000) in this area is that of Gee (1977, Figure 5), who described the intrusions as sills and slightly transgressive sheets, with numerous offshoots in the form of sills, dykes and apophyses. The thickest body of dolerite crops out for about 500 m in the western part of the foreshore section at Parklands (Figure 2). Both its lower (western) and upper (eastern) contacts are subconcordant with the adjacent Oonah Formation, which dips and faces southeast at typically ~30° - 60°; thus the true thickness of the body is probably ~300 m. Further east, around Parsonage Point to West Beach, numerous smaller bodies, mostly a few tens of metres thick, intrude a more tightly folded but mostly steeply southeast dipping sequence. In this area Gee (1977) showed that the intrusions are themselves folded by the dominant third generation folds.

The dolerite crops out poorly away from the foreshore section, and inland exposures are also limited by Cainozoic basalt and sediments that cap the coastal scarp.

Gee (1977) noted that near the western (lower) contact of the main body, the Cooee Dolerite contains a raft of Oonah Formation with strongly contorted bedding and sinuous apophyses suggesting “intrusion into relatively uncompact sediments.” Similar contact relationships, including “extremely intricate, disrupted and apparently scoriaceous forms” and intermixing of dolerite and sediment, particularly between thinner sills and mudrock beds, were described in detail by Crook (1979). Some of the outcrops he described have been since obscured by urban development, but examples of

remaining exposures are illustrated in Figures (4 - 6). These features (now termed peperites) have been considered to indicate that the Cooee Dolerite was intruded into wet unconsolidated sediments shortly after their deposition.

Thus a radiometric determination of the age of the Cooee Dolerite is important in also providing tight constraints on the age of the enclosing sedimentary sequence, and by correlation on the age of the Oonah Formation elsewhere in western and northern Tasmania

3.0 Sampling and sample preparation

Previous sampling of the Cooee Dolerite for petrographic, geochemical or geochronological purposes was undertaken by Spry (1957), A. V. Brown (1988), L. P. Black (1993-95) and J. L. Everard (2004-05) (Appendix 1; Table 1; Figures 2-3). A further eight samples were collected by C. Jackman in 2017 from foreshore outcrops at Parklands, Burnie (Appendix 1; Table 1, Figure 3). Thin sections were cut for petrographic examination from each sample, and seven of the additional samples analysed for major and trace elements by standard XRF techniques (Appendix 1, Table 2). Sample C112167A was chosen for geochronology, based on the abundance and freshness of biotite.

4.0 Petrography

The hand specimens are homogeneous, unfoliated, aphyric, medium- (1 - 2 mm) to coarse-grained (2 - 4 mm) or exceptionally very coarse-grained (≤ 8 mm, C112165) holocrystalline dolerites. Vesicles are absent or small and sparse ($\leq 1\%$, R004580). Veining is rare and banding and other inhomogeneities are absent, other than thin weathering rinds (Figure 7). Equant to narrowly elongate dark green to brown and black mafic minerals (typically up to 3 - 4mm), pinkish brown clinopyroxene and off-white plagioclase are commonly visible.

The eight newly collected samples and twelve previously collected samples were examined in thin section (Appendix 1; Table 3).

All samples are moderately altered, but may be divided into two broad petrographic groups, based on whether clinopyroxene or hornblende is the dominant mafic mineral, although there are some transitional varieties (e.g. R012627, Figure 12) containing both.

The clinopyroxene-rich samples (Figures 8, 9 and 10) generally have higher Mg# (mostly >55 ; see geochemistry section below) and contain more abundant olivine pseudomorphs. A typical sample (C112164, Figure 8) consists mainly of closely packed euhedra of fresh pale pink titaniferous augite (~1 - 4mm; ~40%) and turbid blocky plagioclase (mostly ≤ 1.5 mm long;

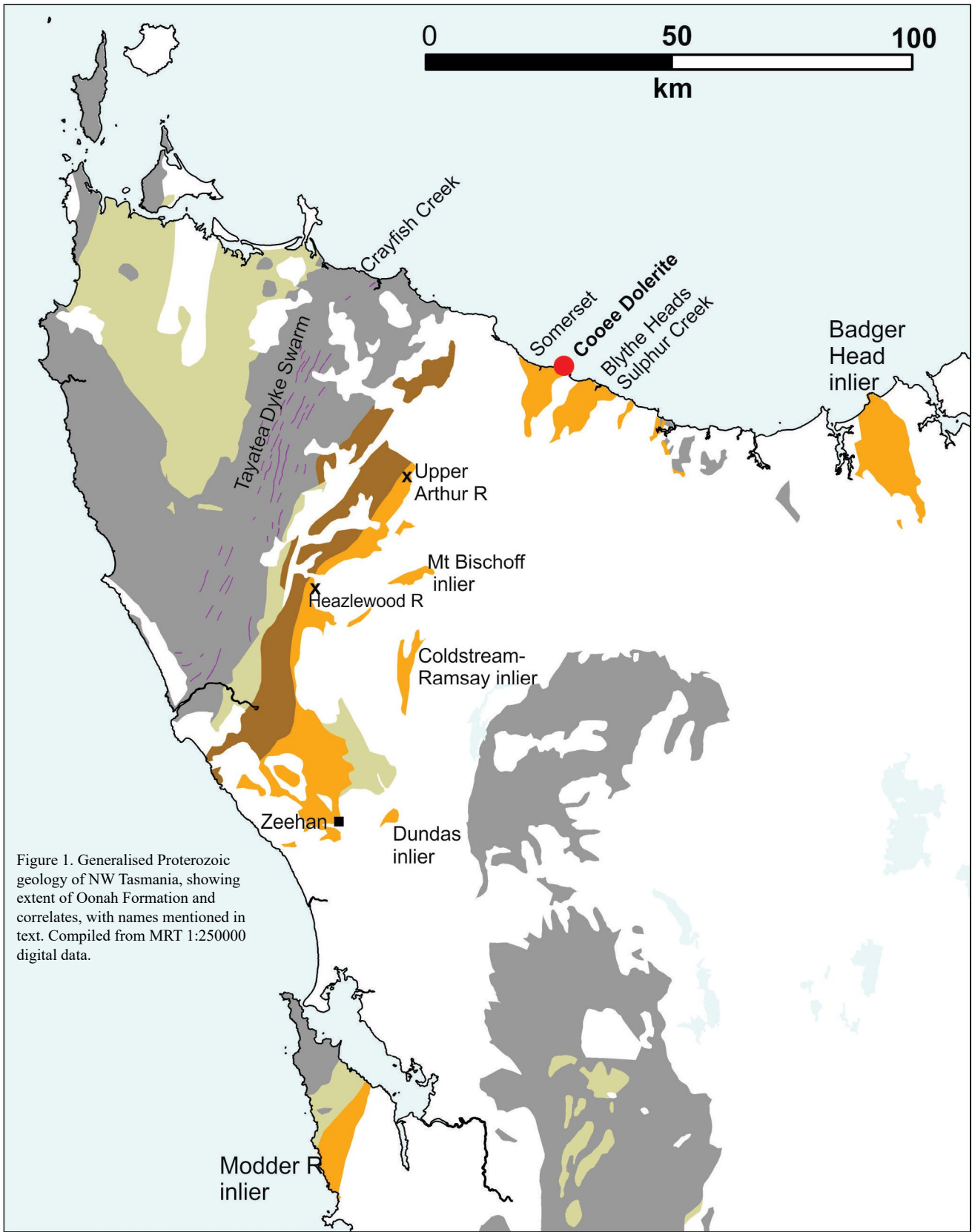
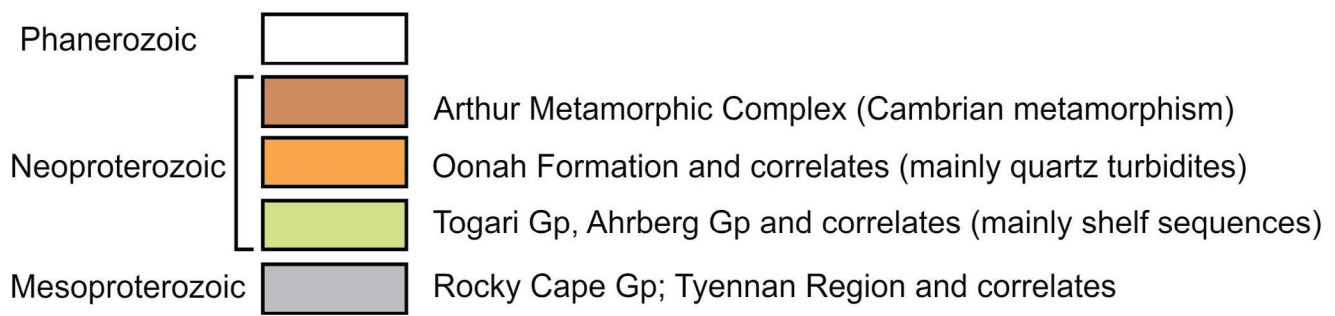


Figure 1. Generalised Proterozoic geology of NW Tasmania, showing extent of Oonah Formation and correlates, with names mentioned in text. Compiled from MRT 1:250000 digital data.



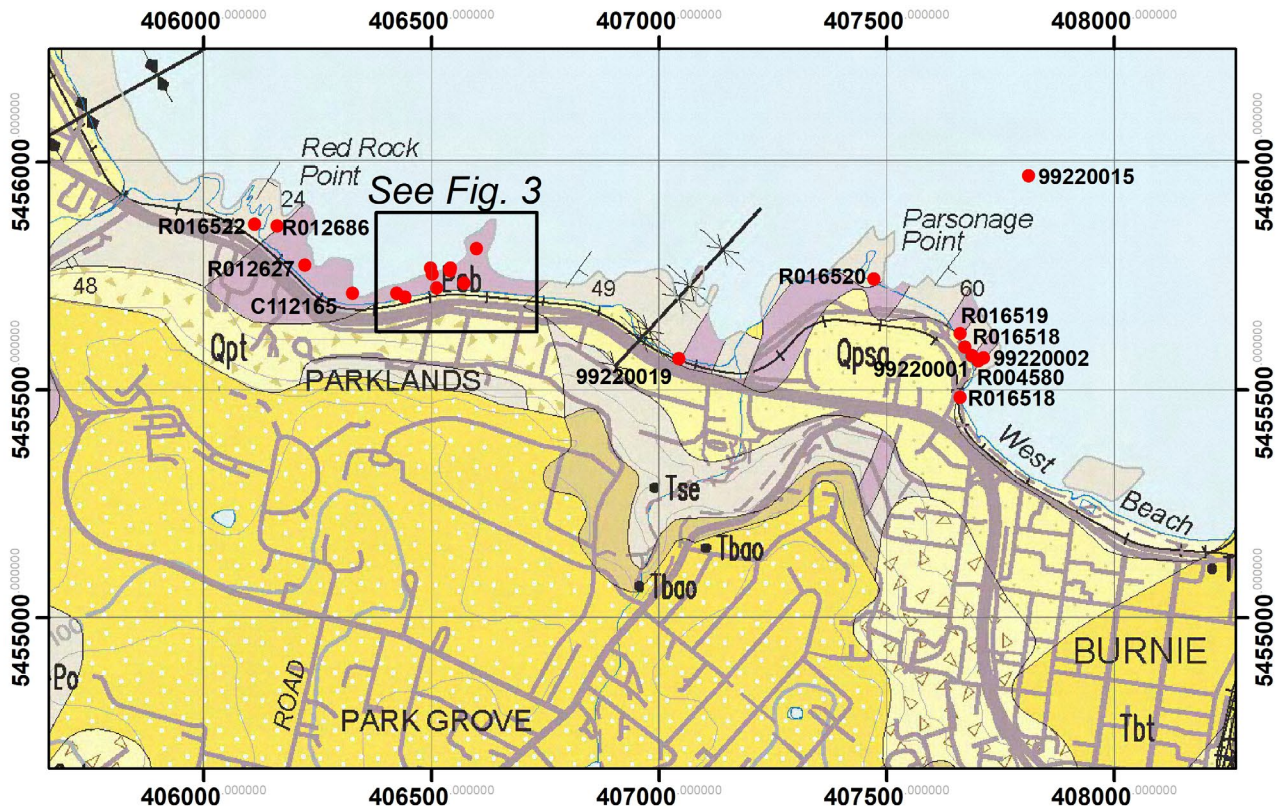


Figure 2. Cooee Dolerite sample locations. 1:25000 geology from Vicary (2004), 500m grid shown.

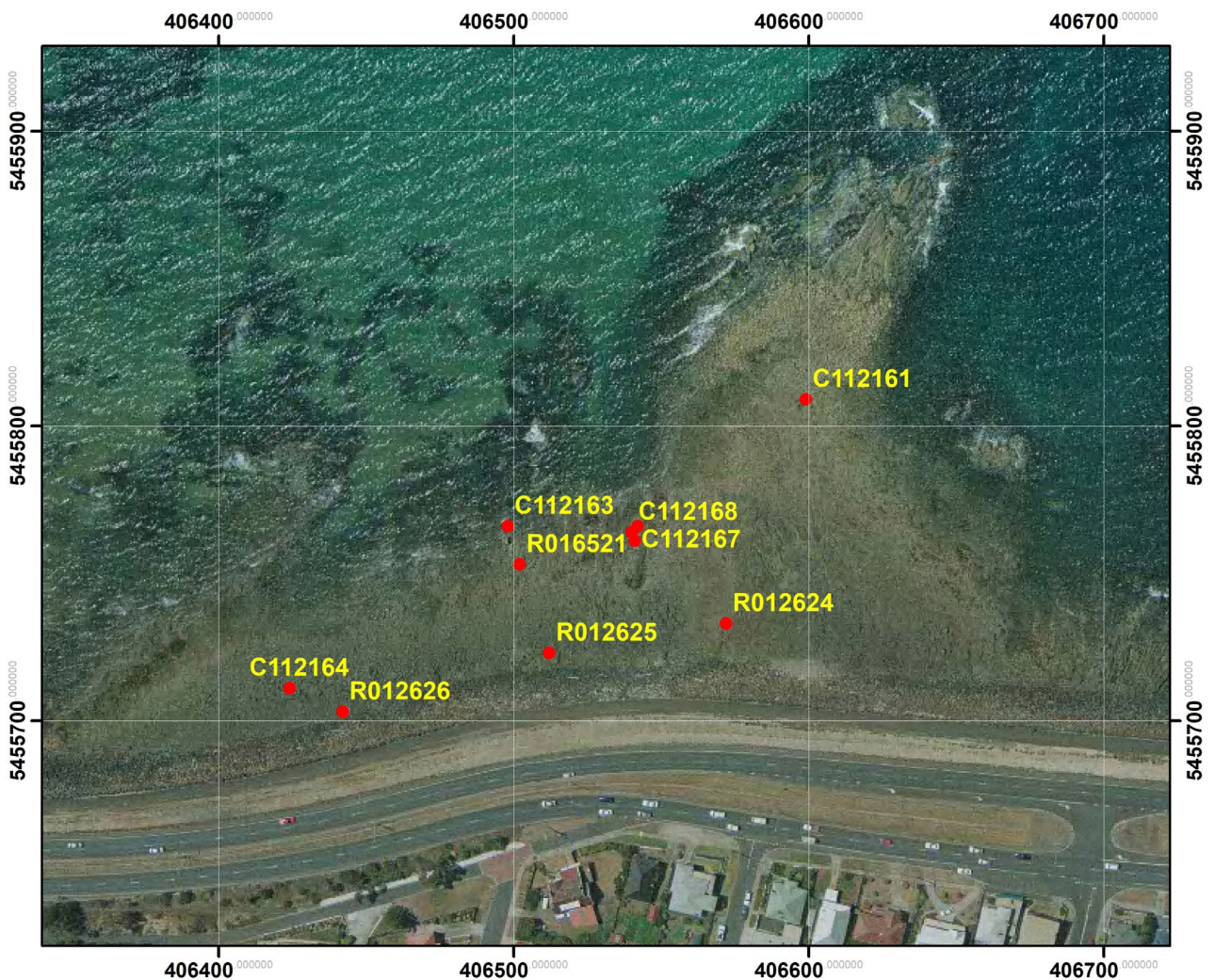


Figure 3. Detail of Cooee Dolerite sample locations, Parklands foreshore. Base imagery from Tasmanian government DPIWE State Orthophoto, 100m grid shown.



Figure 4. Lower contact of small sill of Cooee Dolerite, near west end of West Beach, Burnie (407608mE, 5455521mN). Oonah Formation sandstone bed (bottom) overlain by laminated Oonah Formation mudstone (grey-black, middle); note peperitic interfingering of mudstone with dolerite (brown-weathering, top). Photo- C. J. Jackman.



Figure 5. Detail of peperitic dolerite-mudstone contact, same locality. The carabener is about 10 cm long. Photo- C. J. Jackman.



Figure 6. Peperitic interfingering of Oonah Formation mudstone and Cooee Dolerite, 407705mE, 5455541mN, ~25 NE along strike from Figures 4, 5. Photo- C. J. Jackman.



Figure 7. Sawn hand specimen of $^{40}\text{Ar}/^{39}\text{Ar}$ dated sample (C112167A) of Cooee Dolerite. Dark grey-green mafic minerals including biotite, pinkish-brown partly altered clinopyroxene, cream-white altered plagioclase. Photo- R. S. Bottrill.

~50%), together with pale green chlorite grains in part pseudomorphs after olivine, interstitial ragged grains of red-brown biotite (≤ 1 mm), largely unaltered equant opaque grains (~0.5 mm), platelets of prehnite and traces of acicular apatite. The dense packing of augite, plagioclase and former olivine euhedra, with relatively little interstitial groundmass, is reminiscent of orthocumulate texture (Figures 8 and 9). The rock probably formed by local accumulation of crystals with partial expulsion of intercumulus melt (“filter-pressing”) and thus does not represent a liquid composition. This is also consistent with high Mg# (72.8 for this sample).

Samples containing hornblende (Figures 11, 12 and 13) invariably have low Mg# (<55) and are thus relatively fractionated. A typical sample (C112165, Figure 11) consists mainly of interlocking plagioclase and hornblende, with subordinate titanite, biotite and apatite. Very turbid crystals of original calcic plagioclase, (typically 2 – 5 x 0.5 mm) are largely replaced by albite and fine-grained clinozoisite, prehnite and sericite. Elongate prisms of hornblende (α pale yellow-brown, β and γ dark red-brown, optically negative), up to 7 mm long and 0.5-2 mm wide, are partly to completely (50 – 100 %) replaced by an aggregate of fine-grained chlorite and very finely fibrous pumpellyite. Large (≤ 4 mm) crystals of titanite, with polygonal to skeletal outlines, have largely replaced iron-titanium oxides. Numerous splinters of biotite ($\leq 250 \mu\text{m}$) display pleochroism (α very pale yellow-brown, β and γ very dark red-brown) superficially similar to that of hornblende, but are distinguished by their characteristic cleavage and poorer crystal form. Apatite is common as small elongate prisms ($\leq 600 \mu\text{m}$ long and 50 – 75 μm across) and pseudo-hexagonal basal sections.

In both groups, secondary minerals form fine-grained aggregates which are difficult to characterise optically. Calcic plagioclase is replaced by turbid albite with minute inclusions of clinozoisite and/or prehnite, and olivine is completely replaced by chlorite. Hornblende and clinopyroxene are partly to completely replaced by a fine-grained aggregate of chlorite, clinozoisite, and/or a pale green to pale yellow pleochroic, finely fibrous mineral (e.g. R016519, Figure 13). This was initially thought to be tremolite-actinolite, but a combination of x-ray diffraction and microprobe analysis (see below) identified pumpellyite; tremolite-actinolite was not positively identified in any sample. Iron-titanium oxides (probably ilmenite) are mostly partly or completely replaced by titanite. The groundmass may also contain minor potash feldspar.

Some samples (e.g. R016518, R016520, R016522) contain no primary minerals apart from apatite and in some cases minor biotite. The least altered samples (i.e.

those with at least some fresh clinopyroxene or hornblende) are all from the large intrusion at Parklands, whereas most of the severely altered samples are from the smaller intrusions between Parsonage Point and West Beach.

5.0 X-ray diffraction

Three samples (C112167A, C112167B and C112168A) were chosen for more detailed mineralogical investigation by x-ray diffraction.

The samples were run on an automated Philips X-Ray diffractometer system: PW 1729 generator, PW 1050 goniometer and PW 1710 microprocessor with nickel-filtered copper radiation at 35kV/25mA, a graphite monochromator (PW1752), sample spinner and a proportional detector (sealed gas filled PW1711). The typical step-size was 0.02 degrees, and the standard scanning speed was 0.02 degrees/second. The PW1710 system was driven by the CSIRO XRD software: “VisualXRD”, “PW1710 for Windows” and “XPLOT for Windows”. Interpretation and quantification were largely manual, using a series of prepared standards of the more common minerals to enable some semi-quantitative analysis. Quartz was added to the sample as an internal standard. The semi-quantitative results were calculated using single-peak calibration factors derived from scans of known mixtures of minerals.

The XRD results (Appendix 1; Table 4) indicate that sample C112167A, chosen for dating, comprises mostly plagioclase (~25 - 35 wt%), mica, chlorite and clinopyroxene (all ~15 - 25 wt%), with lesser pumpellyite (~5 – 10 wt%), clinozoisite/epidote (~2 – 5 wt%) and ilmenite (<2 wt %). The mica is mostly trioctahedral (biotite series), but some is dioctahedral (muscovite series). Plagioclase is probably near albite in composition. No amphiboles were detected. The other samples C112167B and C112168B are similar with slightly different proportions of some minerals.

6.0 Mineral chemistry

Mineral compositions were investigated in two samples: C112167A, from which biotite was separated for $^{40}\text{Ar}/^{39}\text{Ar}$ dating, and the more fractionated sample R012627 from which amphibole had been used for K/Ar dating. Analyses were obtained using a Hitachi SU-70 analytical field emission scanning electron microscope (SEM) at the Central Science Laboratory, University of Tasmania. Spatial resolution was of the order of 1 nm and elements sought ranged from B to U, although accuracy is poorer for very light elements; only those detected are reported.

Approximately 300 analyses were made, from both magmatic and secondary minerals. Most of the latter are fine-grained groundmass phases, and approximate-

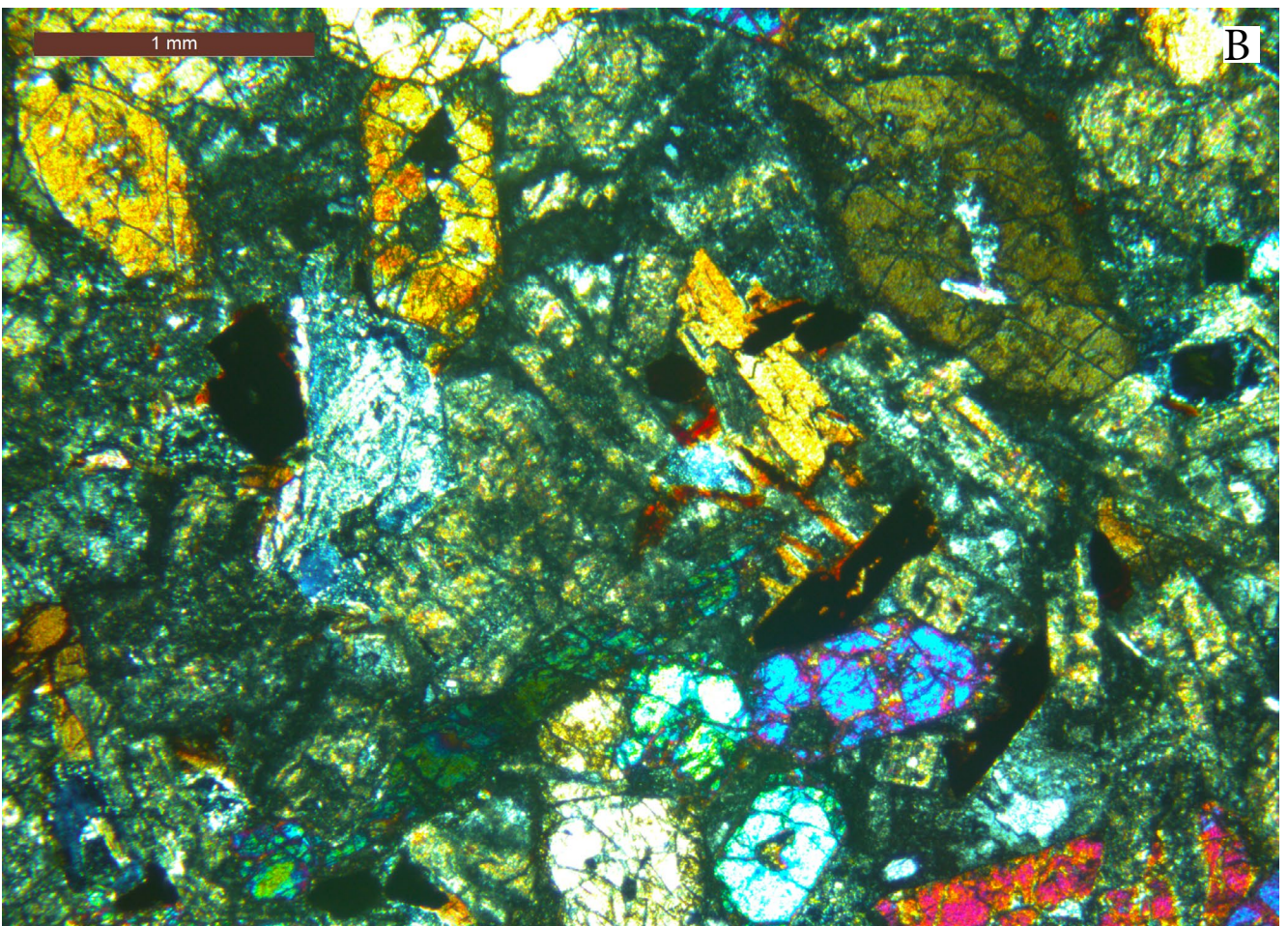
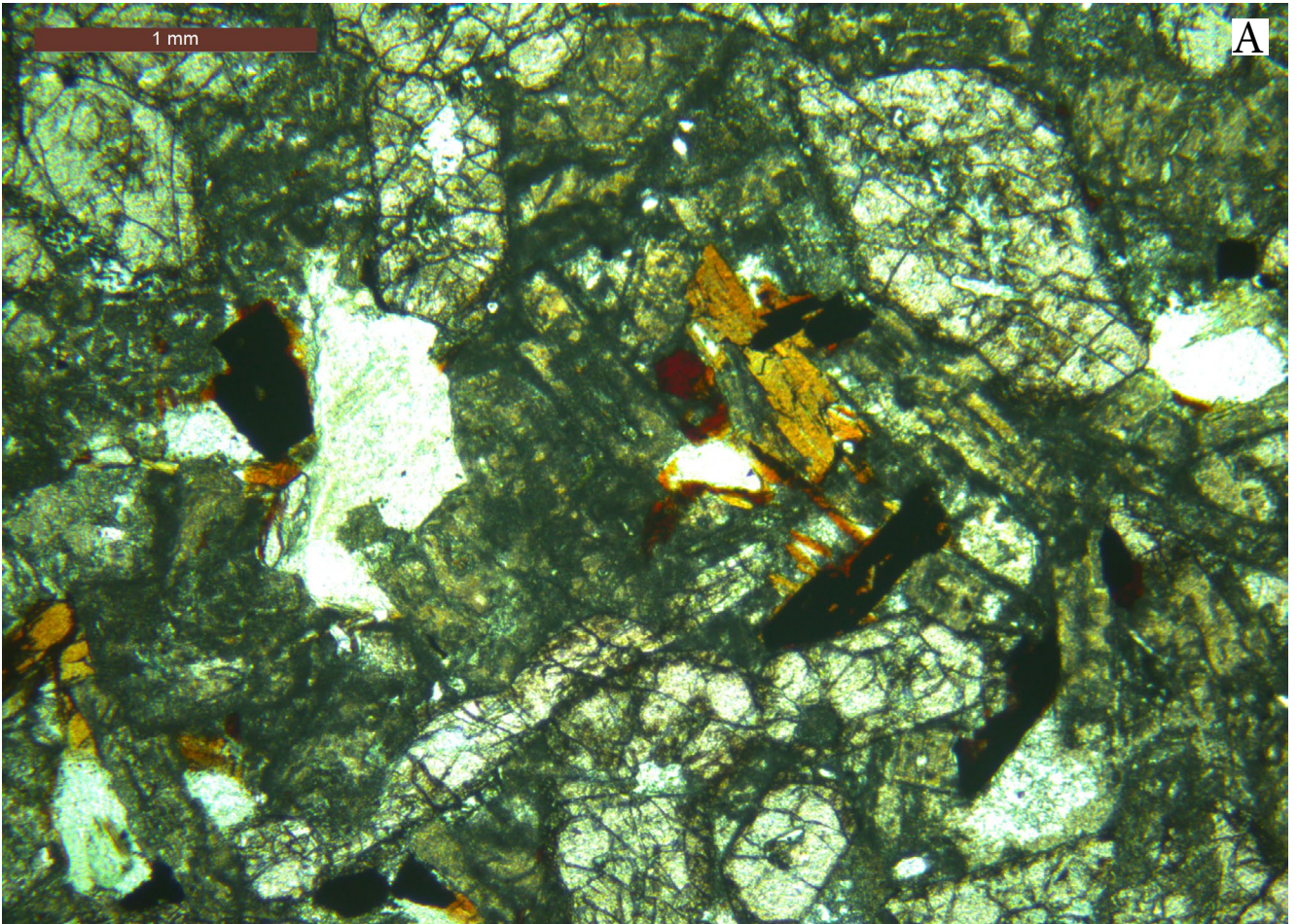


Figure 8. Photomicrograph of sample C112164A. Field of view ~4.6 mm x 3.4 mm (a) plane polarised light (b) crossed nicols. Note biotite flakes (red-brown), augite euhedra (pale yellow, high birefringence), chlorite and clinzoisite (colourless) and turbid plagioclase.

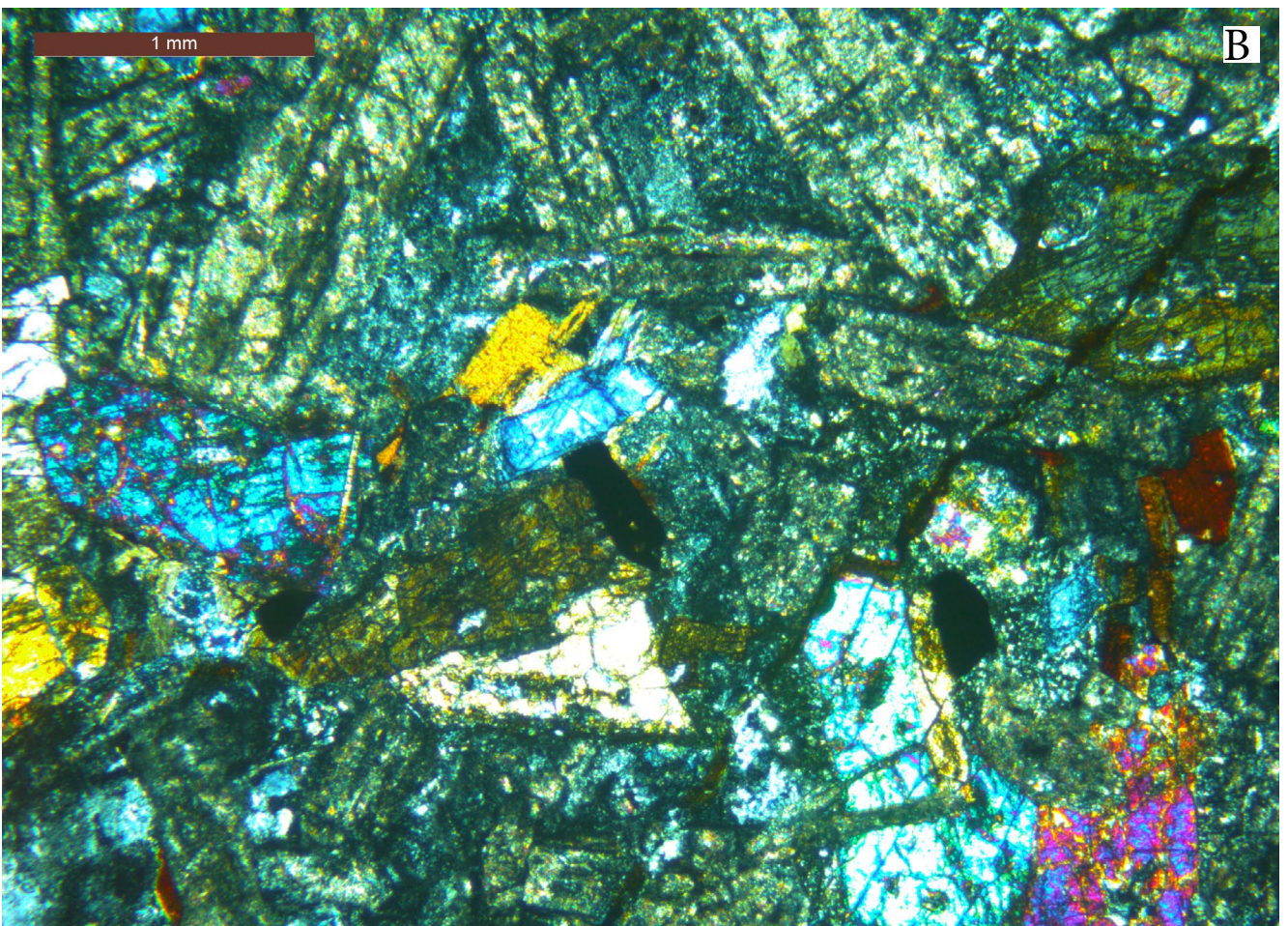
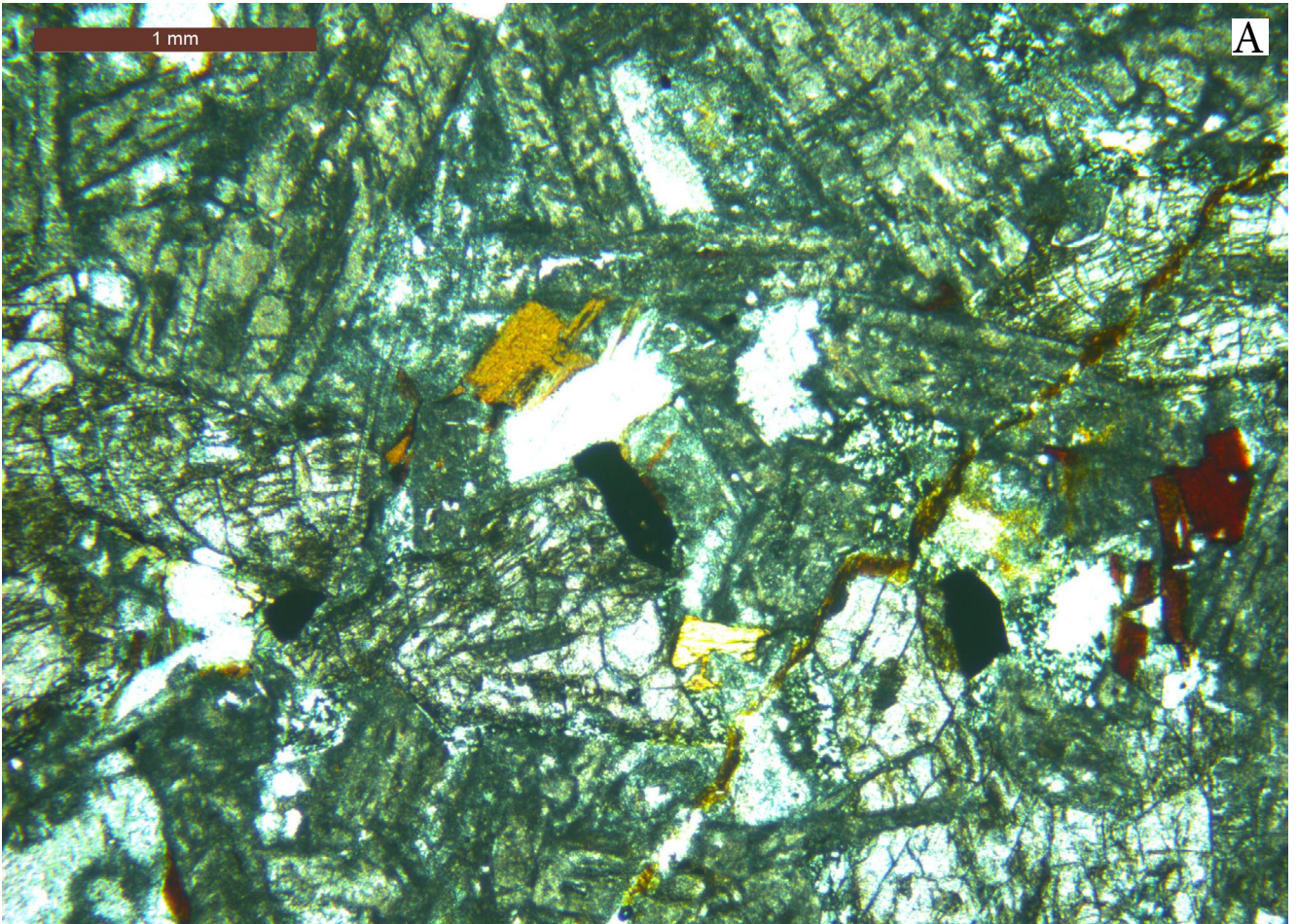


Figure 9. Photomicrograph of sample C112168A. Field of view ~4.6 mm x 3.4 mm (a) plane polarised light (b) crossed nicols. Note biotite (red-brown), closely packed crystals of clinopyroxene and turbid plagioclase laths and chlorite (colourless, centre).

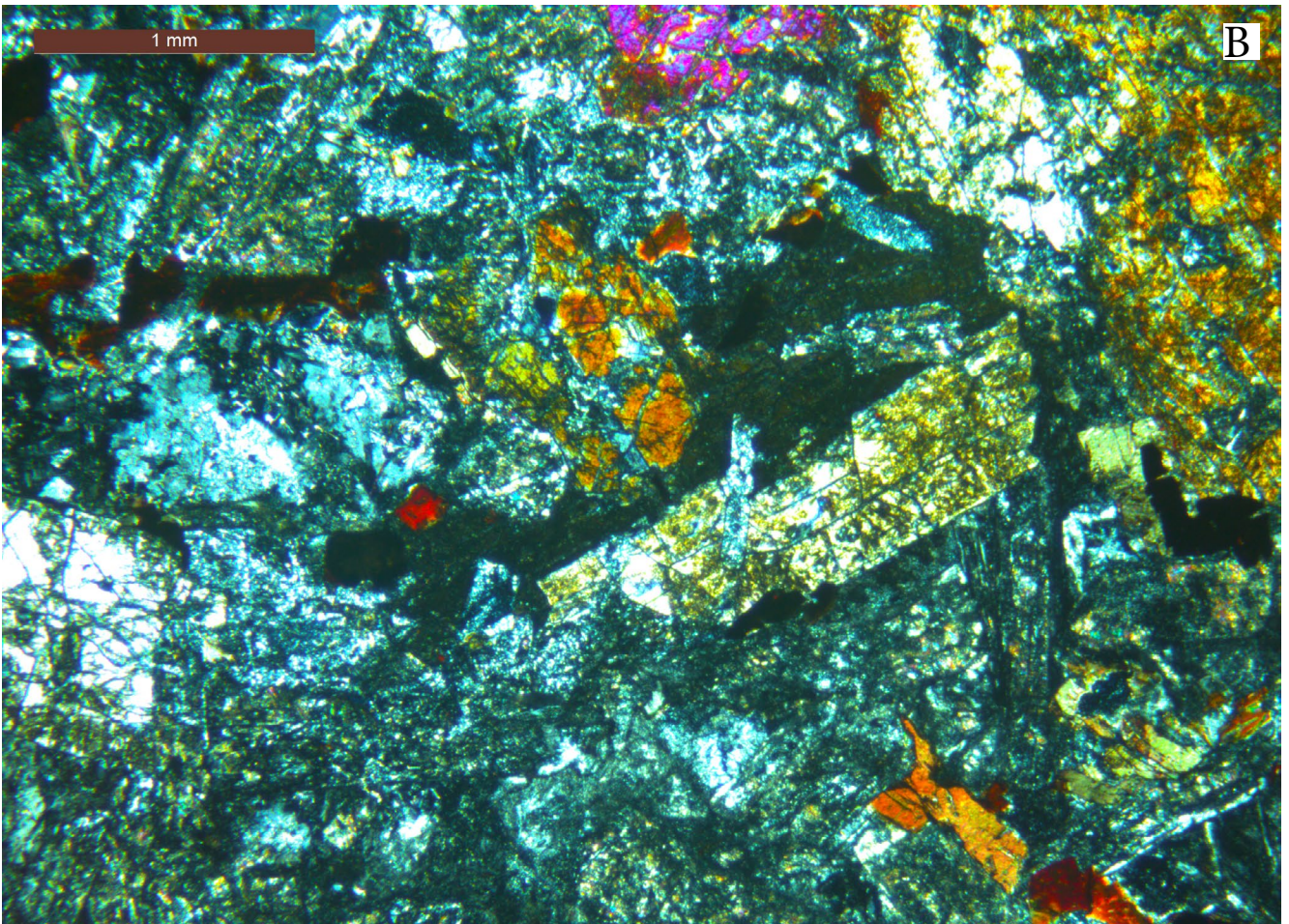
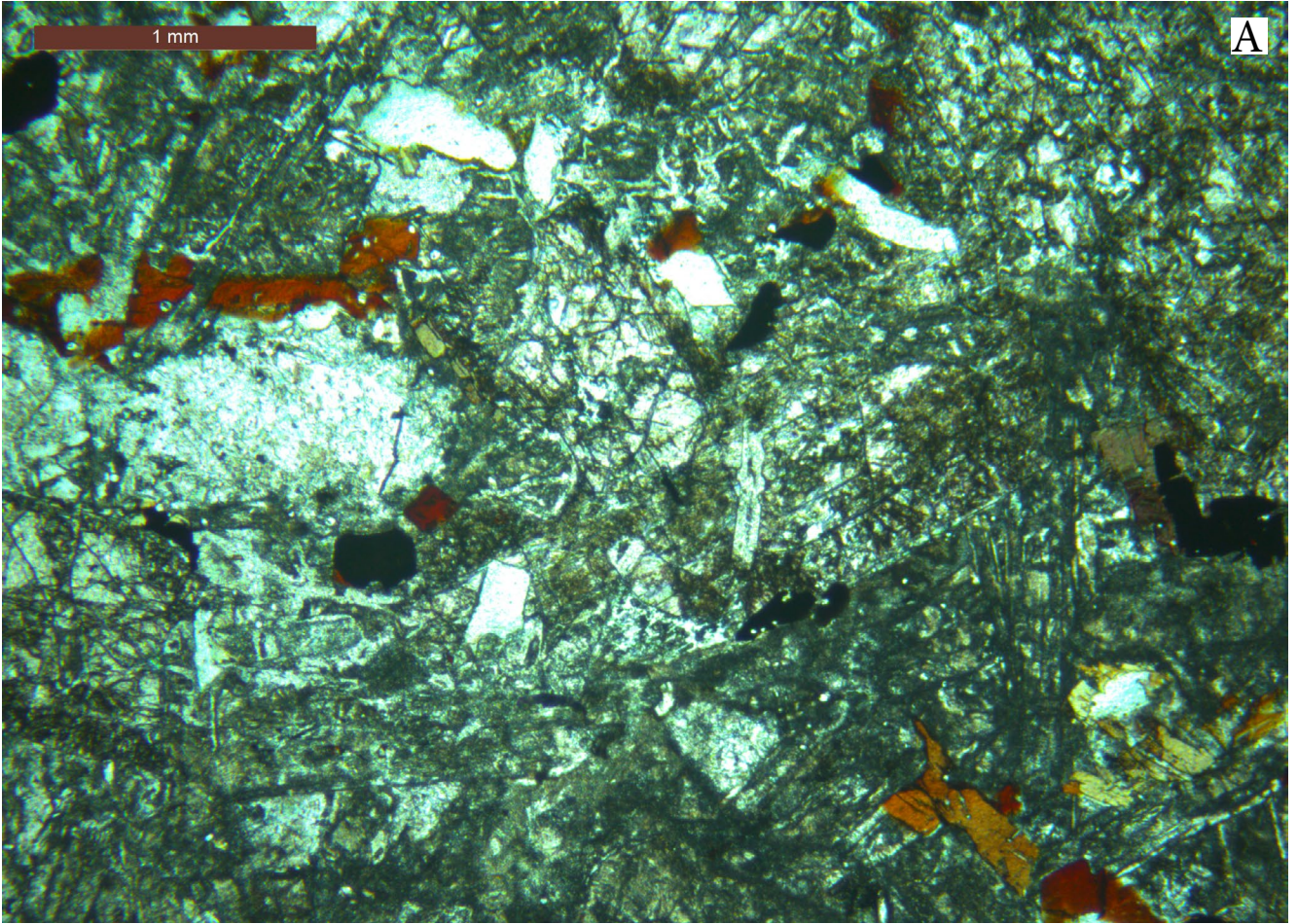


Figure 10. Photomicrograph of dated sample C112167A. Field of view ~4.6 mm x 3.4 mm (a) plane polarised light (b) crossed nicols. Note biotite (red-brown), subophitic texture with clinopyroxene partly enclosing plagioclase, partly altered to a fine-grained aggregate of secondary minerals.

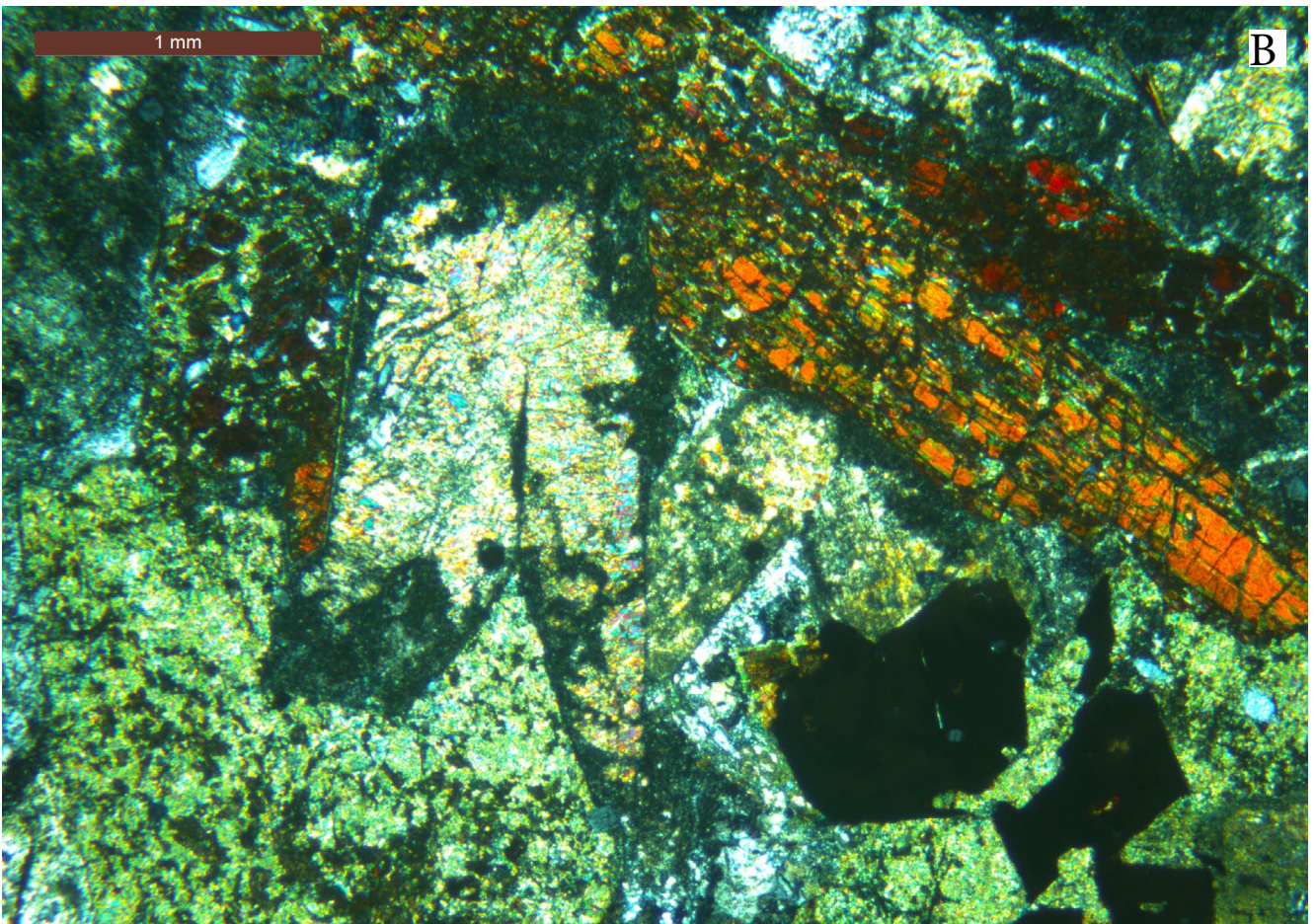
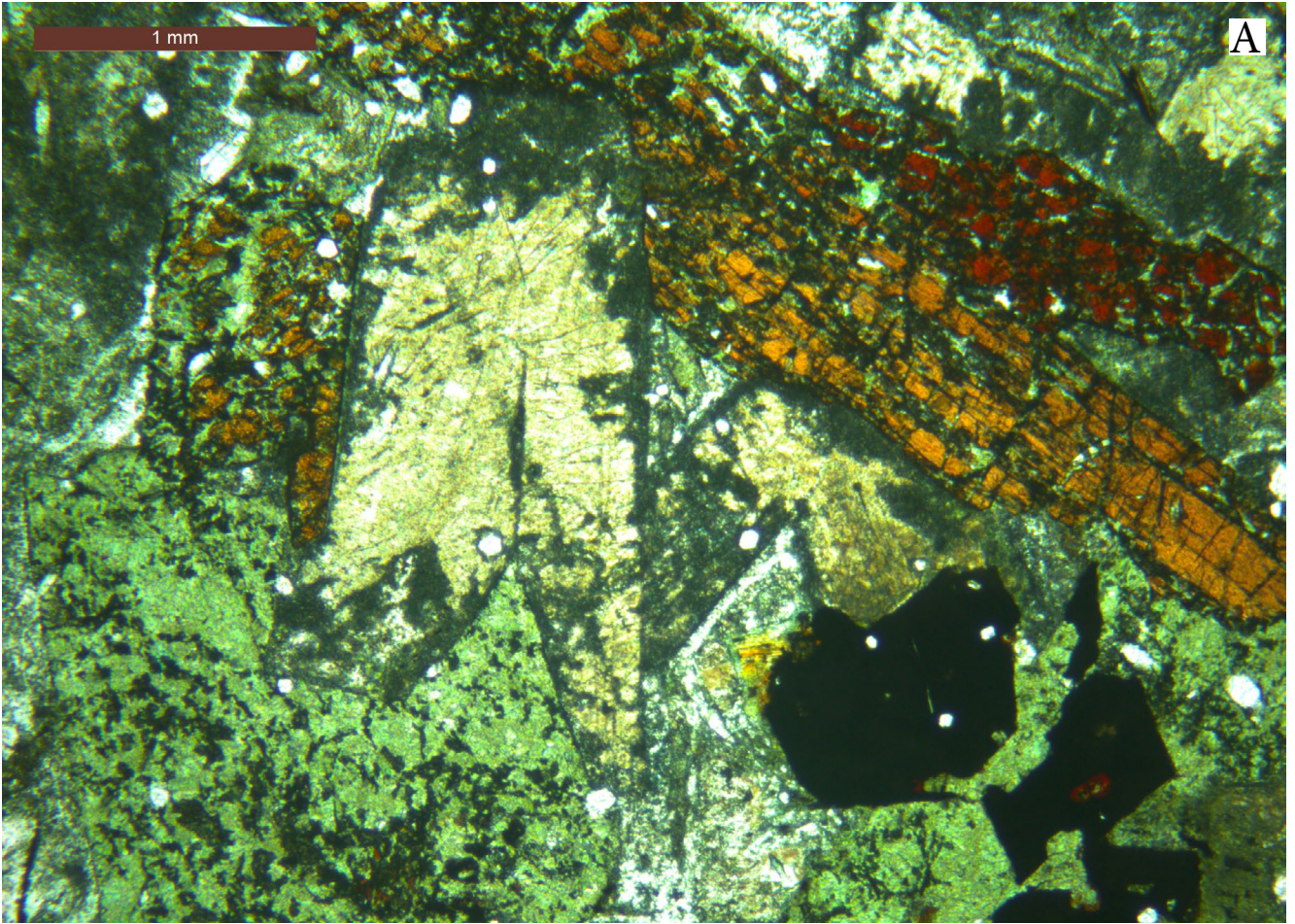


Figure 11. Photomicrograph of sample C112165. Field of view ~4.6 mm x 3.4 mm (a) plane polarised light (b) crossed nicols. Note large partly altered prism of kaersutite (red-brown, upper right), ilmenite largely replaced by titanite grains (lower right), large former plagioclase replaced by clinozoisite (pale yellow, centre left), fine-grained aggregate of pumpellyite (pale green-yellow, lower left), turbid albite (colourless) and scattered small apatite grains (colourless, hexagonal sections).

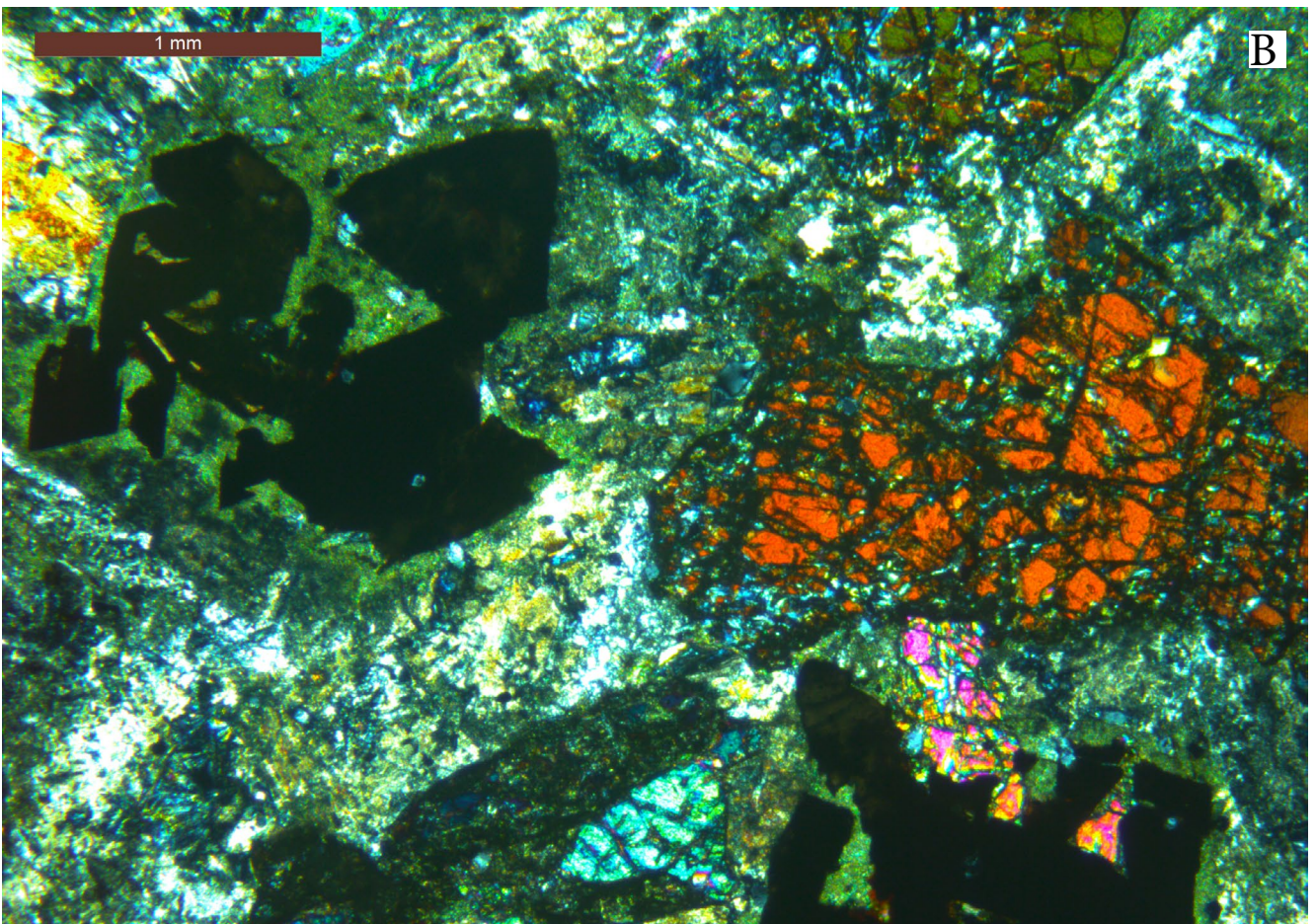
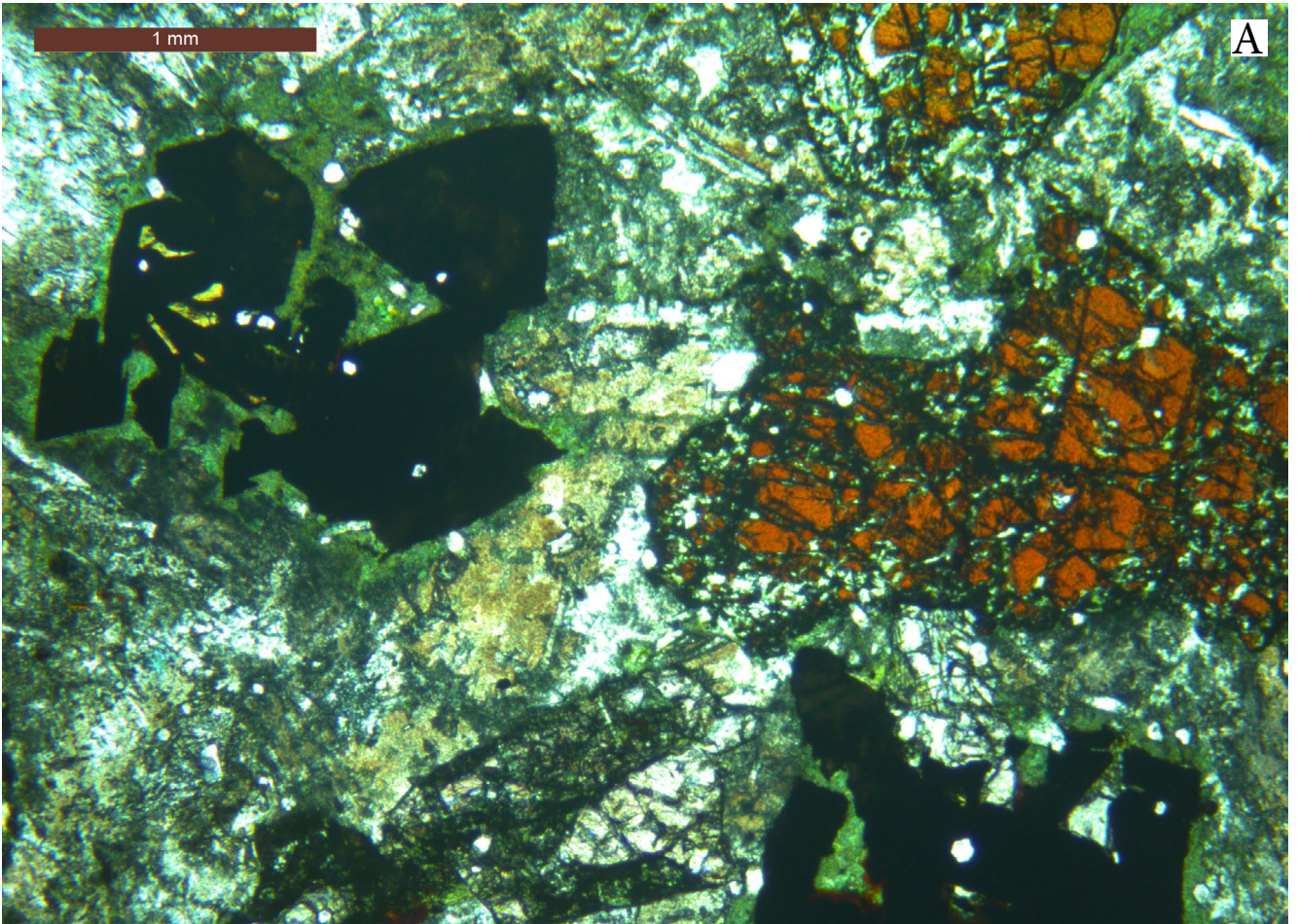


Figure 12. Photomicrograph of sample R012627. Field of view ~4.6 mm x 3.4 mm (a) plane polarised light (b) crossed nicols. Note large partly altered kaersutite euhedra, colourless fresh clinopyroxene (lower right and centre), angular titanite grains surrounded by fine-grained pumpellyite (yellow-green), and plagioclase replaced by fine-grained prehnite and clinozoisite (pale yellow-brown).

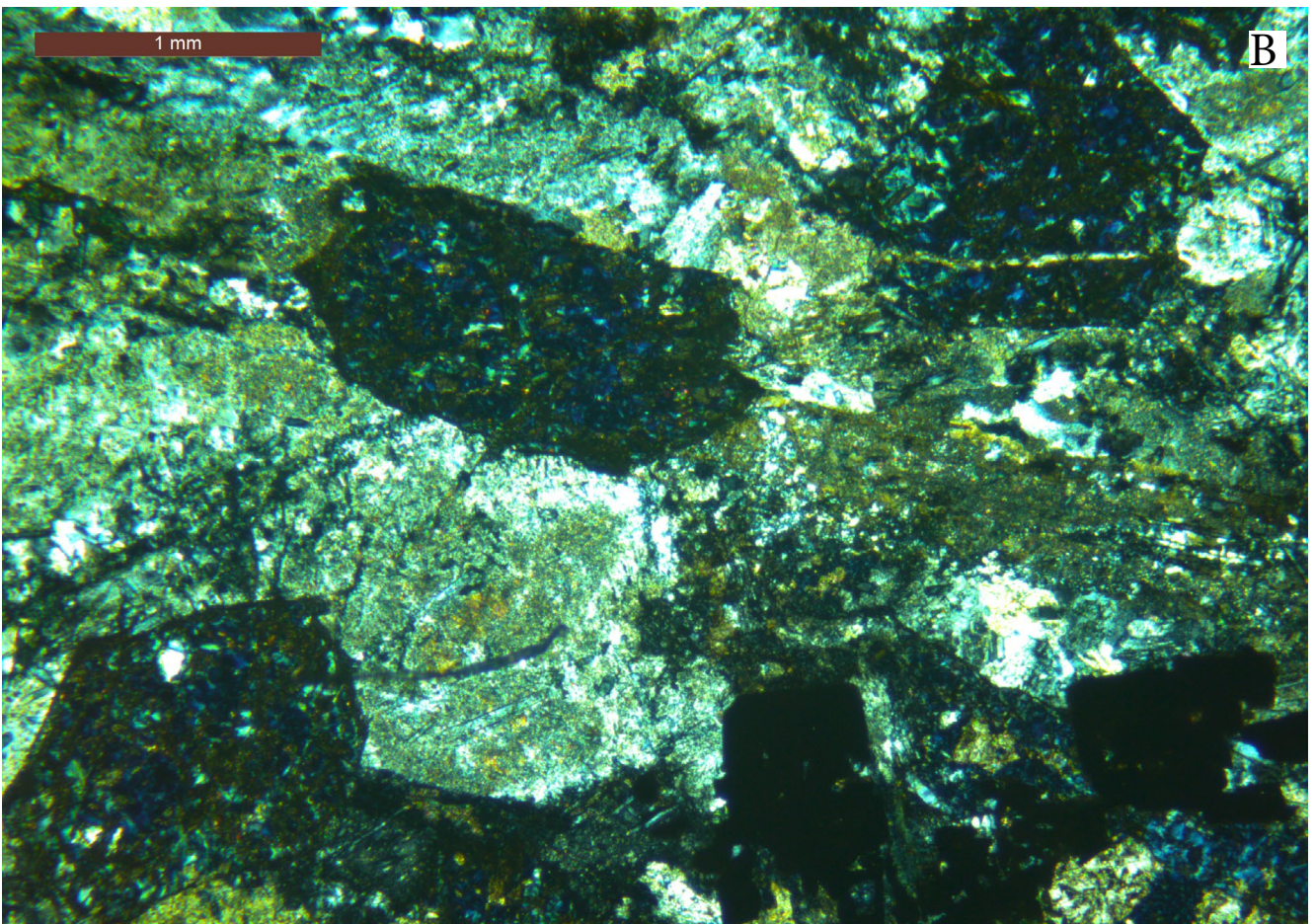
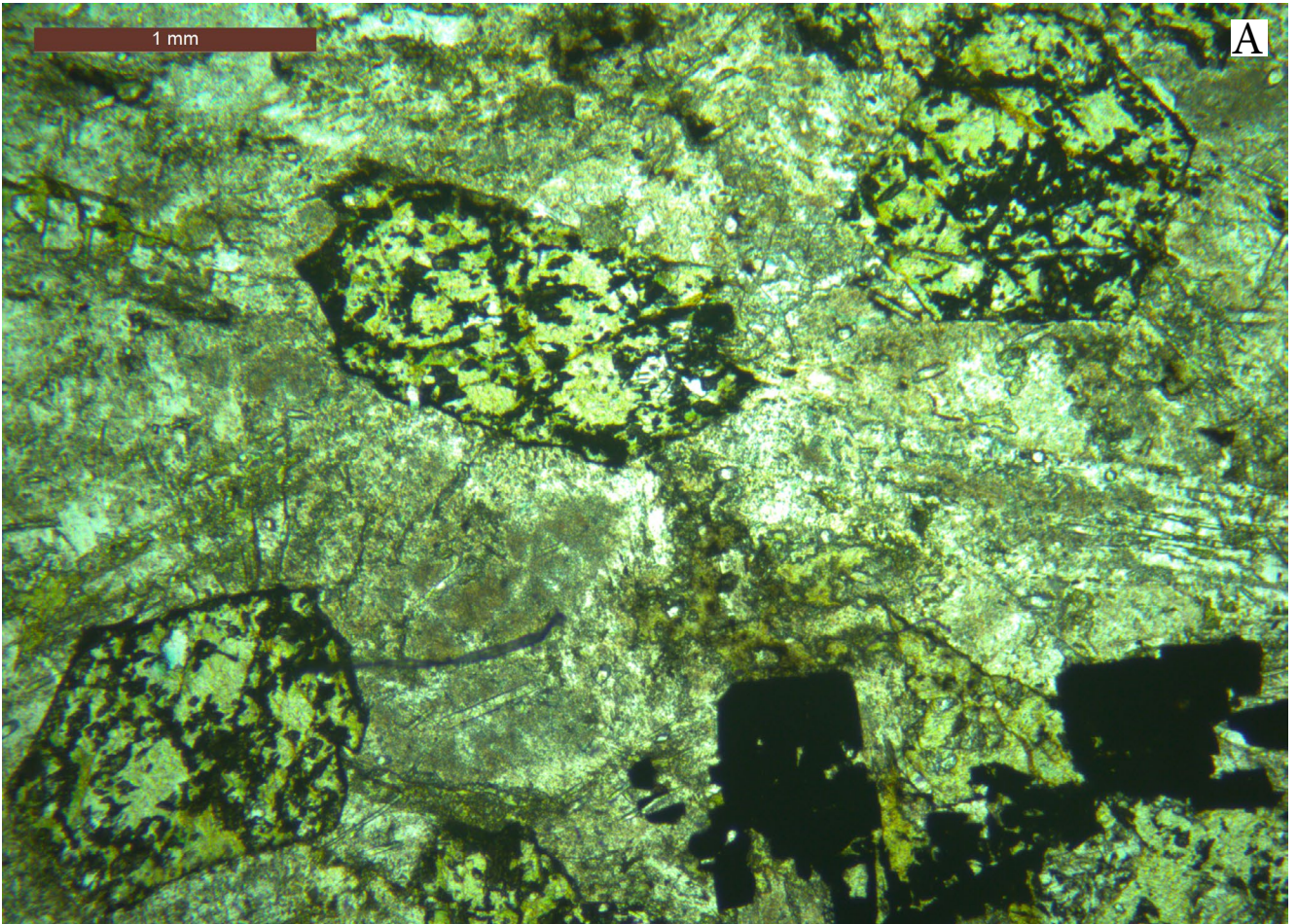


Figure 13. Photomicrograph of sample R016519. Field of view ~4.6 mm x 3.4 mm (a) plane polarised light (b) crossed nicols. Note pseudo-hexagonal pseudomorphs after amphibole, now replaced by chlorite and clinzoisite, turbid plagioclase replaced by prehnite and clinzoisite, chlorite (pale green, just below centre) and titanite (lower right).

ly 30 analyses appear to be of mixtures of two or more minerals. Attempts were made to deconvolute these, but in some cases this cannot be done with any confidence.

Results are reported as oxide weight per cent, together with calculated mineral formulae (tables 5 - 20).

6.1 Biotite

Biotite (Appendix 1; Table 5) from the dated sample (C112167A) is highly titanian (up to 7.3% TiO₂ or 0.42 cations/formula unit) (Figure 14b) with low Si (2.59 - 2.72 cations/formula unit) and little or no octahedral Al. Mg# (molar Mg/(Mg + Fe^{II})) ranges from 0.40 to 0.62 and thus these biotites straddle the phlogopite-biotite boundary (Mg# ~0.50) in the IMA-approved nomenclature scheme of Rieder et al (1998) (Figure 14a). Small amounts of Ba (up to 2.33% BaO or 0.08 cations/formula unit) and Na (up to 1.02% Na₂O or 0.154 cations/formula unit) present in some analyses are assigned to the A sites, although Na may be present as impurities or inclusions (e.g. by traces of albite in the analysed volume). No Mn or Ca was detected.

Two types of biotite are present in the more fractionated sample R012627. One is a titanian biotite (up to 7.5% TiO₂ or 0.43 cations/formula unit), similar to that in C112167A but more iron-rich (Mg# 0.22 - 0.41) and is thus annite (Rieder et al. 1998). Small amounts of Mn (up to 0.54% MnO) and Na (up to 0.69% Na₂O) were recorded in some analyses, but Ba was not detected.

The second type of biotite in R012627 is also annite (Mg# 0.16 - 0.44) but has significant octahedrally coordinated Al (0.28 - 0.71 cations/formula unit) (Figure 14c) and also differs in containing low to undetectable Ti (≤ 0.63% TiO₂) (Figure 14b). Small amounts of Mn are present in some analyses, but Na and Ca (reported in one analysis each) may be due to contamination. These more aluminous biotites are interpreted as a secondary, metamorphic phase in contrast to the titanian biotites which are interpreted as a relict igneous mineral.

6.2 Amphibole

Amphiboles (Appendix 1; Table 6) in sample R012627 (26 analyses) are notable for their high titanium (~ 5.4 - 7.9% TiO₂; ~0.64-0.91 Ti cations/formula unit) and are kaersutites or possibly ferrikaersutites (Figure 15a). Mn (≤ 0.36% as MnO) was detected in only two samples, Sc (0.032% as Sc₂O₃) in one sample, and Cr, Ni and F, among other elements, were not detected. A further two analyses with low totals are considered less reliable and contain minor S (≤ 0.08% as SO₃) and Cl (≤ 0.39%) suggesting small amounts of impurities are present.

Calculation of cations to the standard amphibole formula AB₂C₅T₈O₂₂(OH)₂ with the assumption that all

iron is ferrous (Fe^{II}) yields unsatisfactory results, in particular requiring some Ca (≤ 0.17 cations/ formula unit) to enter the C sites, where it should not be. This anomaly cannot be removed by converting some iron to Fe^{III} (see Leake et al., 1997 for discussion).

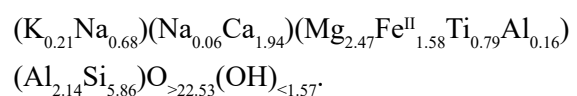
However, it is probable that these basaltic amphiboles are deficient in (OH) and contain some ferric iron (Fe^{III}). An alternative procedure would be to calculate the analyses as ferrikaersutites (NaCa₂Mg₃Fe^{III}TiAl₂Si₆O₂₄), with the assumptions of 24 oxygens and that all iron is ferric. This requires the allocation of some Mg to the B sites or, again, some Ca to the C sites.

The mineral formulae preferred here (Appendix 1; Table 6) were calculated by assuming all iron is Fe^{II} and normalising cations capable of entering the T and C sites (i.e. all but Ca, Na and K) to 13, and then adjusting (O) and (OH) to maintain charge balance. This provides a maximum constraint on (OH) of ~1.39 - 1.80 for these analyses.

The possibility remains that some ferric iron is present. However, this cannot be estimated because the coupled substitution Fe^{II} ↔ Fe^{III}, (O) ↔ (OH) cannot be quantified from microprobe analyses alone. The only constraint is that (OH) cannot be less than zero, which for some analyses provides an estimate of the maximum Fe^{III} that could be present.

In any case, most of the analyses are kaersutites in the IMA-approved nomenclature of Leake (1997) and Hawthorne et al. (2012), with Ti > 0.50 cations/formula unit and Mg#, i.e. Mg/(Mg + Fe^{II}) > 0.50. Two analyses with lower Mg# plot marginally in the ferrokaersutite field. Ti correlates positively with Mg# (Figure 15a), and Na and K, which are largely or wholly in the A sites, have weak negative correlations with Mg#. Octahedrally coordinated Al (i.e. in the C sites) is low (0.08 - 0.26 cations/formula unit, but total Al correlates strongly negatively with Si due to tetrahedrally coordinated Al (up to 2.29 cations/formula unit) (Figure 15c).

In summary, the mean composition calculated from 26 analyses, assuming all iron is ferrous and normalised to Si+Al+Ti+Fe+Mn+Mg=13, is



If any ferric iron is present, (O) will be larger and (OH) proportionally smaller.

Note that Hawthorne et al. (2012) consider kaersutite as a member of the ox-amphibole group, with



for kaersutite-ferrokaersutite-ferroferrikaersutite-ferrikaersutite end-members; i.e. lacking hydroxyl and with greater trivalent ion occupancy of the C sites. Again, these parameters cannot be quantified from microprobe data only.

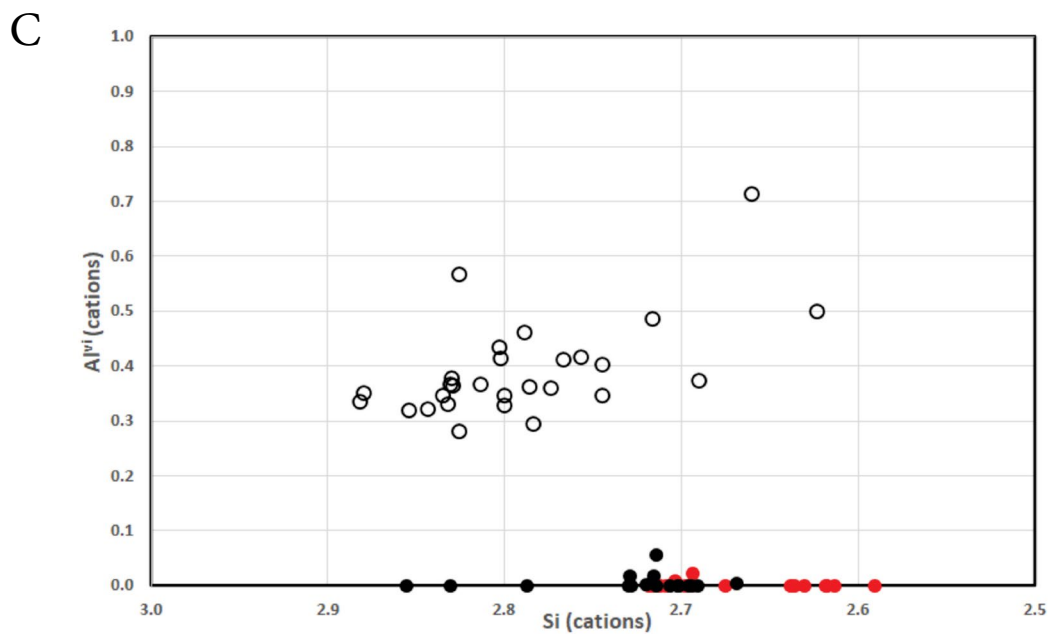
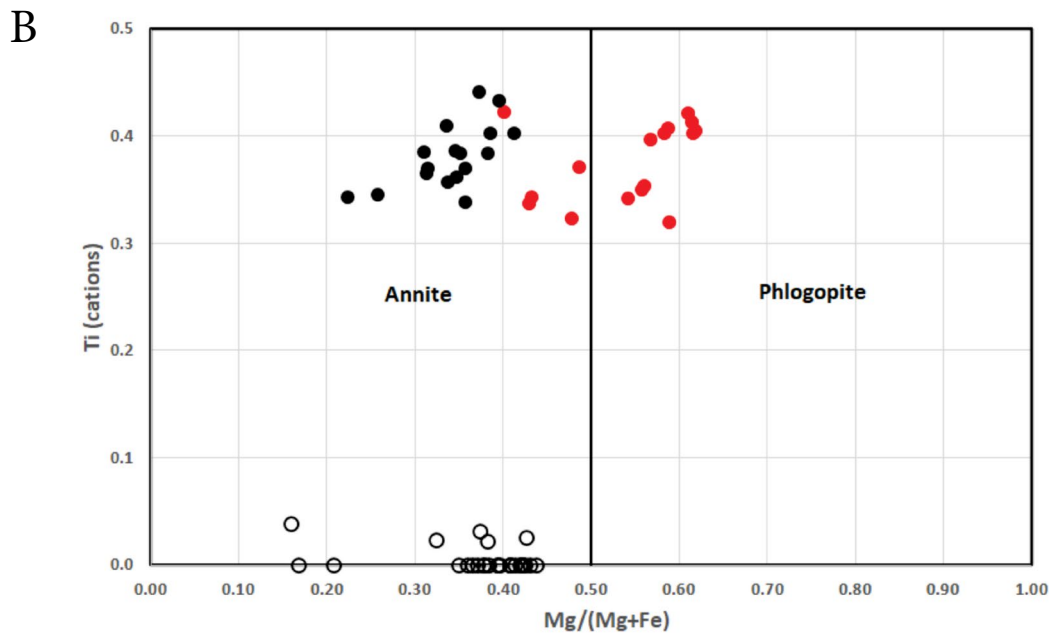
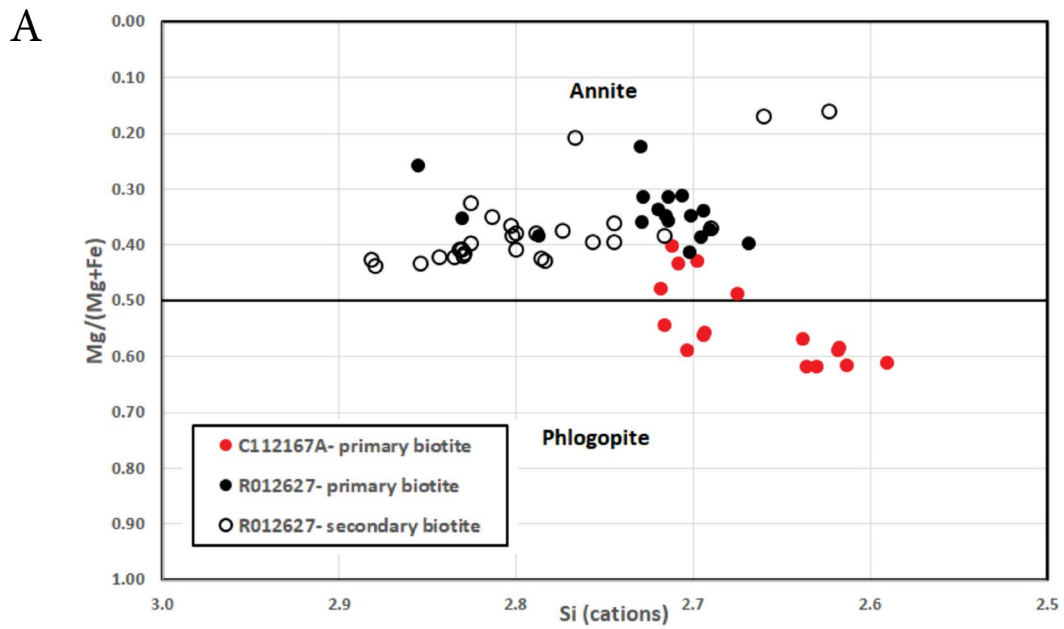
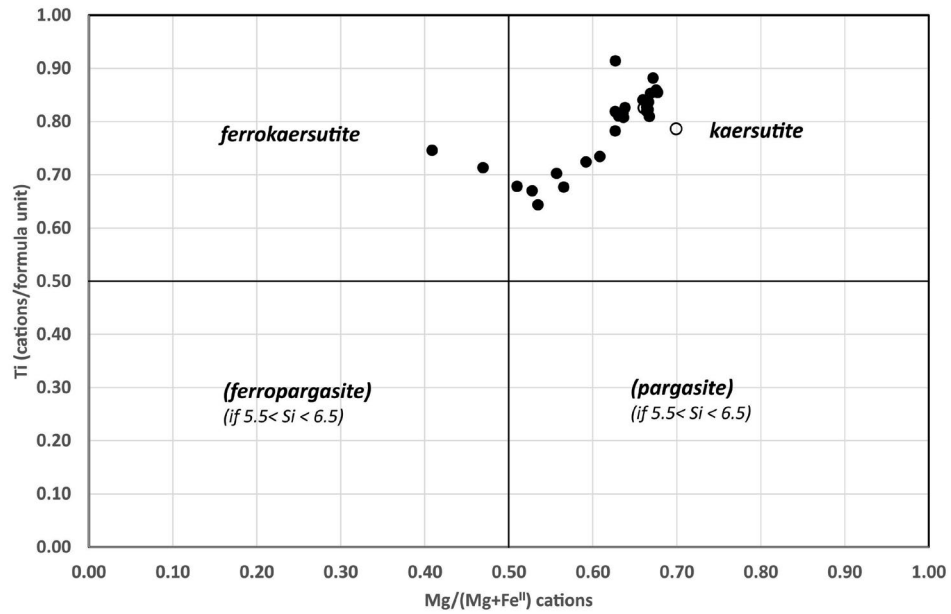
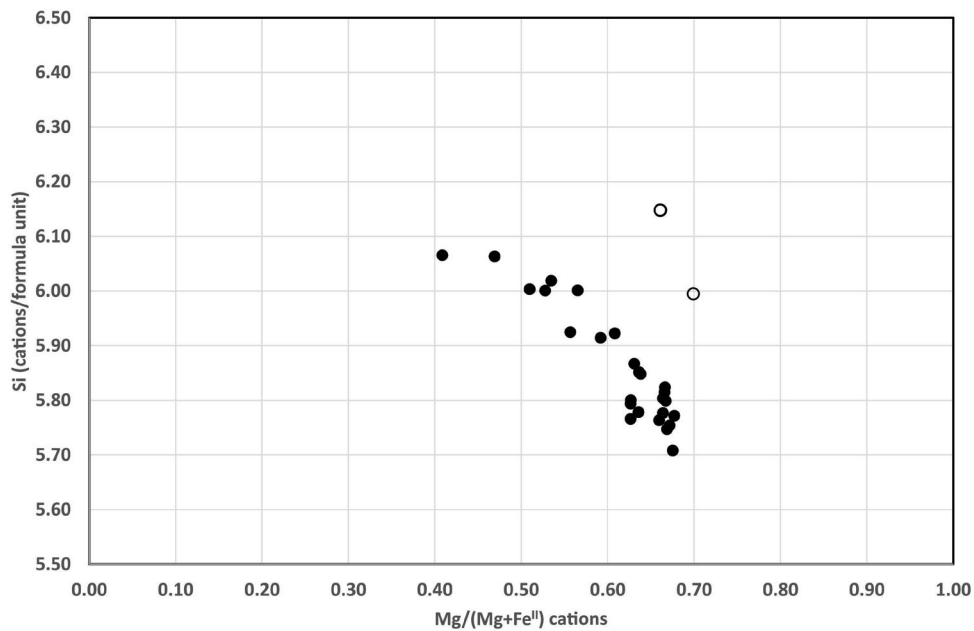


Figure 14. Plot of scanning electron microscope (SEM) analyses of biotite from dated samples C112167A ($^{40}\text{Ar}/^{39}\text{Ar}$) and R012627 (K/Ar) (Appendix 1; Table 5). Biotite nomenclature after Rieder et al. (1998). (a) Mg# vs Si (b) Ti vs Mg# (c) Al^{IV} vs Si.

A



B



C

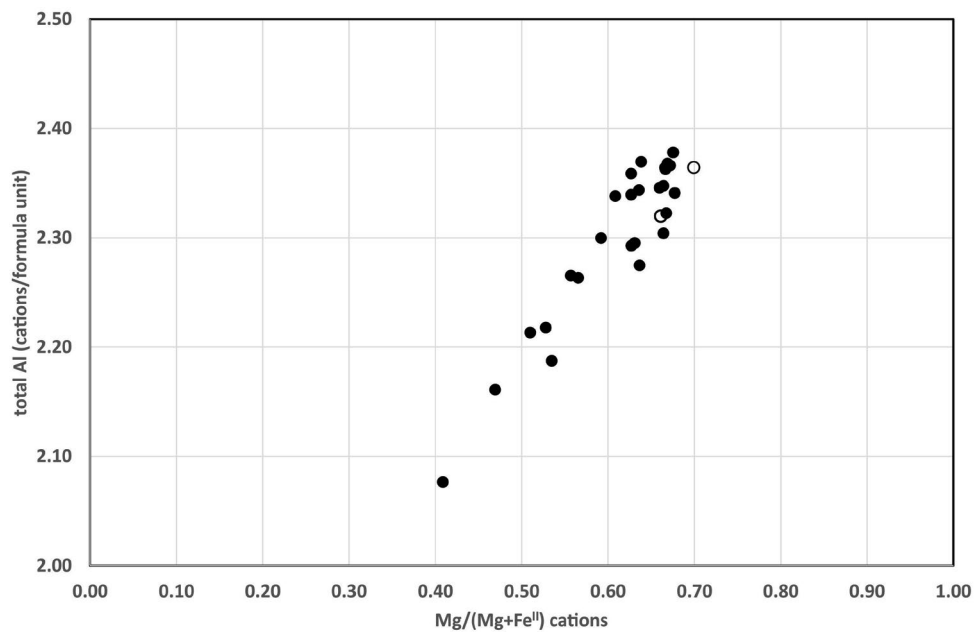


Figure 15. Plot of scanning electron microscope (SEM) analyses of amphibole from dated sample R012627 (Appendix 1; Table 6). Open symbols are from analyses with low totals. Amphibole nomenclature after Leake (1997) and Hawthorne et al. (2012). (a) Ti vs Mg# (b) Si vs Mg# (c) total Al vs Mg#.

No metamorphic amphiboles such as tremolite-actinolite were analysed in R012627, nor was any amphibole detected in C112167A, consistent with the XRD results.

6.3 Clinopyroxene

Sixty-two analyses were obtained (Appendix 1; Table 7) from the two samples and structural formulae calculated on the basis of 4 cations, partitioning Fe^{II} and Fe^{III} on the basis of 4 oxygens.

Almost all analyses are diopside in the IMA-approved nomenclature of Morimoto (1988) (Figure 16a). As might be expected, those from the more fractionated sample R012627 tend to be richer in iron than those from C112167A, although there is considerable overlap. One less calcic analysis plots as augite, and another as hedenbergite.

TiO₂ ranges from 4.47% (0.13 cations/formula unit) to less than 0.6% but only 6 analyses, all from R012627, qualify as titanian (> 0.10 cations/formula unit). Ti correlates negatively with Si (Figure 16b), consistent with the coupled substitution (Mg ↔ Ti, 2Si ↔ 2Al), although tetrahedral Al is apparently also coupled with small amounts of Al and Fe^{III} in the octahedral sites. There is no clear correlation of Ti with Mg#, except that the most iron-rich analyses, all also from R012627, are also low in Ti.

Na₂O is low (< 1% except for one analysis) and does not correlate with Mg# or Si.

MnO ranges up to 1.16% (0.045 cations/formula unit) in the hedenbergite analysis, but otherwise is < 0.83% and was usually not detected (< about 0.3%). Cr was detected in only two analyses (≤ 0.45% Cr₂O₃) and Sc₂O₃ (0.40%) and V₂O₃ (0.32%) in one sample each.

6.4 Feldspars

Feldspars were analysed in both C112167A and R012627 (Appendix 1; Table 8). Several analyses contain significant FeO and MgO, suggesting the presence of some impurities.

Some plagioclase analyses in both samples are near-stoichiometric albite. Others contain up to 1.1% CaO (~5.5 mol % anorthite), although some of this may be due to minor impurities such as prehnite or clinozoisite.

Alkali feldspar in C112167A is mostly low in Na (~4.0 - 8.6 mol% albite) and is probably orthoclase, but contains significant BaO (4.4 - 7.0 wt%, ~8 - 13 mol% celsian), consistent with high Ba (2151 ppm) in the whole rock analysis (Appendix 1; Table 2). Another alkali feldspar analysis plots toward the albite end-member (6.36% Na₂O) and may be anorthoclase, but is less stoichiometric and may contain impurities.

Calcic plagioclase was not detected or analysed in either sample.

6.5 Prehnite

Prehnite analyses from sample R012627 (Appendix 1; Table 9) are near-stoichiometric. Iron (mostly < 1 wt% as FeO) is the main impurity.

6.6 Clinozoisite

Following the IMA-recommended procedure of Armbruster et al. (2006), clinozoisite analyses from sample R012617 (Appendix 1; Table 10) were normalized to 8 cations. Fe was distributed to Fe^{III} and Fe^{II} to account for a cation charge of 25, although this cannot quite be attained for four analyses, even with all trivalent Fe and Mn. Only small amounts of Fe^{II} are inferred in the other five analyses.

The analyses show moderate (~11 - 49 mol%) solid solution toward epidote, Ca₂Fe^{III}Al₂Si₃O₁₂(OH). Two analyses contain minor strontium (≤ 1.05% SrO), one of which has also 0.53% MnO. Most analyses have slightly excess Y site occupancies (≤ 3.046) and are slightly deficient in the A sites (≥ 1.954), possibly due to slight vacancies in the latter.

6.7 Pumpellyite

Pumpellyite was analysed in both C112167A and R012627 (Appendix 1; Table 11). However, 6 of the 11 analyses contain small amounts of Na₂O (≤ 0.51 wt%) or K₂O (≤ 0.33 wt%), possibly due to impurities, which were subtracted as feldspar before calculation of mineral formulae on the basis of 16 cations. Iron was partitioned between Fe^{II} and Fe^{III} to balance 23 oxygens and 3 (OH) if possible. In C112167A, estimated Fe^{III} is low and Mg# (0.41- 0.61) varies over a relatively restricted range. In the more fractionated sample R012627, these all vary more widely. It is possible that the analysed volumes contained small amounts of other phases such as biotite, clinozoisite or chlorite which contributed to this dispersion.

6.8 Grossular

Metamorphic garnet was analysed in one site in the relatively fractionated sample R012627 (Appendix 1; Table 12). The two analyses calculate near-stoichiometrically if all iron is allocated to Fe^{III}, and are grossular (Ca-Al garnet) with about 16-20 mol% andradite component and minor Mn (~2 mol% spessartine).

Both analyses are slightly deficient in Si (2.910, 2.933 cations/formula unit) which is accounted for in Table 12 by assuming some tetrahedrally coordinated Al. Another possibility is that there may be some solid solution toward hydrogrossular (i.e. hibschite Ca₃Al₂(SiO₄)_{4-3x}(OH)_{4x}), but there is no other evidence for this such as low totals. It is not possible from microprobe data to distinguish

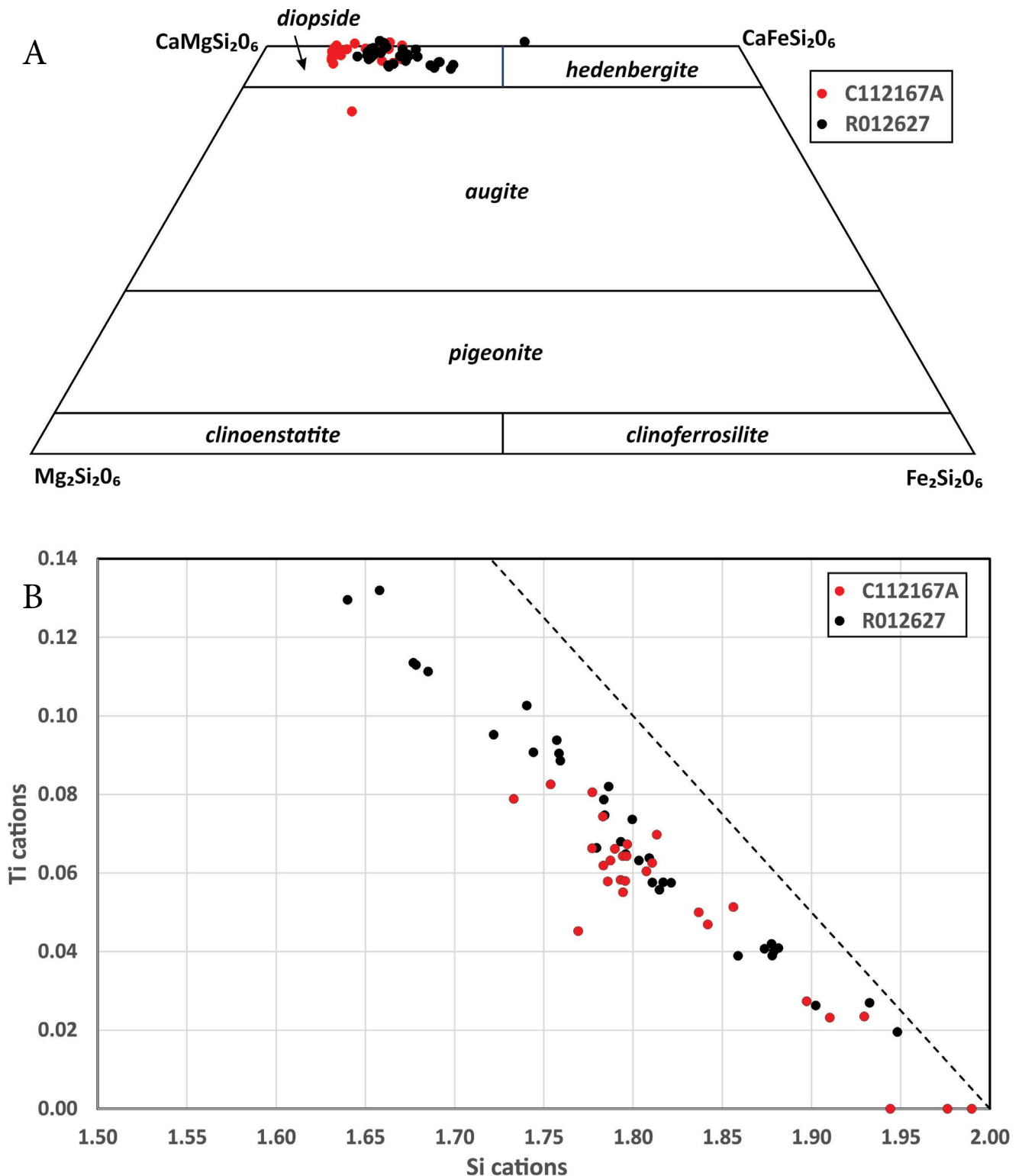


Figure 16. Plot of scanning electron microscope (SEM) analyses of clinopyroxene from dated samples C112167A and R012627 (Appendix 1; Table 7). (a) quadrilateral plot, nomenclature after Morimoto (1988), (b) Ti vs Si; the dotted line represent the ideal coupled substitution $\text{Si} \leftrightarrow \text{Al}^{\text{iv}}, \text{Mg} \leftrightarrow \text{Ti}$.

these substitutions, nor to disentangle them from other possible substitutions such as Fe^{II} for Fe^{III} . However, more significant departures from stoichiometry occur if any Fe^{II} is assumed.

6.9 Chlorite

Most chlorite analyses contain small amounts of K_2O (≤ 0.9 wt%), suggesting some interlayering with, and/or alteration from, biotite (Appendix 1; Tables 13 and 14). In both samples C112167A and R012627, chlorite is relatively aluminous ($\sim 2.77 - 3.07$ Si cations/formu-

la unit with complementary $1.23 - 0.93 \text{ Al}^{\text{iv}}$ /formula unit). However, chlorites in the less fractionated sample (C112167A) are more magnesian ($\text{Mg}\# 0.62 - 0.67$) compared to those in R012627 ($\text{Mg}\# 0.27 - 0.54$) (Figure 17). This merely reflects bulk rock composition. Following Bayliss (1975) and Bailey (1980), trioctahedral chlorites are named after their dominant divalent cation end-member; thus those in C112167A are clinochlore and those in R012627 are predominantly chamosite (Figure 17).

A further ten analyses (Table 14) contain higher amounts of K₂O and in some instances CaO, and are interpreted as mixtures of chlorite, secondary (low Ti-) biotite and other minerals. Again, however, Mg# is higher in those from C112167A (0.60-0.64) than R012627 (0.30 – 0.40).

6.10 Muscovite

Two analyses from sample C112167A (Appendix 1; Table 15) are probably mixtures of dioctahedral mica (muscovite) and albite, with possibly small amounts of other secondary minerals.

6.11 Titanite

Few titanite (sphene) grains appear petrographically homogeneous, and all analyses significantly depart from ideal CaTiSiO₅ (Appendix 1; Table 16). All appear to have some substitution of Al for Ti, whereas significant FeO (≤ 7.5 wt%) and minor MgO (≤ 1.3 %) may indicated iron- rich chlorite impurities (Appendix 1; Table 16). Although titanite probably formed by the replacement of ilmenite, none of the analyses deconvolute well with ilmenite as a component. Several analyses contain small amounts of V, Sc and Zr.

6.12 Apatite

Apatite analyses in both R012627 and C112167A are fluorine-dominant in the X sites (F 2.0 – 3.1 wt%, 0.53-0.91 anions/formula unit) and thus these are fluorapa-

tites (Pasero et al. 2010). All analyses are slightly deficient in Ca. Small amounts of Si, Fe and other elements in the analyses are probably due to inclusions (Appendix 1; Table 17).

6.13 Ilmenite

Eight similar analyses of ilmenite from sample C112167A show that there is significant substitution of Mn for Fe^{II} ($\sim 7 - 8$ mol % MnTiO₃), but suggest that there is minimal (~ 3 mol %) solid solution towards hematite (Appendix 1; Table 18).

6.14 Zircon

A single zircon analysis from sample R012627 (Appendix 1; Table 19) is contaminated with significant impurities, probably chlorite and biotite. The zircon may be a xenocryst derived from the Oonah Formation country rock, since Turner et al. (1998) reported inherited zircons in one sample (93220002), whereas Black et al. (1997) found no zircons in two samples (95220015, 95220019).

Miscellaneous analyses of fine-grained probable mixtures are reported in Appendix 1; Table 20.

7.0 Metamorphism

Although the secondary minerals in the groundmass are unlikely to lie in metamorphic equilibrium, some conclusions on their conditions of formation may be drawn. Prehnite is stable below about 405°C at low

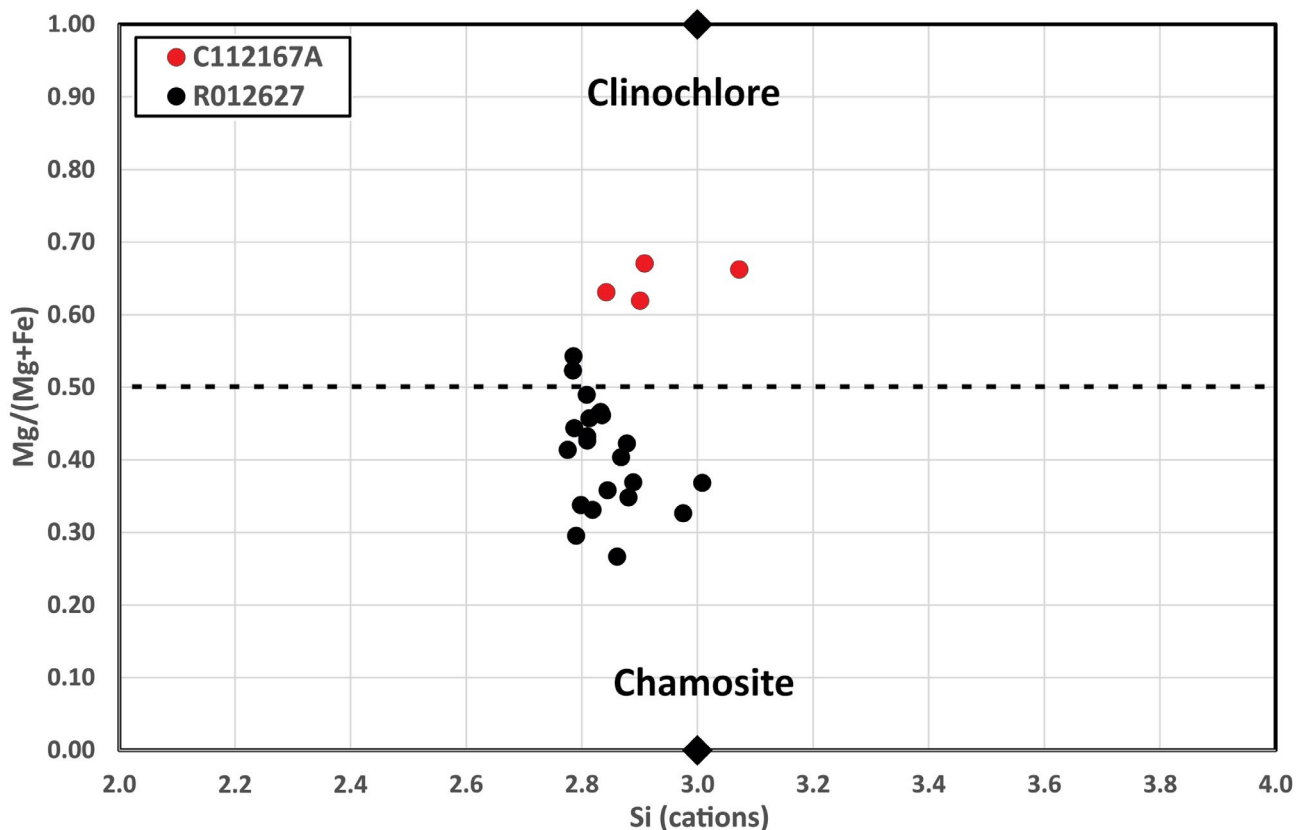
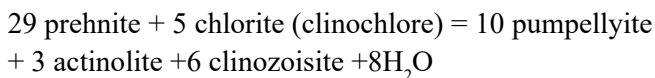


Figure 17. Plot of scanning electron microscope (SEM) analyses of chlorite from dated samples C112167A and R012627 (Table 13), Si vs Mg#. Compositions of ideal end-member clinocllore and chamosite also shown (Bayliss 1975, Bailey 1980).

pressures (Liou, 1971) and its coexistence with chlorite (and the apparent absence of actinolite) suggests that the following reaction (no. 4 of Winkler, 1979, p. 190) was displaced to the left:



Winkler (1979) estimates that this reaction occurs at ~350- 400°C at 0 – 200 MPa. The other reactions considered by him in relation to the very low grade metamorphism of mafic rocks mostly involve quartz and are thus not directly relevant in the present context.

The metamorphic minerals in the Cooee Dolerite probably formed at ~300-400°C within the prehnite-pumpellyite facies or prehnite-pumpellyite-chlorite zone (Winkler, 1979), presumably in the Cambrian Tyennan Orogeny (see K/Ar results below).

8.0 Geochemistry

The geochemistry of the Cooee Dolerite has previously been described by Brown (1989), Crawford and Berry (1992) and Calver and Everard (2014). XRF results for the seven new samples are considered together with 16 previous analyses of the Cooee Dolerite (11 by Mineral Resources Tasmania/Tasmania Department of Mines, 4 by the Australian Geological Survey Organisation/Geoscience Australia, and one by the University of Tasmania).

All samples are alkali dolerites, although with widely ranging degrees of fractionation, quantified by Mg# (molar 100Mg/Mg + Fe^{II}), calculated at Fe₂O₃/FeO = 0.20) which ranges from 72.8 to 46.1 (Table 2). The most fractionated member of the dataset is one of the new samples (C112165) with the lowest Mg# (46.1) and MgO (3.82%). The sample chosen for ⁴⁰Ar/³⁹Ar dating (C112167), with Mg# ~ 69.8, is fairly typical of the less fractionated samples.

Most samples with high Mg# are from the central Parklands outcrops (apart from 99220002 from near West Beach), whereas fractionated samples with low Mg# were collected from throughout the unit, and predominate at the eastern and extreme western ends. Near Parklands, sedimentary structures in the enclosing Oonah Formation indicate easterly or southeasterly younging both at Red Rock Point, which is therefore stratigraphically below the dolerite, and just east of Parklands, therefore stratigraphically above it (Figure 2; Figure 5 of Gee, 1977). However, there does not seem to be any systematic spatial correlation with Mg# in the area that might be attributable to gravitational crystal settling in a thick sheet, as seen in the Jurassic dolerites. Many of the high Mg# samples in the Parklands area are in fact in the upper part of the intrusion.

SiO₂ ranges from 43.50 – 49.87%, except for one very

altered sample (with 11.2% loss-on-ignition). Total iron (FeOt) and Na₂O tend to correlate negatively with Mg#, and CaO positively, although the plots are quite scattered, particularly at low Mg# (Figure 18).

The high field strength elements (HFSE) including TiO₂, P₂O₅, Y, Zr, Nb and the REE correlate negatively with Mg# (i.e. increase with fractionation) (Figure 18, 19a) and show good mutual correlations (Figure 19b), whereas Ni, Cr and Sc correlate positively with Mg# (i.e. decrease with fractionation) (Figure 19c). Levels of Al₂O₃, V, Co and Ga remain more-or-less constant regardless of fractionation state (Figure 19c). The large ion lithophile elements (LILE) K₂O, Rb, Ba and Sr vary more erratically, suggesting of element mobility, although Rb and to a much lesser extent Ba remain correlated with K₂O (Figure 19d). No clear trends can be recognised for Cu (Figure 19c) or Zn (Figure 19a).

The trends shown by MgO, total iron (FeOt), CaO, Ni, Cr, Sc and the HFSE, when plotted against Mg#, are consistent with crystallisation and fractionation of olivine, clinopyroxene ± plagioclase, although some scatter may be attributable to slight mobility during alteration.

The mobility of LILE and relative immobility of the HFSE in the Cooee Dolerite are typical features of mafic rocks that have been undergone low-grade metamorphism. The absolute levels and ratios of the HFSE are diagnostic of alkalic within-plate basaltic magmas, as depicted in various discrimination diagrams developed in the 1970s and 1980s (e.g. see Calver and Everard, 2014).

Seven samples of the Cooee Dolerite have previously been analysed for REE elements, by INAA (4 samples), ICPMS (2 samples) and ion exchange/XRF (1 sample) (Table 21). Normalised against average chondrite, all are strongly light rare-earth element (LREE)-enriched ((La/Yb)_N 9.5 – 13.0), with similar slightly concave patterns and negligible Eu anomalies (Figure 20). No additional REE analyses were made of samples collected for the current study.

Isotopic analyses of four samples of the Cooee Dolerite by Geoscience Australia returned strongly positive εNd values (at 734 Ma) of +5.31 to +5.97, consistent with a mantle source with little crustal input (Table 22, L. P. Black, pers. comm.). Initial Sr isotope ratios (also at 734 Ma) vary widely (~0.7084 – 0.7213) but are discounted due to mobility of Rb and Sr, as are the Pb isotope results due to mobility and low levels of Pb, Th and U (Table 22).

9.0 Magnetic susceptibility and oxidation state

Magnetic susceptibility was measured on planar and unweathered sawn surfaces of ten large samples with a susceptibility meter (Kappameter Model KT⁵). Values from nine of the samples lie within a narrow range

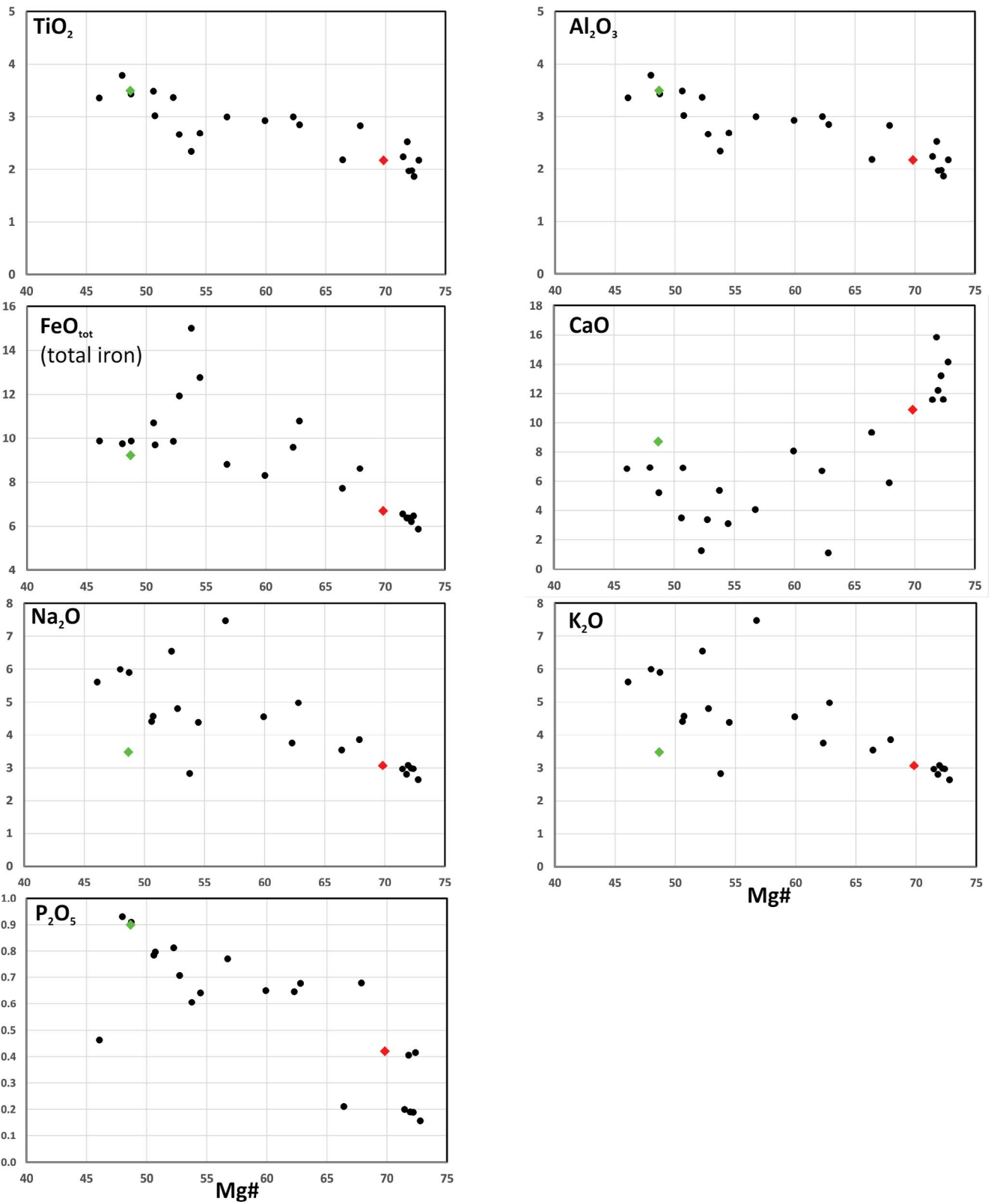


Figure 18. Plot of major elements against Mg# for Cooee Dolerite (Table 2), the dated samples are highlighted (C112167A, red) and R012727 (green).

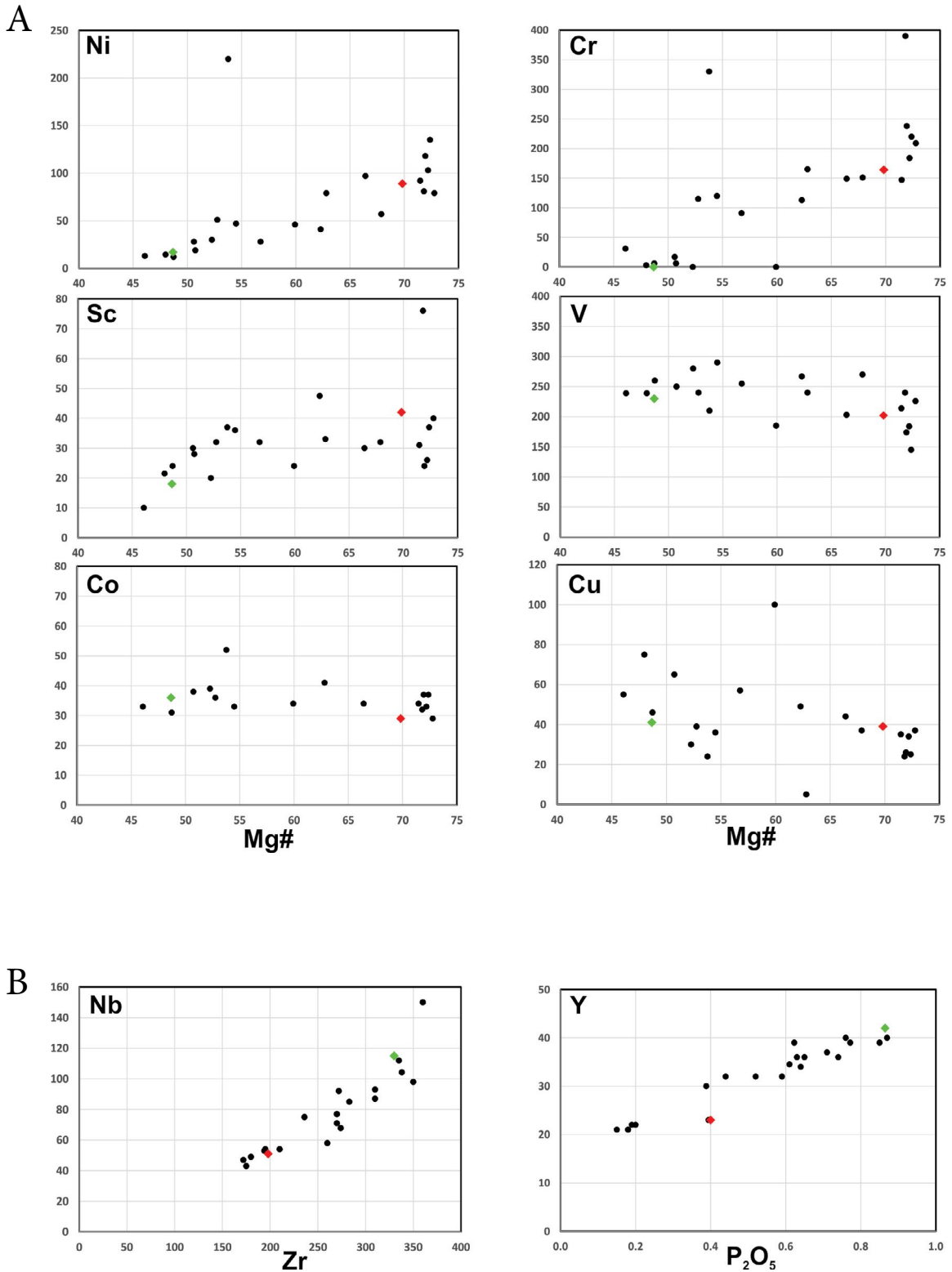
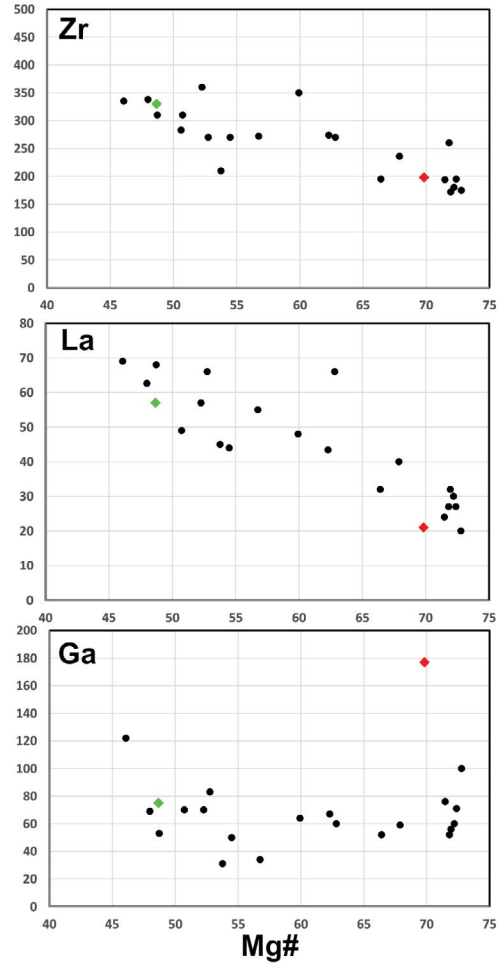
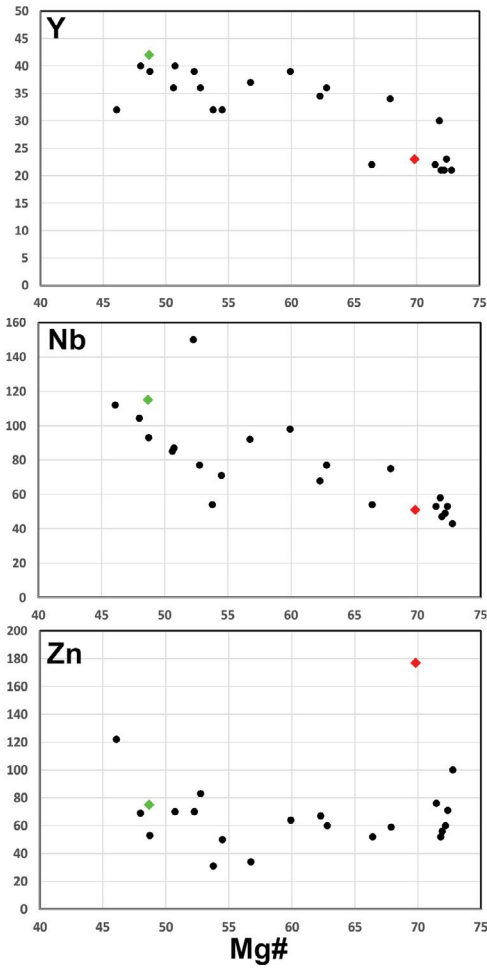
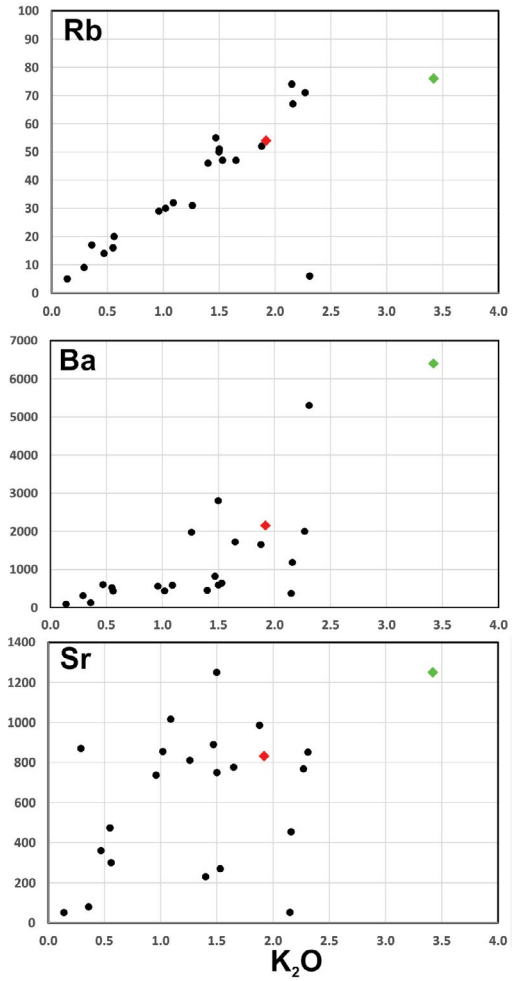
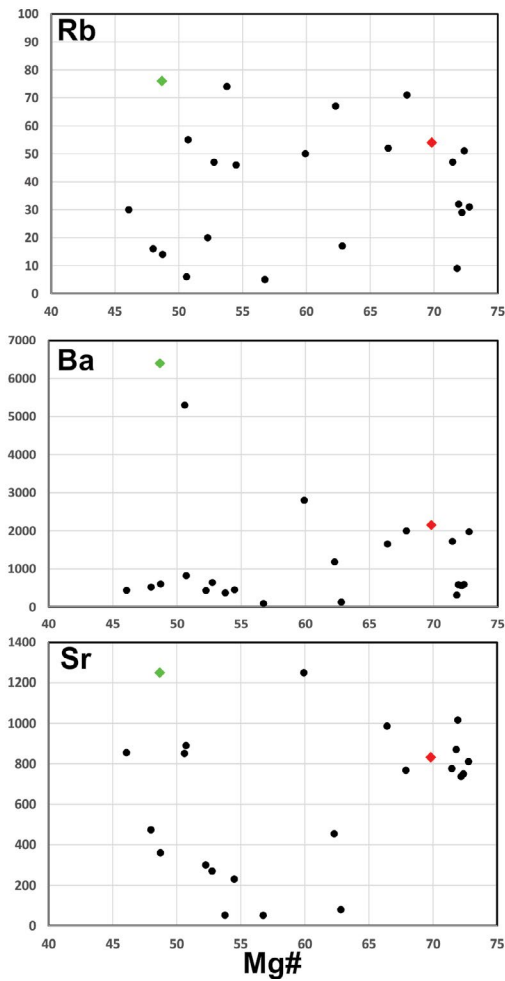


Figure 19. Plot of trace elements for Coocoe Dolerite (Table 2), the dated samples are highlighted (C112167A, red and R012727, green). (a) Y, Zr, Nb, La, Zn and Ga vs Mg#; (b) Nb vs Zr and Y vs P_2O_5 ; (c, following page) Ni, Cr, Sc, V, Co and Cu vs Mg#; (d, following page) Rb, Sr and Ba vs. Mg# and K_2O .

C



D



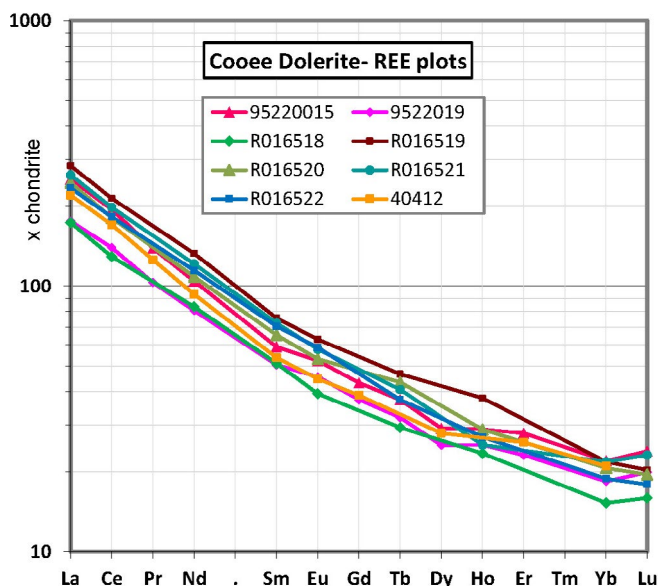


Figure 20. Chondrite-normalised rare-earth element plots for the Cooee Dolerite; data (Table 21) from L. P. Black, A. V. Brown and Crawford and Berry (1992), average CI-chondrite-normalising factors from O'Neill (2016).

(0.38 to 0.52 $\times 10^{-3}$ SI), whereas sample C112165, a strongly fractionated hornblende-bearing sample, returned a higher value of 1.47 $\times 10^{-3}$ SI (Table 1).

These are low values for mafic rocks, and strongly suggest that the samples contain little or no magnetite, or other members of the magnetite-ulvospinel series. Although it is possible that magnetite has been replaced by secondary minerals, a relict opaque phase is present in most samples (Appendix 1; Table 3), and this is confirmed as ilmenite in sample C112167A (Table 18). It seems more likely that little or no magnetite crystallised in the Cooee Dolerite due to a strongly reduced oxidation state (low oxygen fugacity) of the magma. This is supported by the low inferred hematite content (<3 mol%) of the ilmenite analyses (table 18) and the low Fe_2O_3 and $\text{Fe}_2\text{O}_3/\text{FeO}$, where available, of the whole rock analyses (Appendix 1; Table 2).

The Cooee Dolerite has no obvious expression on aeromagnetic imagery, although there are anomalies in the area related to Cenozoic basalt and cultural features.

10 Geochronology

10.1 Previous work

Spry (1962) briefly reported a K/Ar age of 700 Ma from the Cooee Dolerite, attributed to J. Richards. This appears to have been the same determination (702 Ma from biotite) which was reported more fully by McDougall and Leggo (1965), who considered it a minimum age due to the likelihood of argon loss from Precambrian rocks. This age is recalculated to 711 Ma for revised decay constants (Steiger and Jäger 1977). Crook (1979), quoting J. Richards, further revised this age to 725 \pm 35 Ma to account for spike bias. The location is imprecisely described in imperial coordinates

rounded to ± 1000 yards ("Cooee Point, E390 N945") but probably refers to the large body on the foreshore at Parklands, in the western part of the outcrop of the Cooee Dolerite.

Coleman (1974; 1976, p. 601) briefly reported a K/Ar age of 735 \pm 15 Ma from the Cooee Dolerite, which is recalculated to 744 Ma for revised decay constants.

Turner et al. (1998) found common zircon grains in a sample collected from the upper part of a sill about 1m below a peperitic contact, near the western end of West Beach, Burnie, at the extreme eastern end of the outcrops. However, the rounded and pitted morphology of the grains and subsequent SHRIMP dating (^{204}Pb corrected $^{207}\text{Pb}/^{206}\text{Pb}$ ages ranging from 1420-2450 Ma) indicate that they are xenocrysts, probably detrital zircons derived from the country rocks. Three other samples of the Cooee Dolerite failed to yield any zircon (Turner et al. 1998; Black et al. 1997). The lack of magmatic zircon was attributed to the low silica content of the Dolerite (e.g. $\text{SiO}_2 \sim 45.4$ to 48.0% for these samples).

S. Denyszyn and co-workers at the University of Western Australia unsuccessfully attempted to separate baddeleyite from the Cooee Dolerite (pers. comm., c. 2015).

Mulder et al. (2018) obtained a ^{207}Pb -corrected $^{238}\text{U}/^{206}\text{Pb}$ age of 733 \pm 9 Ma age from magmatic apatite separated from the Cooee Dolerite. This is consistent with the maximum depositional ages that they obtained from the enclosing Oonah Formation of ~ 730 Ma (detrital monazite) and was considered to robustly date both units.

11.0 K/Ar

A coarse-grained dolerite (R012627) from near Red Rock Point was despatched to the CSIRO, Kensington, WA for possible $^{40}\text{Ar}/^{39}\text{Ar}$ dating. A hornblende (kaersutite) separate was prepared but due to problems with the $^{40}\text{Ar}/^{39}\text{Ar}$ instrumentation it was decided to first obtain a K/Ar age. The result, 514.5 \pm 10.4 Ma (Table 23; H. Zwingmann, 14th May 2013) is virtually identical to U-Pb SHRIMP ages of rocks associated with the Tyennan Orogeny (e.g. Heazlewood Tonalite $\sim 513.6 \pm 5.0$ Ma, amphibolite from the Forth Metamorphic Complex, 514.1 \pm 4.6 Ma; Black et al. 1997). Although it is unlikely that the kaersutite is a metamorphic mineral, it appears that its K/Ar systematics have been completely re-set during Cambrian metamorphism. It was therefore decided that proceeding with $^{40}\text{Ar}/^{39}\text{Ar}$ analysis on the kaersutite would be futile.

12.0 $^{40}\text{Ar}/^{39}\text{Ar}$: analytical procedure

Sample C112167A was crushed and screened at MRT and dispatched to N. Allen for biotite separation. The crushed sample was washed to remove abundant very

small electrostatically adhering particles, and then passed through several separation stages, including both magnetic lift in a field gradient, and with a superimposed rotating field at 40 to 200Hz. The final concentrate was despatched to the School of Earth Sciences, University of Melbourne.

The supplied biotite mineral separate (~0.5 mm grain-size) was of high purity. A subset of thick, euhedral to subhedral grains was hand-picked using a binocular microscope, taking care to avoid grains with obvious inclusions. Selected grains were then rinsed in acetone, weighed and wrapped in an aluminium foil envelope, and placed into a quartz glass vial together with aliquots of the flux monitor MD-2 biotite (Age = 99.125 ± 0.039 Ma; Phillips et al., 2017). The package (UM#83) was then encapsulated in a secondary glass vial and irradiated in the CLICIT facility of the Oregon State University TRIGA Reactor for 60 MWh.

Following irradiation and cooling, $^{40}\text{Ar}/^{39}\text{Ar}$ analyses were undertaken in the Noble Gas laboratory at the University of Melbourne. Step-heating was undertaken on aliquots of ~10 biotite grains each using a multi-collector Thermo Fisher Scientific ARGUSVI mass spectrometer linked to a stainless steel gas extraction/purification line and a Photon Machines Fusions 10.6 CO₂ laser system (e.g. Phillips and Matchan, 2013). Mass discrimination was monitored by analysis of standard air volumes, assuming the air argon isotopic composition of Lee et al. (2006). Grains were outgassed at 0.5% laser power (6 mm homogenised beam; 0.12 W) to remove absorbed argon. Step-heating experiments were then conducted using the 1 mm beam (range of 1–10% laser power), heating the sample for 2 min, followed by 3 min of gettering (total 5 min gettering time). Blanks were monitored routinely and subtracted from measurements. Blanks were negligible compared to sample signals (<2.0 fA ^{40}Ar blank compared to typical sample values of 400–1200 fA).

Analytical results are summarised below and detailed in Table 24. Unless otherwise stated, reported uncertainties are two-sigma. Inclusion of errors in the J-value and age of MD-2 biotite have a negligible impact on uncertainties. Decay constants are those of Steiger and Jäger (1977). The $^{40}\text{Ar}/^{39}\text{Ar}$ dating technique is described in detail by McDougall and Harrison (1999).

13.0 $^{40}\text{Ar}/^{39}\text{Ar}$: Geochronological results

Age spectra for the two aliquots are highly similar, showing increasing apparent ages of ~610–730 Ma for the low- to mid-temperature heating steps, and concordant ages for subsequent heating steps (Figure 21). The high-temperature steps (3.5–10% laser power; representing 44.2% of the total ^{39}Ar) of aliquot BR-2 yielded

a weighted mean age of 734.2 ± 0.6 Ma (2σ ; MSWD = 1.4, $p = 0.20$). The high-temperature steps (4.5–10% laser power; representing 33.4% of the total ^{39}Ar) of aliquot BR-3 yielded an identical weighted mean age of 733.6 ± 0.5 Ma (2σ ; MSWD = 0.75, $p = 0.56$). The weighted mean value of the two weighted means values is 733.8 ± 0.4 Ma (2σ).

The ascending portion of the age spectrum likely results from a combination of recoil effects, in vacuo breakdown of hydrous structures (e.g. Gaber et al., 1988) and partial thermal resetting, such that the young ages calculated for the low-temperature steps are not considered to have any geological meaning. The concordance of high-temperature age results across the two aliquots suggests negligible isotopic disturbance for gas released in these heating steps. The weighted mean of the high-temperature results, 733.8 ± 0.4 Ma (2σ), is interpreted to reflect the cooling age of the biotite below its closure temperature (ca. 300°C; Harrison et al., 1985); which should be equivalent to the crystallization age (i.e., magma emplacement age) given that the host rock is a shallow-level intrusive.

14.0 Discussion

The 733.8 ± 0.4 Ma magma emplacement age for the Cooee Dolerite provides a tight minimum depositional age for the adjacent Oonah Formation, since peperitic contacts indicate that the dolerite was intruded into wet unconsolidated sediments.

The Oonah Formation crops out semi-continuously on the northwest coast from Somerset to Penguin. Inland of Burnie, it is largely obscured by Cenozoic basalt and Permo-Carboniferous strata, but several small inliers leave little doubt that it is continuous beneath thin cover to the upper Arthur River area. From there, lithologically similar sequences can be traced southward, through the Heazlewood River area to the type area of the Oonah Formation near Zeehan. Alkali basalts, chemically similar to the Cooee Dolerite, are intercalated with the Oonah Formation at Sulphur Creek, Somerset, and near Zeehan (Montana Volcanics) and a small alkali dolerite dyke intrudes it in the upper Arthur River (see review of Calver and Everard 2014 and references therein).

Correlates of the Oonah Formation form fault-bounded inliers near Mt Bischoff (Groves and Solomon, 1964; Williams in Seymour, 1989; Cumming et al., 2016), in the Coldstream River- Ramsay River area NW of Rosebery (Collins et al., 1981; Brown, 1986); near Dundas (Turner, 1979; Mulder et al., 2020) and in the Modder River south of Macquarie Harbour (Turner, 1989; McClenaghan and Findlay, 1993). On the north coast, east of Port Sorell, the Badger Head Group (Gee & Legge, 1979) is also now correlated with the Oonah Formation (Black et al., 2004).

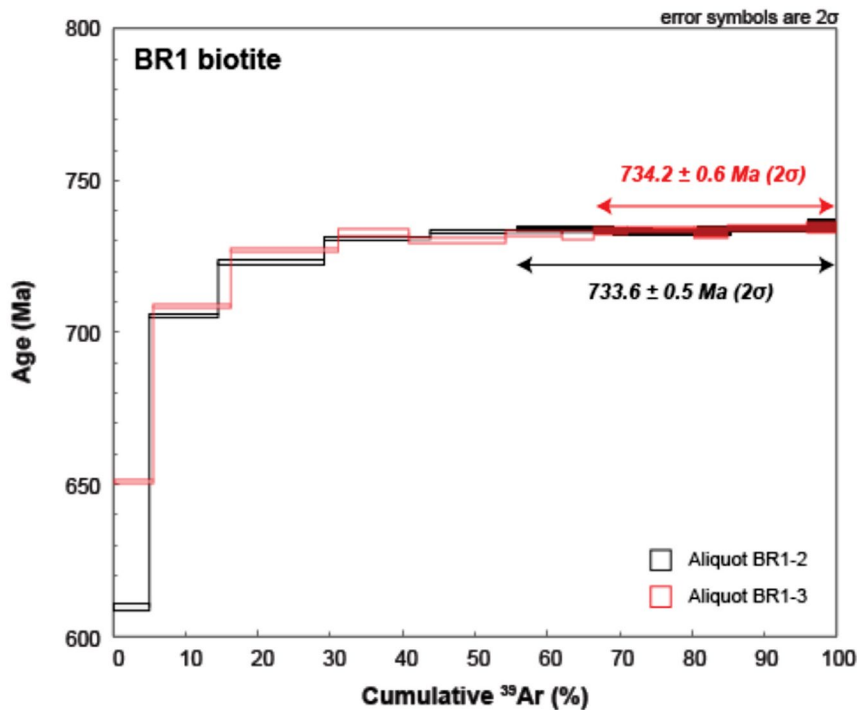


Figure 21. $^{40}\text{Ar}/^{39}\text{Ar}$ age spectra (plotted using Ludwig 2012) for biotite aliquots BR1-2 and BR1-3 (10 grains each) from sample C112167A. Weighted mean age results for concordant high-temperature steps are shown.

Although no intercalated lavas, (other than the Montana Volcanics) are known in these sequences, correlation has in most cases been supported by detrital zircon studies (Black et al., 2004; Cumming et al., 2016; Mulder et al., 2018, 2020). All samples studied display a major peak at ~ 1770 - 1800 Ma, usually accompanied by a subsidiary peak at ~ 1450 Ma and a range of minor peaks between ~ 1100 and ~ 3150 Ma. Unequivocal Neoproterozoic detrital zircons have, however, only been reported from Burnie (Mulder et al., 2018). No detrital zircon data has been reported from the Coldstream-Ramsay or Modder River inliers.

Turner (1992) and Turner et al. (1992) suggested that the Oonah Formation represents the distal turbiditic equivalents of the Donaldson Formation near Corinna, and Forest Conglomerate and Quartzite near Smithton; these are Neoproterozoic units near the base of the Ahrberg and Togari Groups respectively. This coeval relationship is supported by the similarity of their detrital zircon patterns to that of the Oonah Formation (Black et al., 2004; Mulder et al., 2018) and is consistent with the radiometric ages obtained from the Cooe Dolerite (Mulder et al., 2018, and herein).

15.0 Conclusion

The Neoproterozoic (Tonian) $^{40}\text{Ar}/^{39}\text{Ar}$ age of 733.8 ± 0.4 Ma (2σ) is interpreted as that of the crystallisation of the dolerite, and is fully compatible with, but more precise than, previous K/Ar (biotite) and U-Pb (apatite) age determinations. It further demonstrates that the enclosing Oonah Formation is coeval with, and a likely distal turbiditic facies equivalent of, the basal units of the Togari Group and Ahrberg Group.

16.0 Acknowledgements

MRT technical staff including T. Coyte, L. Unwin and R. S. Woolley assisted with the laboratory work. A. McNeill critically reviewed the manuscript, which was prepared for publication by C. Large.

17.0 References

- Armbruster T., Bonazzi P., Akasaka M., Bermanec V., Chopin C., Heuss-Assbichler S., Liebcher A., Menchetti S., Pan Y. and Pasero M. 2006. Recommended nomenclature of epidote-group minerals. *European Journal of Mineralogy* 18, 551-567.
- Bailey S. W. 1980. Summary of recommendations of AIPEA nomenclature committee on clay minerals. *American Mineralogist* 65, 1-7.
- Bayliss P. 1975. Nomenclature of the trioctahedral chlorites. *Canadian Mineralogist* 13, 178-180.
- Black L. P., Seymour D.B., Corbett K.D., Cox S.E., Streit J.E., Bottrill R.S., Calver C.R., Everard J.L., Green G.R., McClenaghan M.P., Pemberton J., Taheri J. and Turner N.J. 1997. Dating Tasmania's oldest geological events. Australian Geological Survey Organisation Record 1997/15.
- Black L. P., Calver C. R., Seymour D. B. and Reed A. 2004. SHRIMP U-Pb detrital zircon ages from Proterozoic and Early Palaeozoic sandstones and their bearing on the early geological evolution of Tasmania. *Australian Journal of Earth Sciences* 51, 885-900.
- Brown A. V. 1986. Geology of the Dundas - Mt Lindsay - Mt Youngbuck region. *Tasmanian Geological Survey Bulletin* 62, 221pp. Tasmania Department of Mines.
- Brown A. V. 1989 (compiler). Geological Survey Explanatory Report, Geological Atlas 1:50,000 Series, Sheet 21 (7916S), *Smithton*. Tasmania Department of Mines.
- Calver C. R. and Everard J. L. 2014. Cooee Dolerite and related rocks, in Corbett K. D., Quilty P. G. and Calver C. R. (eds.). The Geological Evolution of Tasmania. *Geological Society of Australia Special Publication* 24, p.54-58.
- Coleman R. C. 1974. *The Savage River magnetite deposits*. Ph. D. thesis, University of Tasmania.
- Coleman R.C. 1976. Savage River magnetite deposits, in Knight C. L. (ed.), *Economic geology of Australia and Papua New Guinea*, p. 598-604. Australasian Institute of Mining and Metallurgy.
- Collins P. L. F., Gulline A. B. and Williams E. 1981. Geological Survey Explanatory Report, Geological Atlas 1 mile Series, Sheet 44 (8014N), *Mackintosh*. Tasmania Department of Mines.
- Crawford A. J. and Berry R. F. 1992. Tectonic implications of Late Proterozoic- Early Palaeozoic igneous rock associations in western Tasmania. *Tectonophysics* 214, 37-56.
- Crook K. A. W. 1979. Tectonic implications of some field relations of the Adelaidean Cooee Dolerite, Tasmania. *Journal Geological Society of Australia* 26, 353-361.
- Cumming G., Everard J. L. and Meffre S. 2016. Age constraints and provenance of the Mount Bischoff inlier and the Luina Group: evidence from LA-ICPMS U-Pb dating of detrital zircon. *Tasmanian Geological Survey Record* 2016/04.
- Everard J. L., Seymour D. B., Reed A. R., McClenaghan M. P., Green D. C. and Calver C. R. 2007. Regional geology of the Southern Smithton Synclinorium. Explanatory Report for the Roger, Sumac and Dempster 1:25 000 scale geological map sheets, far northwestern Tasmania, *1:25 000 Scale Digital Geological Map Series Report 2*. Mineral Resources Tasmania.
- Gaber L. J., Foland K. A. and Corbato C. E. 1988. On the significance of argon release from biotite and amphibole during $^{40}\text{Ar}/^{39}\text{Ar}$ vacuum heating. *Geochimica Cosmochimica Acta* 52, 2457-2465.
- Gee R. D. 1977. Geological Survey Explanatory Report, Geological Atlas 1 mile series. Sheet 28 (8015N), *Burnie*. Tasmania Department of Mines.
- Gee R. D. and Legge P. J. 1977. Geological Survey Explanatory Report, Geological Atlas 1 mile series. Sheet 30 (8215N), *Beaconsfield* (2nd edition). Tasmania Department of Mines.
- Groves D. I. & Solomon M. 1964. The geology of the Mt Bischoff district. *Papers and Proceedings of the Royal Society of Tasmania* 98, 1-22.
- Harrison T.M., Duncan, I. and McDougall I. 1985. Diffusion of Ar-40 in biotite- temperature, pressure and compositional effects. *Geochimica et Cosmochimica Acta* 49, 2461-2468.
- Hawthorne F. C., Oberti R., Harlow G. E., Maresch W. V., Martin R. F., Schumacher J. C. and Welch M. D. 2012. Nomenclature of the amphibole supergroup. *American Mineralogist* 97, 2031-2048.
- Hess J. C. and Lippolt H. J. 1994. Compilation of K-Ar measurements on HD-B1 standard biotite, in Odin. G. S. 1994. Phanerozoic time scale. Bull. Lias. Inform., *IUGS Subcommission on Geochronology* 12, Paris, p. 19-23.
- Leake B.E. (Compiler). 1997. Nomenclature of amphiboles: Report of the Subcommittee on Amphiboles of the International Mineralogical Association, Commission on New Minerals and Mineral Names. *American Mineralogist* 82, 1019 - 1037.
- Lee J.-Y., Mart K., Severinghaus J., Kawamura K., Yoo S.-S., Lee J. and Kim J. 2006. A redetermination of

- the isotopic abundances of atmospheric Ar. *Geochimica et Cosmochimica Acta* 70, 4507–4512.
- Liou J. G. 1971. Synthesis and stability relations of prehnite, $\text{Ca}_2\text{Al}_2\text{Si}_3\text{O}_{10}(\text{OH})_2$. *American Mineralogist* 56, 507-531.
- Ludwig, K. 2012. User's Manual for Isoplot 3.75. A Geochronological Toolkit for Microsoft Excel. *Special Publication 5*, Berkeley Geochronology Center, Berkeley, California 75.
- McClenaghan M. P. and Findlay R. H. 1993. Geological Survey Explanatory Report, Geological Atlas 1:50 000 series, Sheet 64 (7913S), *Macquarie Harbour*. Tasmania Department of Mines
- McDougall I. and Leggo P. J. 1965. Isotopic age determinations on granitic rocks from Tasmania. *Journal of the Geological Society of Australia* 12, 295-332.
- McDougall I. and Harrison T.M. 1999. *Geochronology and Thermochronology by the $^{40}\text{Ar}/^{39}\text{Ar}$ Method*, 2nd edition. Oxford University Press, New York.
- Morimoto N. 1988: Nomenclature of pyroxenes. *American Mineralogist* 73, 1123 - 1133.
- Mulder J. A., Berry R. F., Halpin J. A., Meffre S. and Everard J. L. 2018. Depositional age and correlation of the Oonah Formation: refining the timing of Neoproterozoic basin formation in Tasmania. *Australian Journal of Earth Sciences* 65:3, 391-407.
- Mulder J. A., Everard J. L., Cumming G., Meffre S., Bottrill R. S., Merdith A. S., Halpin J. A., McNeill A. W. and Cawood P. A. 2020. Neoproterozoic opening of the Pacific Ocean recorded by multi-stage rifting in Tasmania, Australia. *Earth-Science Reviews* 201, 1-29.
- O'Neill H. St.C. 2016. The smoothness and shapes of chondrite-normalised rare-earth element patterns in basalts. *Journal of Petrology* 57 (8), 1463 - 1508.
- Pasero M., Kampf A. R., Ferraris C., Pekov I. V., Rakovan J. & White T. J. 2010. Nomenclature of the apatite supergroup minerals. *European Journal of Mineralogy* 22, 163-179.
- Phillips D. and Matchan E.L. 2013. Ultra-high precision $^{40}\text{Ar}/^{39}\text{Ar}$ ages for Fish Canyon Tuff and Alder Creek Rhyolite sanidine: New dating standards required? *Geochimica et Cosmochimica Acta* 121, 229–239.
- Phillips D., Matchan E.L., Honda M. and Kuiper K.F. 2017. Astronomical calibration of $^{40}\text{Ar}/^{39}\text{Ar}$ reference minerals using high-precision, multi-collector (ARGUSVI) mass spectrometry. *Geochimica et Cosmochimica Acta* 196 (1), 351–369.
- Rieder M. (comp.).1998. Nomenclature of the micas. *Canadian Mineralogist* 36, 905-912.
- Seymour D. B. 1989 (compiler). Geological Survey Explanatory Report, Geological Atlas 1:50 000 Series, Sheet 36 (8015N), *St Valentines*. Tasmania Department of Mines.
- Spry A. 1957. The Precambrian rocks of Tasmania, Part I. Dolerites of the north-west coast of Tasmania. *Papers and Proceedings of the Royal Society of Tasmania* 91, 81-93.
- Spry A.H. 1958. Some observations on the Jurassic dolerite of the Eureka cone sheet near Zeehan, Tasmania, in: Carey S.W. (ed). *Dolerite, a Symposium*. University of Tasmania, Hobart
- Spry A. H. 1962. The Precambrian rocks. In: Spry A. and Banks M. R. (eds.). The Geology of Tasmania. *Journal of the Geological Society of Australia* 9, 107-126.
- Steiger R.H. and Jäger E. 1977. Subcommission on geochronology: Convention on the use of decay constants in geo- and cosmochronology. *Earth and Planetary Science Letters* 36, 359-362.
- Turner N. J. 1979. The boundary relationship of the Concert Schist and the Oonah Quartzite and Slate at Dundas. *Papers & Proceedings of the Royal Society of Tasmania* 113, 15–20.
- Turner N. J. 1989. Precambrian, in: Burrett C. F. and Martin E. L. (eds.). Geology and Mineral Resources of Tasmania. *Geological Society of Australia Special Publication* 15, p. 5-46.
- Turner N. J. 1992. *Corinna 1:50 000 Geological Map: Field guide to selected rock exposures*. Tasmania Department of Mines Report 1992/06.
- Turner N. J., Black L. P. and Kamperman M. 1998. Dating of Neoproterozoic and Cambrian orogenies in Tasmania. *Australian Journal of Earth Sciences* 45, 789-806.
- Turner N. J., Bottrill R. S., Crawford A. J. and Villa I. 1992. Geology and prospectivity of the Arthur Mobile Belt, in: Tasmania: An Island of Potential; New perspectives on mineral exploration. *Tasmanian Geological Survey Bulletin* 70, 227-233.
- Vicary M. J. (comp.) 2004. Digital geological atlas 1:25000 scale series, Sheet 4045, *Burnie*. Mineral Resources Tasmania.
- Winkler H. G. F. 1979. *Petrogenesis of Metamorphic Rocks* (Fifth Edition). Springer-Verlag.

APPENDIX 1

Tables 1 - 24



File Download

Table 1. Sample location and treatment, Cooee Dolerite.														
Reg No	Field No	Locality	mEagd66	mNagd66	mEgda94	mNgda94	Acc±	ORIG	TS	CA	χ^*	Analysis No	lab	comments
C112161	C112161	Foreshore, Parklands			406599	5455809	5	CJJ	Y	Y	0.38		MRT	
C112162	C112162	Foreshore, Parklands			406542	5455766	5	CJJ	Y	Y	0.45		MRT	
C112163	C112163	Foreshore, Parklands			406498	5455766	5	CJJ	Y	Y	0.43		MRT	
C112164	C112164	Foreshore, Parklands			406424	5455711	5	CJJ	Y	Y	0.44		MRT	
C112165	C112165	Foreshore, Parklands			406327	5455711	5	CJJ	Y	Y	1.47		MRT	
C112167	C112167	Foreshore, Parklands			406541	5455761	5	CJJ	Y	Y	0.38		MRT	
C112168	C112168	Foreshore, Parklands			406540	5455764	5	CJJ	Y	Y	0.45		MRT	
R012624	DBJ 90	Foreshore, Parklands	406460	5455550	406572	5455733	10	JLE	Y	Y		20070001	MRT	
R012625	DBJ 91	Foreshore, Parklands	406400	5455540	406512	5455723	10	JLE	Y	Y	0.49	20070002	MRT	
R012626	DBJ 92	Foreshore, Parklands	406330	5455520	406442	5455703	10	JLE	Y	Y	0.52	20070003	MRT	
R012627	DBJ 93	~130m E of Red Rock Point	406110	5455590	406222	5455773	10	JLE	Y	Y		20070004	MRT	
R012686	DBJ552	Red Rock Point, Cooee	406049	5455676	406161	5455859	10	JLE	Y	-		-	-	not analysed
R004580	CDL	N of end of West Beach	407590	5455380	407702	5455563	10	JLE	Y	Y	0.52	20070385	MRT	
R016517	ABS102	West end of West Beach	407550	5455300	407662	5455483	20	AVB	Y	Y		883172	DoM	
R016518	ABS103	E of Parsonage Point	407560	5455410	407672	5455593	20	AVB	Y	Y		883173	DoM	sill
R016519	ABS104	E of Parsonage Point	407550	5455440	407662	5455623	20	AVB	Y	Y		883174	DoM	dyke
R016520	ABS105	Parsonage Point	407360	5455560	407472	5455743	20	AVB	Y	Y		883175	DoM	sill
R016521	ABS106	Foreshore, Parklands	406390	5455570	406502	5455753	20	AVB	Y	Y		883176	DoM	dyke
R016522	ABS107	Red Rock Point	406000	5455680	406112	5455863	20	AVB	Y	Y		883177	DoM	sill
93220001	LB34	N of end of West Beach	407576	5455391	407688	5455574	10	LPB	na	Y			AGSO	
93220002	LB45	N of end of West Beach	407601	5455386	407713	5455569	10	LPB	na	Y			AGSO	
95220015	LB48	near Parsonage Point (?)	407700#	5455786#	407812#	5455969#	500	LPB	na	Y			AGSO	Black et al. (1997)
95220019	LB43	E end of foreshore, Parklands	406932	5455384	407044	5455567	10	LPB	na	Y			AGSO	Black et al. (1997)
4864	-	Foreshore, Parklands	406500	5455500	406612	5455683	500	AHS	na	Y			DoM	Spry (1957)
4852	-	beach west of Hilder St	406200	5455600	406312	5455783	200	AHS	na	Y			DoM	Spry (1957)
		#coordinates plot offshore, incorrect in reference												
		# magnetic susceptibility, x 10 ⁻³ SI												

Table 2. Whole rock (XRF) analyses of the Cooee Dolerite													
Reg No	C112161	C112162	C112163	C112164	C112165	C112167	C112168	R012624	R012625	R012626	R012627	R004580	R016517
Field No	-	-	-	-	-	-	-	DBJ 90	DBJ 91	DBJ 92	DBJ 93	CDL	ABS102
SiO ₂ (%)	45.04	45.93	44.66	46.11	47.16	46.03	45.94	47.30	44.62	45.70	46.10	49.87	43.50
TiO ₂	1.89	2.08	1.87	2.09	3.20	2.07	2.14	2.80	1.77	2.42	3.36	3.20	2.47
Al ₂ O ₃	18.68	18.47	19.07	17.38	18.12	17.97	17.86	17.72	19.03	15.58	17.65	18.88	18.48
Fe ₂ O ₃	6.60*	8.18*	6.72*	6.27*	10.45*	7.08*	6.96*	1.06	0.63	0.80	1.09	1.30	0.54
FeO								7.00	5.58	5.39	7.89	8.20	11.25
MnO	0.16	0.19	0.16	0.15	0.22	0.19	0.19	0.16	0.13	0.13	0.18	0.14	0.23
MgO	7.33	6.92	7.37	7.17	3.82	7.01	7.46	5.65	7.66	7.40	4.00	4.90	6.68
CaO	12.62	8.90	11.59	13.60	6.53	10.36	11.06	7.73	11.02	15.18	8.36	1.20	2.86
Na ₂ O	2.85	3.37	2.92	2.53	5.34	2.92	2.83	4.36	2.82	2.68	3.34	6.22	4.03
K ₂ O	0.96	1.88	1.09	1.26	1.02	1.92	1.65	1.50	1.50	0.29	3.42	0.56	1.40
P ₂ O ₅	0.18	0.20	0.18	0.15	0.44	0.40	0.19	0.62	0.39	0.39	0.86	0.77	0.59
H ₂ O+								3.05	4.17	3.28	2.55	4.31	5.35
H ₂ O-													
CO ₂								0.43	0.23	0.24	0.06	0.10	1.49
C tot	0.00	0.20	0.00	0.00	0.10	0.00	0.00						
SO ₃ tot								0.01	0.01	0.01	0.04	0.02	0.33
S	0.06	0.05	0.05	0.05	0.22	0.06	0.05						
LOI	3.69	4.06	4.24	3.34	2.80	3.66	3.55						
rest													
TOTAL	100.24	100.18	99.87	100.05	99.10	99.61	99.83	99.39	99.56	99.49	98.90	99.67	99.2
Mg#(0.20)	72.19	66.42	71.94	72.78	46.08	69.83	71.47	59.92	72.38	71.81	48.67	52.26	54.49
Be (ppm)													
F													
S													
Sc	26	30	24	40	10	42	31	24	37	76	18	20	36
V	184	203	174	226	239	202	214	185	145	240	230	280	290
Cr	184	149	238	209	31	164	147	-5	220	390	-5	-5	120
Mn													
Co	33	34	37	29	33	29	34	34	37	32	36	39	33
Ni	103	97	118	79	13	89	92	46	135	81	17	30	47
Cu	34	44	26	37	55	39	35	100	25	24	41	30	36
Zn	60	52	56	100	122	177	76	64	71	52	75	70	50
Ga	16	16	16	15	20	17	17	20	19	17	21	21	14
Ge													
As	<3	<3	<3	<3	<3	2	<3	<20	<20	<20	<20	<20	<22
Se													
Rb	29	52	32	31	30	54	47	50	51	9	76	20	46
Sr	737	986	1016	811	855	832	776	1250	750	870	1250	300	230
Y	21	22	21	21	32	23	22	39	23	30	42	39	32
Zr	180	195	172	175	335	198	194	350	195	260	330	360	270
Nb	49	54	47	43	112	51	53	98	53	58	115	150	71
Mo	3	3	3	3	6	2	3	<5	<5	<5	5	<5	
Ag													
Sn	<2	<2	<2	<2	3	<2	<2	<9	<9	<9	<9	<9	<8
Sb	<2	<2	<2	<2	<2	<2	<2						
Cs	5	2	2	<3	5	<3	2						
Ba	556	1652	583	1974	435	2151	1720	2800	590	310	6400	430	450
La(xrf)	30	32	32	20	69	21	24	48	27	27	57	57	44
Ce(xrf)	57	66	65	54	130	59	71	66	62	63	<28	115	91
Nd(xrf)	30	27	30	28	55	21	31	43	23	42	39	52	46
Hf													
Ta													
W	<2	2	2	2	3	<2	<2	<10	<10	<10	<10	52	
Pb	13	12	8	35	43	68	15	<10	<10	<10	<10	<10	<11
Bi	<1	<1	<1	<1	1	<1	<1	<5	<5	<5	<5	<5	<6
Th	9	8	8	5	12	7	8	<10	<10	<10	<10	11	<11
U	2	3	2	2	2	1	2	<10	<10	<10	<10	<10	<13
*Total iron as Fe2O3													
Mg#(0.20)- molar 100Mg/(Mg + Fe ^{II}) calculated at Fe ₂ O ₃ /FeO = 0.20													

Table 2 (cont.). Whole rock (XRF) analyses of the Coee Dolerite												
Reg No	R016518	R016519	R016520	R016521	R016522	93220001	93220002	95220015	95220019	40412	-	-
Field No	ABS103	ABS104	ABS105	ABS106	ABS107						4864	4861*
SiO ₂ (%)	37.20	47.67	44.48	47.40	47.79	45.41	48.04	46.58	45.52	47.90	44.44	58.32
TiO ₂	2.01	3.21	2.45	2.88	2.65	2.67	2.76	3.54	2.83	3.29	3.00	0.41
Al ₂ O ₃	16.49	17.35	18.30	18.00	17.77	17.71	16.55	16.69	17.12	17.40	17.97	15.03
Fe ₂ O ₃	0.54	1.01	1.29	0.86	1.33	0.89	0.72	1.21	0.96		1.74	0.96
FeO	12.41	8.32	9.82	8.48	8.84	7.33	7.48	8.03	8.19	10.10#	8.32	2.60
MnO	0.46	0.17	0.26	0.22	0.10	0.14	0.13	0.13	0.17	0.25	0.22	0.11
MgO	7.13	4.17	5.83	4.53	8.06	8.17	5.07	4.00	7.11	4.92	4.74	4.36
CaO	4.62	4.89	3.11	6.60	1.03	5.56	3.74	6.49	6.34	3.30	9.42	8.46
Na ₂ O	2.42	5.51	4.41	4.36	4.63	3.63	6.89	5.61	3.54	4.16	2.86	3.24
K ₂ O	2.15	0.47	1.53	1.47	0.36	2.27	0.14	0.55	2.16	2.31	3.04	1.41
P ₂ O ₅	0.52	0.85	0.65	0.76	0.63	0.64	0.71	0.87	0.61	0.74	0.72	0.12
H ₂ O+	6.04	3.70	4.79	3.39	5.19						3.53	5.04
H ₂ O-											0.26	0.14
CO ₂	6.52	1.03	2.02	0.35	0.25							
C tot												
SO ₃ tot	0.14	0.04	0.92	0.08	0.60							
S												
LOI						4.85	7.39	5.95	5.06	2.48		
rest						0.76	0.41	0.25	0.35			
TOTAL	98.65	98.39	99.86	99.38	99.23	100.03	100.03	99.90	99.96	96.85	100.26	100.20
Mg#(0.20)	53.77	48.73	52.76	50.73	62.81	67.88	56.75	47.99	62.29	50.61	50.21	72.58
Be (ppm)						3.0	3.0		2.0			
F								1200	1300			
S						770	790	80	710			
Sc	37	24	32	28	33	32.0	32.0	21.5	47.5	30		
V	210	260	240	250	240	270	255	239	267			
Cr	330	6	115	6	165	151	91	3	113	17		
Mn						1401	1194					
Co	52	31	36	38	41							
Ni	220	12	51	19	79	57	28	14.5	41	28		
Cu	24	46	39	65	5	37	57	75	49			
Zn	31	53	83	70	60	59	34	69	67			
Ga	13	13	13	15	15	16	16	18.2	16.5			
Ge						2	1	2.2	1.9			
As	<22	<22	<22	<22	<22	3	2	0.8	0.8			
Se						<1	<1					
Rb	74	14	47	55	17	71	5	16	67	6		
Sr	52	360	270	890	79	768	51	474	454	851		
Y	32	39	36	40	36	34	37	40	34.5	36		
Zr	210	310	270	310	270	236	272	338	274	283		
Nb	54	93	77	87	77	75	92	104.3	67.8	85		
Mo						3	4	1.5	2.3			
Ag						2	2	<0.5	<0.5			
Sn	<8	<8	<8	<8	<8	2	4	2.5	2			
Sb								0.1	<0.1			
Cs						12	3	1.9	20.6			
Ba	370	600	640	820	125	1996	89	519	1180	5299		
La(xrf)	45	68	66	49	66	40	55	62.6	43.4			
Ce(xrf)	79	140	110	110	125	79	106	122.7	88.1			
Nd(xrf)	34	58	41	45	48	37	43	50.1	38.8			
Hf						7	8	6.9	6.5			
Ta						3	5	7.1	4.9			
W												
Pb	<11	<11	<11	<11	<11	6	3	1.5	6			
Bi	<6	<6	<6	<6	<6	<2	<2	<0.1	<0.1			
Th	<11	<11	<11	<11	14	7	7	8.8	6.1			
U	<13	<13	<13	<13	<13	2	1	1.9	1.4			

Table 3. Summary of petrography of Cooee Dolerite (samples sorted by Mg#)										
Reg No	Field No	Mg#	plag	cpx	olivine	hbl	biotite	FeTiOx	apatite	Notes
R012686	DBJ552	-	A	X	A?		X	P	X	
C112164	C112164	72.78	A	X	A		X	X	X	prehnite
R012625	DBJ 91	72.38	A	X	A		X	P	X	
C112161	C112161	72.19	A	X	A		X	X	X	
C112163	C112163	71.94	A	P	A		X	X	X	
R012626	DBJ 92	71.81	P	X	A		X	P	X	albite
C112168	C112168	71.47	A	X	A		X	X	X	
C112167	C112167	69.83	A	X	A		X	X	X	
C112162	C112162	66.42	A	X	A		X	P	X	
R016522	ABS107	62.81	A	A?	?	A		A	X	severely altered
R012624	DBJ 90	59.92	P	P	A		X	P	X	albite
R016517	ABS102	54.49	A	A?	A?		X	P	X	fine-grained
R016518	ABS103	53.77	A	A?	A?	A	tr	A	X	altered
R016520	ABS105	52.76	A	A?		A	P	A	X	severely altered
R004580	CDL	52.26	A			A	tr	A	X	altered
R016521	ABS106	50.73	P	P		A?		A	X	albite
R016519	ABS104	48.73	A			A	tr	A	X	albite
R012627	DBJ 93	48.67	A	P		P	X	P	X	
C112165	C112165	45.08	A			P	X	A	X	act, epidote

A= altered; P- partly altered; X-present ; tr-trace

Table 4: XRD Analysis Report

Client: C. Jackman
Sample Source: Cooee
MRT Job Number: LJN2017/081
Analysis: Approximate Mineralogy
Method: X-Ray Diffraction
Analyst: R. N. Woolley
Date: 9th August 2017

Results (approx wt %)

Reg. No.	C112167A	C112167B	C112168D
35%-50%		Albite	Albite
25%-35%	Albite		Chlorite
15%-25%	Mica ¹ , Chlorite, Clinopyroxene	Chlorite, Clinopyroxene	Clinopyroxene
10%-15%			
5%-10%	Pumpellyite	Mica ²	Mica ²
2%-5%	Epidote	Pumpellyite, Epidote	Pumpellyite, Epidote
<2%	Ilmenite	Ilmenite	Ilmenite

Peak overlap may interfere with identifications and quantitative calculations
Amorphous material and minerals present in trace amounts may not be detected

¹ both trioctahedral and dioctahedral Mica present

² predominantly dioctahedral Mica

Table 5. Biotite analyses																																		
Sample	Primary biotite																																	
Sample	C112167A														R012627																			
Site	2	2	2	2	2	3	3	3	3	4	4	4	6	6	6	6	3	3	3	3	10	10	10	13	13	13	13	16	16	17	19	19	19	
Analysis	231	232	233	234	242	246	247	248	249	258	259	260	270	271	272	277	24	25	26	27	122	123	124	172	173	175	176	200	201	206	207	208	213	
SiO2	36.154	35.149	35.812	36.112	35.598	34.229	34.101	34.871	34.593	33.865	34.079	35.063	34.186	33.737	34.400	34.208	32.218	32.368	32.389	32.325	33.117	33.138	32.689	36.047	35.919	35.705	33.010	34.550	33.972	35.170	34.529	34.614	34.357	
TiO2	5.705	5.571	6.205	6.055	6.222	6.322	6.822	7.223	7.089	5.721	5.671	7.273	7.189	7.306	6.989	7.022	5.821	6.138	6.172	5.838	5.838	5.888	5.438	6.605	6.489	5.755	7.206	7.473	6.756	6.989	6.922	6.205	5.755	
Al2O3	14.813	14.058	14.983	14.473	14.530	13.850	14.265	15.342	15.305	13.699	13.831	13.661	14.832	15.116	14.606	14.776	12.735	12.943	12.981	12.943	13.566	13.491	13.718	12.716	12.093	12.055	13.359	14.681	13.888	14.247	13.812	13.774	13.264	
FeOt	16.724	20.236	17.316	18.191	17.162	19.889	16.686	15.850	15.824	21.767	22.475	22.552	14.769	14.756	14.537	14.306	23.851	23.684	22.552	22.308	24.160	23.311	22.668	23.221	24.225	27.042	21.690	22.153	22.076	21.960	24.147	25.460	28.907	
MnO	-	-	-	-	-	-	-	-	-	-	-	-	-	-	-	-	0.452	0.374	-	0.413	-	-	0.413	-	0.439	-	-	-	-	-	0.426	0.542		
MgO	13.399	10.364	12.205	12.039	12.238	10.547	12.221	12.636	12.371	9.286	9.452	8.441	13.183	12.918	13.067	12.951	6.102	5.953	6.683	6.948	6.882	6.948	7.031	8.059	7.363	5.240	7.197	8.109	7.744	8.640	6.849	6.500	4.660	
CaO	-	-	-	-	-	-	-	-	-	-	-	-	-	-	-	-	-	-	-	-	-	-	-	-	-	-	-	-	-	-	-	-	-	-
BaO	-	-	-	-	1.050	-	1.172	2.255	2.333	-	-	-	2.099	2.255	2.333	2.568	-	-	-	-	-	-	-	-	-	-	-	-	-	-	-	-	-	-
Na2O	0.661	1.024	0.701	0.822	0.890	0.607	0.634	0.836	0.890	-	-	-	0.782	0.768	0.917	0.863	-	0.580	0.674	-	-	-	-	-	-	-	0.674	0.000	0.566	0.687	-	0.499	0.431	
K2O	8.480	8.360	8.492	8.372	8.179	8.372	8.203	7.770	7.818	7.685	7.673	8.673	7.685	7.589	7.758	7.565	8.023	7.938	7.950	7.734	8.408	8.432	8.167	8.444	8.396	8.408	7.722	8.601	8.444	8.191	8.372	8.685	8.806	
Cl	-	0.190	-	-	-	-	-	-	-	-	-	-	-	-	-	-	0.130	-	-	-	0.120	-	-	-	-	-	-	-	-	-	-	-	-	
TOTAL	95.937	94.953	95.715	96.064	95.868	93.815	94.105	96.782	96.222	92.024	93.182	95.663	94.726	94.445	94.607	94.258	88.881	90.056	89.775	88.215	92.384	91.208	89.710	96.086	94.484	94.644	90.857	95.567	93.446	95.885	94.631	96.163	96.723	
<i>Cations on the basis of 10 oxygens, 2 (OH)</i>																																		
Si	2.704	2.718	2.694	2.717	2.694	2.675	2.639	2.619	2.618	2.709	2.698	2.713	2.613	2.591	2.637	2.631	2.729	2.707	2.702	2.730	2.695	2.716	2.715	2.788	2.831	2.856	2.691	2.669	2.696	2.702	2.720	2.714	2.730	
Aliv	1.296	1.281	1.306	1.283	1.296	1.276	1.301	1.358	1.365	1.291	1.291	1.246	1.336	1.368	1.319	1.339	1.271	1.276	1.276	1.270	1.301	1.284	1.285	1.159	1.123	1.136	1.284	1.331	1.299	1.290	1.280	1.273	1.242	
T	4.000	4.000	4.000	4.000	3.991	3.951	3.940	3.977	3.983	4.000	3.989	3.958	3.950	3.959	3.956	3.970	4.000	3.982	3.978	4.000	3.996	4.000	3.947	3.954	3.992	3.975	4.000	3.995	3.992	4.000	3.987	3.972		
Alvi	0.009	-	0.023	-	-	-	-	-	-	0.001	-	-	-	-	-	-	-	-	-	0.018	-	0.019	0.057	-	-	-	0.006	-	-	-	-	-		
Ti	0.321	0.324	0.351	0.343	0.354	0.372	0.397	0.408	0.403	0.344	0.338	0.423	0.413	0.422	0.403	0.406	0.371	0.386	0.387	0.371	0.357	0.363	0.340	0.384	0.385	0.346	0.442	0.434	0.403	0.404	0.410	0.366	0.344	
Fe	1.046	1.309	1.089	1.144	1.086	1.300	1.080	0.995	1.002	1.456	1.488	1.459	0.944	0.948	0.932	0.920	1.690	1.656	1.573	1.575	1.644	1.598	1.574	1.502	1.597	1.809	1.479	1.431	1.465	1.411	1.591	1.670	1.921	
Mn	-	-	-	-	-	-	-	-	-	-	-	-	-	-	-	-	-	0.032	0.026	-	0.028	-	-	0.027	-	0.030	-	-	-	-	-	-	-	
Mg	1.494	1.195	1.369	1.350	1.381	1.229	1.410	1.415	1.396	1.107	1.116	0.973	1.502	1.479	1.493	1.485	0.771	0.742	0.831	0.875	0.835	0.849	0.870	0.929	0.865	0.625	0.875	0.934	0.916	0.990	0.804	0.760	0.552	
Ca	-	-	-	-	-	-	-	-	-	-	-	-	-	-	-	-	-	-	-	-	-	-	-	-	-	-	-	-	-	-	-	-	-	-
C	2.870	2.828	2.832	2.837	2.821	2.901	2.886	2.818	2.801	2.909	2.942	2.856	2.860	2.848	2.828	2.811	2.831	2.817	2.818	2.839	2.865	2.829	2.842	2.842	2.846	2.809	2.795	2.805	2.785	2.804	2.808	2.824	2.853	
Na	0.096	0.154	0.102	0.120	0.131	0.092	0.095	0.122	0.131	-	-	-	0.116	0.114	0.136	0.129	-	0.094	0.109	-	-	-	-	0.087	-	-	0.107	-	0.087	0.102	-	0.076	0.066	
K	0.809	0.825	0.815	0.804	0.790	0.835	0.810	0.744	0.755	0.784	0.775	0.856	0.750	0.743	0.759	0.742	0.867	0.847	0.846	0.833	0.873	0.882	0.865	0.833	0.844	0.858	0.803	0.848	0.855	0.803	0.841	0.869	0.893	
Ba	-	-	-	-	0.031	-	0.036	0.066	0.069	-	-	-	0.063	0.068	0.070	0.077	-	-	-	-	-	-	-	-	-	-	-	-	-	-	-	-	-	-
A	0.905	0.978	0.917	0.923	0.951	0.927	0.940	0.932	0.955	0.784	0.775	0.856	0.928	0.926	0.965	0.948	0.867	0.941	0.955	0.833	0.873	0.882	0.865	0.920	0.844	0.858	0.910	0.848	0.942	0.905	0.841	0.945	0.959	
Cl	-	0.025	-	-	-	-	-	-	-	-	-	-	-	-	-	-	0.019	-	-	-	0.017	-	-	-	-	-	-	-	-	-	-	-	-	
Mg#	0.588	0.477	0.557	0.541	0.560	0.486	0.566	0.587	0.582	0.432	0.428	0.400	0.614	0.609	0.616	0.617	0.313	0.309	0.346	0.357	0.337	0.347	0.356	0.382	0.351	0.257	0.372	0.395	0.385	0.412	0.336	0.313	0.223	

Table 6. Amphibole (kaersutite) analyses																													
Sample	R012627																												
Site	2	2	2	2	2	2	2	9	9	9	9	9	9	9	9	9	9	11	11	11	11	15	15	15	15	15	15	2	2
Analysis	13	14	15	16	17	18	23	104	105	106	107	108	109	111	115	121	141	143	145	146	191	192	193	195	196	197	19	20	
comment																												low tot	low tot
SiO2	37.245	36.475	36.668	36.775	36.112	36.625	36.176	38.358	38.144	38.294	37.973	37.738	37.738	38.443	37.395	38.080	37.609	37.181	37.780	37.417	38.593	39.064	37.802	38.550	38.486	38.529	31.170	29.330	
TiO2	7.006	6.772	7.006	6.906	7.006	6.972	7.373	5.454	5.721	5.755	5.988	5.905	6.222	6.289	6.088	5.655	7.406	7.022	7.456	7.489	7.089	7.173	7.923	6.922	7.223	7.239	5.438	5.238	
Al2O3	12.848	12.395	12.622	12.622	12.470	12.395	12.622	11.828	12.206	11.979	12.319	11.412	12.641	11.167	12.338	11.941	12.943	12.905	13.207	13.226	12.811	12.886	12.678	13.207	13.245	13.245	10.430	9.391	
Sc2O3	-	-	-	-	-	-	-	-	-	-	-	-	-	-	-	-	0.322	-	-	-	-	-	-	-	-	-	-	-	
FeOt	10.228	10.176	9.983	10.253	10.330	10.421	9.867	14.717	13.405	15.348	13.946	16.042	11.951	18.230	12.530	14.730	10.035	11.681	10.498	10.318	11.694	11.797	11.475	12.132	11.784	11.270	7.204	7.166	
MnO	-	-	-	-	-	-	-	-	-	-	-	-	-	0.336	-	-	-	-	-	-	-	-	-	0.362	-	-	-	-	
MgO	11.442	11.459	11.193	11.376	11.227	11.558	11.326	9.485	9.784	8.955	9.834	7.960	10.414	7.064	10.198	9.237	11.807	10.994	11.890	12.039	11.210	11.591	10.812	11.426	11.542	11.160	9.402	7.844	
CaO	11.585	11.557	11.613	11.781	11.753	11.683	11.515	11.221	11.305	11.095	11.543	11.012	11.725	11.081	11.403	11.109	11.949	11.753	11.921	12.075	12.061	12.313	12.145	11.739	12.299	11.935	9.263	9.347	
Na2O	2.251	2.130	2.251	2.426	2.319	2.238	2.251	2.575	2.682	2.709	2.561	2.602	2.669	2.682	2.602	2.480	2.251	2.332	2.265	2.332	2.615	2.399	2.319	2.521	2.426	2.332	1.901	1.631	
K2O	0.976	0.928	1.024	0.952	1.024	0.940	0.940	1.265	1.144	1.265	1.132	1.277	0.952	1.397	0.903	1.132	1.048	1.193	1.000	1.000	1.060	1.048	1.060	0.976	1.048	0.952	0.879	0.903	
SO3	-	-	-	-	-	-	-	-	-	-	-	-	-	-	-	-	-	-	-	-	-	-	-	-	-	-	0.550	0.500	
Cl	-	-	-	-	-	-	-	-	-	-	-	-	-	-	-	-	-	-	-	-	-	-	-	-	-	-	0.390	0.370	
TOTAL	93.581	91.892	92.360	93.090	92.240	92.831	92.069	94.904	94.392	95.400	95.296	93.947	94.311	96.689	93.459	94.365	95.370	95.062	96.017	95.896	97.133	98.271	96.576	97.473	98.053	96.662	76.626	71.718	
<i>cations on basis of Si+Al+Ti+Sc+Fe+Mg+Mn=13; O+OH=24</i>																													
Si	5.815	5.799	5.824	5.803	5.763	5.777	5.754	6.019	6.001	6.003	5.925	6.063	5.923	6.066	5.914	6.001	5.772	5.766	5.747	5.708	5.867	5.851	5.800	5.794	5.778	5.848	5.995	6.148	
Aliv	2.185	2.201	2.176	2.197	2.237	2.223	2.246	1.981	1.999	1.997	2.075	1.937	2.077	1.934	2.086	1.999	2.228	2.234	2.253	2.292	2.133	2.149	2.200	2.206	2.222	2.152	2.005	1.852	
T sites	8																												
Alvi	0.179	0.122	0.187	0.151	0.109	0.081	0.120	0.206	0.265	0.217	0.190	0.224	0.261	0.142	0.214	0.219	0.113	0.124	0.115	0.086	0.162	0.126	0.093	0.133	0.122	0.218	0.359	0.467	
Ti	0.823	0.810	0.837	0.820	0.841	0.827	0.882	0.644	0.677	0.678	0.703	0.713	0.734	0.746	0.724	0.670	0.855	0.819	0.853	0.859	0.810	0.808	0.914	0.782	0.815	0.826	0.786	0.826	
Sc	-	-	-	-	-	-	-	-	-	-	-	-	-	-	-	-	0.043	-	-	-	-	-	-	-	-	-	-	-	
FeII	1.335	1.353	1.326	1.353	1.379	1.375	1.313	1.931	1.764	2.012	1.820	2.156	1.569	2.405	1.657	1.941	1.288	1.515	1.336	1.316	1.487	1.478	1.473	1.525	1.480	1.431	1.159	1.256	
Mg	2.663	2.716	2.650	2.676	2.671	2.718	2.686	2.219	2.295	2.093	2.287	1.907	2.436	1.662	2.405	2.170	2.701	2.542	2.696	2.738	2.541	2.588	2.473	2.560	2.583	2.525	2.696	2.451	
Mn	-	-	-	-	-	-	-	-	-	-	-	-	-	0.045	-	-	-	-	-	-	-	-	-	0.047	-	-	-	-	
C sites	5																												
Ca	1.938	1.969	1.976	1.992	2.010	1.974	1.962	1.887	1.906	1.864	1.930	1.896	1.972	1.873	1.932	1.876	1.965	1.953	1.943	1.974	1.964	1.976	1.997	1.890	1.978	1.941	1.909	2.099	
NaB	0.062	0.031	0.024	0.008	-	0.026	0.038	0.113	0.094	0.136	0.070	0.104	0.028	0.127	0.068	0.124	0.035	0.047	0.057	0.026	0.036	0.024	0.003	0.110	0.022	0.059	0.091	0.000	
B sites	2	2	2	2	2.010	2	2.099																						
NaA	0.619	0.625	0.670	0.734	0.717	0.659	0.657	0.670	0.724	0.687	0.705	0.706	0.784	0.694	0.730	0.634	0.635	0.654	0.611	0.663	0.735	0.673	0.686	0.625	0.685	0.627	0.617	0.663	
K	0.194	0.188	0.207	0.192	0.208	0.189	0.191	0.253	0.230	0.253	0.225	0.262	0.191	0.281	0.182	0.228	0.205	0.236	0.194	0.195	0.206	0.200	0.208	0.187	0.201	0.184	0.216	0.242	
A sites	0.814	0.813	0.877	0.926	0.926	0.848	0.847	0.923	0.954	0.940	0.930	0.968	0.974	0.975	0.912	0.861	0.840	0.890	0.805	0.858	0.941	0.873	0.894	0.812	0.885	0.812	0.833	0.904	
(O)	22.391	22.322	22.538	22.512	22.500	22.334	22.447	22.322	22.479	22.381	22.380	22.578	22.598	22.548	22.421	22.297	22.442	22.371	22.316	22.345	22.556	22.442	22.612	22.194	22.395	22.471	22.669	23.369	
(OH)	1.609	1.678	1.462	1.488	1.500	1.666	1.553	1.678	1.521	1.619	1.620	1.422	1.402	1.452	1.579	1.703	1.558	1.629	1.684	1.655	1.444	1.558	1.388	1.806	1.605	1.529	1.331	0.631	
S	-	-	-	-	-	-	-	-	-	-	-	-	-	-	-	-	-	-	-	-	-	-	-	-	-	-	-	0.079	0.079
Cl	-	-	-	-	-	-	-	-	-	-	-	-	-	-	-	-	-	-	-	-	-	-	-	-	-	-	-	0.127	0.131
Mg/(Mg+Fe)	0.666	0.667	0.667	0.664	0.660	0.664	0.672	0.535	0.565	0.510	0.557	0.469	0.608	0.409	0.592	0.528	0.677	0.627	0.669	0.675	0.631	0.637	0.627	0.627	0.636	0.638	0.699	0.661	

Table 7. Clinopyroxene analyses																																				
Sample	R012627																																			
Site	1	1	1	3	3	3	3	3	3	4	5	5	5	5	5	5	5	7	7	11	11	12	12	12	12	12	12	14	14	14	14	14				
Analysis	9	11	12	32	33	34	35	36	37	48	54	55	56	57	58	59	61	62	83	84	150	154	155	156	157	158	159	160	164	180	182	183	184	185		
SiO2	47.022	47.750	47.792	45.696	45.011	48.006	46.979	46.658	44.926	47.151	44.348	43.813	46.102	44.519	42.572	42.337	42.765	42.273	43.599	43.278	49.696	50.231	46.252	46.616	45.247	45.888	47.022	45.503	49.076	48.113	47.578	48.028	47.086	47.921		
TiO2	1.301	1.368	1.435	1.902	2.502	0.884	1.284	2.235	1.284	1.318	2.235	3.436	2.502	2.986	3.736	4.454	3.820	4.470	3.203	3.903	0.901	0.651	2.819	2.168	3.203	3.119	2.369	2.652	-	2.018	2.235	1.968	1.985	2.302		
Al2O3	3.099	3.099	3.099	4.308	5.385	1.984	2.948	2.910	5.385	2.891	5.895	6.046	4.875	5.895	7.312	8.295	7.274	8.049	6.500	7.690	2.116	1.398	5.309	4.384	6.311	6.046	4.875	5.007	-	5.083	4.894	4.913	4.950	5.253		
Sc2O3	-	-	-	-	-	-	-	-	-	-	-	-	-	-	-	-	-	-	-	-	-	-	-	-	-	-	-	-	-	-	-	-	-	-	-	0.399
V2O3	-	-	-	-	-	-	-	-	-	-	-	-	-	-	-	-	-	-	-	-	-	-	-	-	-	-	-	-	-	-	-	-	-	-	-	-
Cr2O3	-	-	-	-	-	-	-	-	-	-	-	-	-	-	-	-	-	-	-	-	-	-	-	-	-	-	-	-	-	-	-	-	-	-	-	-
FeOt	8.066	8.246	8.131	9.327	8.568	10.601	10.588	10.073	8.967	10.575	6.304	6.291	5.879	6.278	6.690	7.114	7.024	6.767	6.986	6.561	12.196	11.977	6.883	6.741	6.780	6.342	6.921	6.458	14.653	8.594	8.787	9.263	8.735	8.748		
MnO	0.323	-	-	-	-	0.529	0.387	0.349	-	0.387	-	-	-	-	-	-	-	-	-	-	-	-	0.452	-	-	-	-	-	-	-	-	-	-	-	-	1.162
MgO	12.255	12.503	12.454	10.911	11.127	10.994	10.431	10.663	10.829	10.513	12.653	12.006	13.250	12.304	11.575	11.707	11.857	11.525	12.039	11.906	10.281	10.646	12.503	13.084	12.619	12.802	13.100	12.752	7.379	11.824	12.006	11.840	11.741	12.188		
CaO	21.645	21.575	21.547	21.351	21.295	21.575	21.323	20.918	21.701	21.421	21.561	21.449	21.897	21.715	21.687	21.771	21.631	21.575	21.491	22.233	21.757	21.939	22.051	22.037	21.883	22.135	22.317	21.813	23.156	22.807	22.247	22.569	22.163	22.653		
Na2O	0.539	0.458	0.445	0.620	0.566	0.566	0.553	0.634	0.580	0.458	0.445	0.539	0.310	0.350	0.512	0.566	0.539	0.472	0.404	0.472	0.593	0.499	0.499	0.458	-	0.472	0.404	0.418	-	0.526	0.566	0.485	0.539	0.593		
Cl	-	-	-	-	-	-	-	-	-	-	-	-	-	-	-	-	-	-	-	-	-	-	-	-	-	-	-	-	-	-	-	-	-	-	-	-
TOTAL	94.250	94.999	94.902	94.115	94.455	95.140	94.493	93.522	94.622	94.765	94.258	93.581	94.815	94.048	94.085	96.244	94.910	95.131	94.222	96.044	97.541	97.793	96.316	95.488	96.042	96.805	97.407	94.604	95.427	98.964	98.752	99.065	97.200	99.657		
Formulae on the basis of 4 cations, 6 oxygens																																				
Si	1.859	1.874	1.878	1.821	1.784	1.902	1.878	1.879	1.779	1.881	1.744	1.741	1.800	1.759	1.685	1.640	1.678	1.658	1.722	1.677	1.933	1.948	1.786	1.809	1.757	1.758	1.793	1.784	2.001	1.817	1.803	1.815	1.811	1.796		
Aliv	0.141	0.126	0.122	0.179	0.216	0.093	0.122	0.121	0.221	0.119	0.256	0.259	0.200	0.241	0.315	0.360	0.322	0.342	0.278	0.323	0.067	0.052	0.214	0.191	0.243	0.242	0.207	0.216	-	0.183	0.197	0.185	0.189	0.204		
T	2	2	2	2	2	1.9954	2	2	2	2	2	2	2	2	2	2	2	2	2	2	2	2	2	2	2	2	2	2	2	2	2	2	2	2	2	
Alvi	0.003	0.016	0.021	0.024	0.036	-	0.017	0.016	0.032	0.018	0.017	0.024	0.024	0.033	0.026	0.018	0.014	0.030	0.025	0.028	0.029	0.012	0.027	0.010	0.046	0.032	0.012	0.015	-	0.043	0.021	0.034	0.036	0.027		
Ti	0.039	0.041	0.042	0.057	0.075	0.026	0.039	0.040	0.066	0.041	0.091	0.103	0.074	0.089	0.111	0.130	0.113	0.132	0.095	0.113	0.027	0.020	0.082	0.064	0.094	0.090	0.068	0.079	-	0.058	0.063	0.056	0.058	0.065		
Sc	-	-	-	-	-	-	-	-	-	-	-	-	-	-	-	-	-	-	-	-	-	-	-	-	-	-	-	-	-	-	-	-	-	-	-	0.013
V	-	-	-	-	-	-	-	-	-	-	-	-	-	-	-	-	-	-	-	-	-	-	-	-	-	-	-	-	-	-	-	-	-	-	-	-
Cr	-	-	-	-	-	-	-	-	-	-	-	-	-	-	-	-	-	-	-	-	-	-	-	-	-	-	-	-	-	-	-	-	-	-	-	-
Fe3	0.101	0.063	0.051	0.087	0.075	0.093	0.070	0.074	0.101	0.054	0.092	0.072	0.053	0.058	0.105	0.124	0.122	0.084	0.093	0.104	0.029	0.039	0.059	0.089	0.009	0.064	0.075	0.077	0.000	0.064	0.091	0.076	0.078	0.091		
Fe2	0.167	0.208	0.216	0.224	0.210	0.258	0.284	0.266	0.196	0.299	0.116	0.137	0.139	0.150	0.116	0.106	0.108	0.138	0.138	0.108	0.368	0.349	0.163	0.131	0.211	0.140	0.145	0.135	0.500	0.208	0.188	0.217	0.203	0.184		
Mn	0.011	-	-	-	-	0.018	0.013	0.011	-	0.013	-	-	-	-	-	-	-	-	-	-	-	-	0.015	-	-	-	-	-	-	-	-	-	-	-	-	-
Mg	0.722	0.731	0.729	0.649	0.657	0.649	0.621	0.641	0.639	0.625	0.741	0.710	0.771	0.724	0.683	0.676	0.693	0.673	0.709	0.687	0.596	0.615	0.719	0.756	0.730	0.731	0.744	0.746	0.448	0.666	0.678	0.668	0.672	0.681		
Ca	0.916	0.906	0.907	0.912	0.904	0.916	0.914	0.902	0.921	0.916	0.908	0.913	0.916	0.919	0.920	0.904	0.909	0.907	0.910	0.923	0.906	0.912	0.912	0.916	0.910	0.909	0.912	0.917	1.011	0.923	0.903	0.914	0.913	0.909		
Na	0.041	0.035	0.034	0.047	0.044	0.043	0.043	0.049	0.045	0.035	0.035	0.041	0.024	0.027	0.039	0.042	0.041	0.036	0.030	0.036	0.045	0.038	0.037	0.035	-	0.035	0.030	0.032	-	0.039	0.042	0.036	0.040	0.043		
Oct	2	2	2	2	2	2.0046	2	2	2	2	2	2	2	2	2	2	2	2	2	2	2	2	2	2	2	2	2	2	2	2	2	2	2	2	2	
Cl	-	-	-	-	-	-	-	-	-	-	-	-	-	-	-	-	-	-	-	-	-	-	-	-	-	-	-	-	-	-	-	-	-	-	-	-

Table 7. Clinopyroxene analyses																																				
Sample	C112167A																																			
Site	1	1	1	1	1	1	1	3	3	5	5	5	5	5	5	5	5	6	6	6	6	8	8	8	8	8	8	8	8	8	8	8	8			
Analysis	218	219	220	221	222	223	224	251	253	263	264	265	266	267	268	269	273	274	275	276	292	293	294	295	296	298	299	300								
SiO2	48.648	48.798	48.990	47.728	49.247	49.461	49.461	49.611	50.188	49.119	50.916	49.397	47.386	51.707	48.776	49.311	45.525	47.685	46.380	47.899	47.878	47.279	52.477	48.370	50.081	52.606	49.354	49.654								
TiO2	2.285	2.419	2.335	2.869	2.252	2.118	2.519	-	0.951	2.118	0.801	2.118	2.852	0.817	2.419	2.369	2.852	1.952	1.568	2.635	2.152	2.185	-	2.402	1.835	-	1.668	1.801								
Al2O3	5.461	5.668	5.687	5.744	5.479	5.385	4.913	0.850	2.626	5.555	2.400	5.479	7.426	1.738	5.687	5.498	5.631	5.158	5.782	5.290	5.385	5.102	-	5.139	3.949	-	4.043	3.987								
Sc2O3	-	-	-	-	-	-	-	-	-	-	-	-	-	-	-	-	-	-	-	-	-	-	-	-	-	-	-	-	-	-	-	-	-	-	-	-
V2O3	-	-	-	-	-	-	-	-	-	-	-	-	-	-	-	-	-	-	-	-	-	-	-	-	-	-	-	-	-	-	-	-	-	-	-	-
Cr2O3	-	-	-	-	-	-	-	-	-	-	-	-	-	-	-	-	-	-	-	-	-	-	-	-	-	-	-	-	-	-	-	-	-	-	-	-
FeOt	4.799	4.477	4.670	5.210	4.593	4.902	7.899	6.651	8.671	4.580	7.950	4.477	5.532	8.864	5.017	4.464	6.175	4.593	7.860	5.107	4.824	4.335	8.349	4.670	5.069	7.462	4.747	4.709								
MnO	-	-	-	-	-	-	-	-	0.374	0.387	-	-	-	-	-	-	-	-	-	-	-	-	-	-	-	-	-	-	-	-	-	-	-	-	-	-
MgO	14.593	14.560	14.692	14.012	14.941	15.273	12.603	12.404	12.354	14.858	13.134	14.974	13.697	12.951	14.643	14.991	12.918	14.808	15.223	14.543	14.328	14.444	12.835	14.825	15.372	13.100	15.090	15.090								
CaO	23.226	23.842	23.548	23.184	23.576	24.010	23.366	23.100	22.751	23.870																										

Table 8. Feldspar analyses																												
Sample	R012627														C112167A													
Site	1	1	1	3	3	3	3	4	7	7	8	10	10	10	11	1	2	2	2	2	2	2	2	2	2	6	6	7
Analysis	1	2	3	43	44	45	46	47	75	76	91	133	136	214	151	228	235	236	237	238	239	240	243	245	279	282	290	
mineral	Ab	Ab	mixture*	Ab	Ksp	Ksp	Ksp	Ab	Ksp	Ksp	Ksp	mixture*	Ksp	Afp	mixture*													
SiO2	63.752	65.356	58.489	63.752	64.864	63.281	61.955	64.436	64.329	66.148	66.511	63.901	64.115	67.495	65.228	68.244	59.687	59.280	58.810	66.511	60.821	59.922	57.612	58.467	59.580	55.964	53.847	
Al2O3	19.820	19.594	19.934	18.611	18.989	18.649	17.969	19.046	18.876	19.386	20.009	20.142	20.520	19.764	20.387	20.350	20.236	20.142	20.463	20.803	19.783	20.274	20.179	20.217	19.348	25.810	22.674	
FeO ^t	1.454	-	7.320	0.373	-	-	-	-	-	-	0.630	0.412	-	-	-	0.733	-	-	-	-	-	-	-	0.939	-	0.592	1.840	
MgO	0.199	-	0.763	-	-	-	-	-	-	-	-	-	-	-	-	0.448	-	-	-	-	-	-	-	1.211	-	0.348	1.227	
CaO	-	0.336	-	-	-	-	-	0.448	-	-	-	0.812	1.133	0.308	0.965	-	-	-	-	0.979	-	-	-	3.708	-	-	10.536	
BaO	-	-	-	-	-	-	-	-	-	-	-	-	-	-	-	-	6.297	5.984	6.956	-	4.399	5.448	6.844	0.837	5.192	-	-	
Na2O	10.420	10.824	9.139	10.272	10.420	10.325	10.123	10.312	10.218	10.555	10.609	9.935	9.935	10.770	10.298	11.283	0.580	0.647	0.580	10.595	0.485	0.714	0.903	7.090	0.431	6.362	6.767	
K2O	-	-	-	-	-	-	-	-	-	-	-	0.301	0.422	-	-	-	13.082	13.142	12.974	-	13.889	13.359	12.648	2.216	13.745	3.939	-	
Cl	-	-	-	-	-	-	-	-	-	-	-	-	-	-	-	-	-	-	-	-	-	-	0.170	-	-	-	-	
TOTAL	95.645	96.110	95.645	93.007	94.273	92.255	90.047	94.242	93.423	96.088	97.760	95.502	96.124	98.337	96.879	101.057	99.882	99.196	99.782	98.889	99.377	99.718	98.357	94.686	98.296	93.016	96.890	
<i>Cations on the basis of 8 oxygens</i>																												
Si	2.928	2.967	2.780	2.988	2.993	2.986	2.995	2.979	2.993	2.993	2.969	2.930	2.921	2.988	2.940	2.956	2.8674	2.8651	2.8452	2.938	2.902	2.8699	2.8359	2.787	2.8960	2.677	2.549	
Al	1.073	1.048	1.117	1.028	1.033	1.037	1.024	1.038	1.035	1.034	1.053	1.089	1.102	1.031	1.083	1.039	1.1458	1.1473	1.1668	1.083	1.112	1.1444	1.1707	1.136	1.1084	1.455	1.265	
Fe	0.056	-	0.291	0.015	-	-	-	-	-	-	0.024	0.016	-	-	-	0.027	-	-	-	-	-	-	-	0.037	-	0.024	0.073	
Mg	0.014	-	0.054	-	-	-	-	-	-	-	-	-	-	-	-	0.029	-	-	-	-	-	-	-	0.086	-	0.025	0.087	
Ca	-	0.016	-	-	-	-	-	0.022	-	-	-	0.040	0.055	0.015	0.047	-	-	-	-	0.046	-	-	-	0.189	-	-	0.534	
Na	0.928	0.953	0.842	0.933	0.932	0.945	0.949	0.924	0.922	0.926	0.918	0.883	0.877	0.924	0.900	0.948	0.0540	0.0606	0.0544	0.907	0.045	0.0663	0.0862	0.655	0.0407	0.590	0.621	
Ba	-	-	-	-	-	-	-	-	-	-	-	-	-	-	-	-	0.1185	0.1133	0.1319	-	0.082	0.1023	0.1320	0.016	0.0989	-	-	
K	-	-	-	-	-	-	-	-	-	-	-	0.018	0.025	-	-	-	0.8018	0.8103	0.8007	-	0.845	0.8163	0.7943	0.135	0.8523	0.240	-	
Cl	-	-	-	-	-	-	-	-	-	-	-	-	-	-	-	-	-	-	-	-	-	-	0.0142	-	-	-	-	
sum	4.999	4.985	5.083	4.964	4.957	4.968	4.968	4.964	4.950	4.953	4.964	4.976	4.980	4.958	4.969	4.998	4.9875	4.9967	4.9990	4.974	4.987	4.9992	5.0190	5.041	4.9963	5.011	5.129	
*R012627/1/3- probably ~80% albite, ~20% chlorite																												
*C112167A/2/245- probably ~80% alkali feldspar, ~20% clinzoisite ± chlorite																												
*C112167A/7/290- probably ~59% albite, ~41% clinzoisite or pumpellyite ± chlorite																												

Table 9. Prehnite analyses																			
Sample	R012627																		
Site	6	6	6	6	6	7	7	7	7	7	7	7	8	8	10	10	10	11	11
Analysis	70	71	72	73	74	77	78	79	80	81	82	90	92	93	130	132	139	148	152
SiO ₂	36.711	40.626	40.647	40.946	42.016	41.353	41.866	41.545	41.075	41.353	41.160	41.738	42.701	42.209	41.909	41.417	42.187	42.145	41.310
Al ₂ O ₃	20.690	23.599	24.053	23.562	24.317	24.374	24.242	23.769	23.637	23.902	23.713	24.317	25.130	24.450	24.110	23.788	24.374	24.374	23.751
FeO _t	1.196	-	-	-	0.708	-	0.682	0.399	0.386	0.476	0.515	0.566	0.476	-	0.566	0.450	0.888	0.360	0.373
MgO	0.265	-	-	-	-	-	-	-	-	-	-	-	-	-	-	-	-	-	-
CaO	22.793	25.395	25.773	25.381	26.263	25.871	25.759	25.829	25.423	25.731	25.731	25.549	25.927	25.395	25.801	26.221	26.291	26.123	25.675
Na ₂ O	-	-	-	-	-	-	-	-	-	-	-	-	-	-	-	0.189	-	-	-
K ₂ O	0.169	-	-	-	-	-	-	-	-	-	-	-	-	-	-	-	-	-	-
TOTAL	81.823	89.620	90.473	89.889	93.304	91.598	92.549	91.543	90.521	91.462	91.119	92.170	94.233	92.053	92.386	92.065	93.740	93.001	91.109
<i>Cations on the basis of O₁₀(OH)₂</i>																			
Si	2.960	2.976	2.953	2.988	2.962	2.963	2.970	2.981	2.979	2.971	2.970	2.971	2.969	2.998	2.978	2.964	2.961	2.975	2.978
Aliv	0.040	0.024	0.047	0.012	0.038	0.037	0.030	0.019	0.021	0.029	0.030	0.029	0.031	0.002	0.022	0.036	0.039	0.025	0.022
T	3.000	3.000	3.000	3.000	3.000	3.000	3.000	3.000	3.000	3.000	3.000	3.000	3.000	3.000	3.000	3.000	3.000	3.000	3.000
Al	1.966	2.037	2.059	2.026	2.020	2.058	2.027	2.010	2.021	2.024	2.016	2.040	2.059	2.047	2.019	2.006	2.016	2.028	2.018
Alvi	1.926	2.013	2.012	2.014	1.982	2.022	1.997	1.992	2.000	1.994	1.986	2.011	2.028	2.045	1.997	1.970	1.977	2.003	1.996
FeIII	0.081	-	-	-	0.042	-	0.040	0.024	0.023	0.029	0.031	0.034	0.028	-	0.034	0.027	0.052	0.021	0.022
Y	2.007	2.013	2.012	2.014	2.024	2.022	2.038	2.016	2.023	2.023	2.017	2.044	2.056	2.045	2.031	1.997	2.029	2.024	2.019
Mg	0.032	-	-	-	-	-	-	-	-	-	-	-	-	-	-	-	-	-	-
Ca	1.969	1.993	2.006	1.984	1.984	1.986	1.958	1.986	1.976	1.980	1.989	1.948	1.931	1.933	1.964	2.010	1.977	1.976	1.983
Na	-	-	-	-	-	-	-	-	-	-	-	-	-	-	-	0.026	-	-	-
K	0.017	-	-	-	-	-	-	-	-	-	-	-	-	-	-	-	-	-	-
X	2.018	1.993	2.006	1.984	1.984	1.986	1.958	1.986	1.976	1.980	1.989	1.948	1.931	1.933	1.964	2.036	1.977	1.976	1.983
sum	7.025	7.006	7.018	6.999	7.007	7.008	6.996	7.002	6.999	7.003	7.006	6.993	6.987	6.978	6.995	7.033	7.005	7.000	7.002

Table 10. Clinozoisite analyses									
Sample	R012627								
Site	10	10	10	10	10	11	14	19	19
Analysis No	129	131	134	135	138	153	186	209	212
SiO ₂	36.005	36.882	37.545	37.310	36.689	37.032	38.165	38.657	37.545
Al ₂ O ₃	26.301	29.419	28.928	30.099	29.136	28.852	30.685	32.140	28.833
FeO _t	7.912	5.030	4.953	3.538	4.490	5.468	4.091	2.972	6.304
MnO	-	-	-	0.529	-	-	-	-	-
CaO	21.687	22.527	23.184	22.807	22.765	22.946	23.562	23.002	23.198
SrO	-	-	-	0.769	1.053	-	-	-	-
Cl	-	-	-	-	0.100	-	-	-	-
TOTAL	91.905	93.858	94.610	95.051	94.232	94.298	96.503	96.771	95.880
<i>Cations on the basis of (O)₁₂(OH)</i>									
Si	2.967	2.951	2.984	2.959	2.949	2.958	2.964	2.974	2.955
Aliv	0.033	0.049	0.016	0.041	0.051	0.042	0.036	0.026	0.045
<i>T</i>	<i>3.000</i>								
Alvi	2.522	2.726	2.693	2.773	2.709	2.673	2.773	2.887	2.629
Fe as Fe ^{III}	0.545	0.337	0.329	0.235	0.302	0.365	0.266	0.191	0.415
<i>Y</i>	<i>3.067</i>	<i>3.062</i>	<i>3.023</i>	<i>3.008</i>	<i>3.011</i>	<i>3.038</i>	<i>3.038</i>	<i>3.078</i>	<i>3.044</i>
Mn	-	-	-	0.036	-	-	-	-	-
Ca	1.915	1.931	1.974	1.938	1.960	1.964	1.961	1.896	1.956
Sr	-	-	-	0.035	0.049	-	-	-	-
<i>X</i>	<i>1.915</i>	<i>1.931</i>	<i>1.974</i>	<i>2.009</i>	<i>2.009</i>	<i>1.964</i>	<i>1.961</i>	<i>1.896</i>	<i>1.956</i>
<i>sum</i>	<i>7.983</i>	<i>7.993</i>	<i>7.997</i>	<i>8.017</i>	<i>8.020</i>	<i>8.002</i>	<i>7.999</i>	<i>7.974</i>	<i>8.000</i>
Cl	-	-	-	-	0.014	-	-	-	-

Table 11. Pumpellyite analyses												
Sample	C112167A				R012627							
Site	1	6	7	7	9	9	9	9	9	10	19	
Analysis	226	281	289	291	100	101	102	103	117	140	215	
SiO2	36.796	36.112	37.994	37.224	34.764	36.133	35.876	34.550	35.277	36.090	36.261	
Al2O3	28.436	26.056	28.474	28.021	23.033	25.149	25.149	23.467	22.069	26.245	26.131	
V2O3	-	-	-	-	-	-	-	-	0.309	-	-	
FeOt	2.226	2.753	2.290	2.907	8.607	5.776	5.468	7.462	9.147	7.372	6.291	
MgO	1.227	2.056	0.879	1.277	1.343	1.675	1.857	1.791	1.526	0.298	0.862	
CaO	23.254	22.079	21.939	22.429	21.799	22.037	21.939	21.953	21.771	21.491	22.331	
Na2O	-	0.270	0.755	0.512	-	-	0.243	-	-	-	0.324	
K2O	-	-	-	-	-	-	-	-	-	0.325	-	
TOTAL	91.94	89.33	92.33	92.37	89.55	90.77	90.53	89.223	90.10	91.82	92.20	
<i>Cations on the basis of Z=16, O₂₃(OH)₃</i>												
		*	*	*			*			*	*	
Si	5.952	5.895	5.817	5.789	5.888	5.978	5.836	5.841	5.955	5.869	5.789	
Aliv	0.048	0.105	0.183	0.211	0.112	0.022	0.164	0.159	0.045	0.131	0.211	
Z	6.000	6.000	6.000	6.000								
Alvi	5.373	5.047	5.373	5.205	4.486	4.881	4.776	4.517	4.345	5.009	4.869	
V	-	-	-	-	-	-	-	-	0.042	-	-	
Fe3	-	0.058	-	0.006	0.626	0.141	0.387	0.642	0.658	0.123	0.342	
Y	5.373	5.105	5.373	5.211	5.112	5.022	5.164	5.159	5.045	5.131	5.211	
Fe2	0.301	0.335	0.332	0.405	0.593	0.659	0.387	0.413	0.633	0.916	0.544	
Mg	0.296	0.523	0.227	0.322	0.339	0.413	0.469	0.451	0.384	0.075	0.216	
X	0.597	0.858	0.558	0.727	0.932	1.072	0.856	0.865	1.017	0.991	0.760	
Ca	4.030	4.037	4.069	4.063	3.956	3.906	3.981	3.977	3.938	3.878	4.029	
charge	49.325	49.000	49.190	49.000	49.000	49.000	49.000	49.000	49.000	49.000	49.000	
Mg/(Mg+Fe2)	0.496	0.610	0.406	0.443	0.364	0.385	0.548	0.522	0.377	0.076	0.285	
<i>* albite or orthoclase subtracted before calculation of mineral formula</i>												

Table 12. Grossular analyses			
Sample	R012627		
Site	19	19	
Analysis	211	216	
SiO2	37.802	37.780	
Al2O3	18.989	19.386	
FeOt	6.098	4.940	
MnO	1.007	0.981	
ZnO	-	0.473	
CaO	35.665	34.881	
TOTAL	99.561	98.442	
<i>cations on the basis of (O)=12, all iron as Fe^{III}</i>			
Si	2.910	2.933	
Aliv	0.090	0.067	
T	<i>3.000</i>	<i>3.000</i>	
Alvi	1.633	1.706	
Fe3	0.393	0.321	
Y	<i>2.025</i>	<i>2.027</i>	
Mn	0.066	0.065	
Zn	-	0.027	
Ca	2.942	2.901	
X	<i>3.007</i>	<i>2.993</i>	
sum	8.032	8.020	

Table 13. Chlorite analyses																										
Sample	C112167A										R012627															
Site	1	1	2	7	1	1	2	3	5	5	6	6	6	7	7	8	8	9	9	9	9	11	11	12	15	15
Analysis	225	229	241	287	7	10	21	40	53	63	66	67	68	88	89	95	96	110	113	116	120	142	144	162	188	194
SiO2	28.132	28.752	28.474	28.859	23.918	24.367	24.495	24.495	23.725	24.752	24.131	25.073	26.100	25.436	24.046	25.137	23.982	24.602	24.174	25.458	24.944	25.394	25.565	25.244	26.335	25.950
Al2O3	18.781	19.386	19.953	17.270	18.063	18.876	17.874	19.367	18.725	19.386	17.383	17.723	16.778	16.042	18.611	17.515	17.648	18.347	18.649	18.403	18.498	19.008	18.932	18.857	18.895	19.065
FeOt	20.841	18.152	21.021	17.226	30.811	28.328	25.691	22.346	29.499	22.089	29.692	30.618	32.111	28.933	32.934	30.142	32.587	27.466	26.476	28.509	25.151	28.226	26.296	26.682	28.444	26.836
MnO	-	-	-	-	0.581	0.465	0.400	0.400	0.826	-	0.581	0.555	0.775	0.387	0.646	0.387	0.968	0.439	0.374	0.568	0.633	0.659	0.659	0.529	0.542	0.710
MgO	19.054	20.762	20.198	18.971	8.573	11.227	12.487	13.764	8.441	14.725	9.303	9.187	8.739	9.469	7.761	9.900	6.650	11.475	11.857	10.829	13.548	12.072	12.885	12.619	11.691	12.918
CaO	0.294	0.294	-	-	-	-	-	0.238	-	0.196	0.364	0.252	-	-	-	-	-	0.308	-	-	-	-	-	0.224	-	-
K2O	0.265	0.277	0.554	0.928	-	-	0.229	0.193	0.313	-	0.313	0.530	0.650	0.795	-	0.446	0.337	0.301	-	0.566	-	-	-	-	0.578	0.398
TOTAL	87.367	87.623	90.200	83.253	81.947	83.262	81.177	80.803	81.529	81.148	81.768	83.938	85.153	81.062	83.998	83.528	82.171	82.939	81.530	84.333	82.774	85.358	84.336	84.155	86.485	85.876
<i>Cations on the basis of O₁₀ (OH)_s</i>																										
Si	2.901	2.908	2.842	3.072	2.818	2.775	2.830	2.785	2.798	2.785	2.844	2.881	2.975	3.008	2.790	2.889	2.861	2.809	2.787	2.868	2.808	2.809	2.833	2.813	2.878	2.835
Aliv	1.099	1.092	1.158	0.928	1.182	1.225	1.170	1.215	1.202	1.215	1.156	1.119	1.025	0.992	1.210	1.111	1.139	1.191	1.213	1.132	1.192	1.191	1.167	1.187	1.122	1.165
Alvi	1.183	1.220	1.189	1.238	1.327	1.309	1.264	1.379	1.401	1.356	1.259	1.280	1.229	1.244	1.335	1.261	1.342	1.278	1.320	1.311	1.263	1.288	1.305	1.289	1.311	1.289
Al	2.282	2.311	2.347	2.166	2.509	2.534	2.434	2.595	2.603	2.571	2.415	2.400	2.254	2.236	2.545	2.372	2.481	2.469	2.534	2.443	2.454	2.478	2.472	2.476	2.433	2.455
Fe	1.797	1.536	1.755	1.533	3.036	2.698	2.482	2.124	2.910	2.079	2.927	2.942	3.061	2.862	3.196	2.897	3.251	2.623	2.552	2.686	2.368	2.611	2.437	2.486	2.599	2.452
Mn	-	-	-	-	0.058	0.045	0.039	0.039	0.083	-	0.058	0.054	0.075	0.039	0.063	0.038	0.098	0.042	0.037	0.054	0.060	0.062	0.062	0.050	0.050	0.066
Mg	2.929	3.131	3.005	3.010	1.506	1.906	2.151	2.333	1.484	2.470	1.635	1.573	1.485	1.669	1.342	1.696	1.183	1.953	2.038	1.819	2.274	1.991	2.128	2.096	1.904	2.104
Ca	0.032	0.032	-	-	-	-	-	0.029	-	0.024	0.046	0.031	-	-	-	-	-	0.038	-	-	-	-	-	0.027	-	-
K	0.035	0.036	0.071	0.126	-	-	0.034	0.028	0.047	-	0.047	0.078	0.095	0.120	-	0.065	0.051	0.044	-	0.081	-	-	-	-	0.081	0.055
cations	9.976	9.954	10.020	9.908	9.927	9.958	9.970	9.932	9.924	9.929	9.972	9.958	9.945	9.934	9.937	9.958	9.924	9.978	9.947	9.951	9.965	9.952	9.931	9.949	9.946	9.966
Mg/Mg+Fe	0.620	0.671	0.631	0.663	0.332	0.414	0.464	0.523	0.338	0.543	0.358	0.348	0.327	0.368	0.296	0.369	0.267	0.427	0.444	0.404	0.490	0.433	0.466	0.457	0.423	0.462

Table 14. Chlorite-biotite mixtures										
Sample	C112167A			R012627						
Site	2	3	4	4	1	1	1	7	8	12
Analysis	244	252	261	262	4	5	8	87	97	165
SiO2	22.056	29.373	30.057	34.229	25.458	28.474	26.720	29.116	27.533	33.523
TiO2	-	-	-	-	-	-	-	-	-	0.534
Al2O3	12.905	17.780	17.723	24.639	16.835	17.534	18.196	16.911	18.233	10.279
FeOt	10.704	18.204	19.953	12.042	27.904	28.946	31.184	24.649	29.358	25.691
MnO	-	-	-	-	0.633	0.542	0.994	0.568	0.594	-
MgO	10.580	18.191	16.550	12.271	8.988	8.358	7.860	8.275	7.877	9.485
CaO	1.539	-	-	-	-	-	-	-	-	4.337
Na2O	1.631	-	-	-	-	-	-	-	-	-
K2O	0.602	2.084	2.686	3.927	1.313	3.180	1.518	5.095	1.349	5.192
Cl	0.570	-	-	-	-	-	-	-	-	-
TOTAL	60.587	85.632	86.970	87.107	81.130	87.035	86.472	84.614	84.944	89.041
Mg#	0.638	0.640	0.597	0.645	0.365	0.340	0.310	0.374	0.324	0.397
C112167A/2/244	possibly chlorite, albite or scapolite, pumpellyite or clinozoisite, and biotite									
C112167A/3/252	~75% chlorite, 25% secondary biotite									
C112167A/4/261	~68% chlorite, 32% secondary biotite									
C112167A/4/262	possibly chlorite, K-feldspar +-sericite									
R012627/1/4	~83% chlorite, 17% secondary biotite									
R012627/1/5	~62% chlorite, 38% secondary biotite									
R012627/1/8	~82% chlorite, 18% secondary biotite									
R012627/7/87	~36% chlorite, 64% secondary biotite									
R012627/8/97	~84% chlorite, 16% secondary biotite									
R012627/12/165	possibly biotite, chlorite and a Ca-silicate									

Table 15. Muscovite (sericite) analyses			
Sample	C112167A		
Site	1	6	
Analysis	230	280	
SiO2	51.386	46.894	
Al2O3	32.877	35.616	
FeOt	0.682	0.849	
MgO	-	0.216	
CaO	0.574	-	
Na2O	3.141	1.227	
K2O	7.854	9.336	
TOTAL	96.513	94.137	
<i>Cations on the basis of O₁₀(OH)₂</i>			
TOTAL	96.513	94.137	
Si	3.3224	3.1276	
Aliv	0.6776	0.8724	
Alvi	1.8276	1.9273	
Fe	0.0369	0.0474	
Mg	0.0000	0.0214	
Ca	0.0397	-	
Na	0.3937	0.1586	
K	0.6478	0.7943	
sum	6.9458	6.9490	
C112167A/1/230 - probably a mixture of ~73% muscovite, ~27% albite			
C112167A/6/280 - probably a mixture of ~89% muscovite, ~11% albite			

Table 16. Titanite analyses													
Sample	R012627												C112167
Site	2	4	5	5	9	9	10	12	13	14	16	16	8
Analysis	22	49	50	60	118	119	127	161	166	181	198	199	297
SiO2	29.266	28.988	28.667	29.672	31.170	29.630	29.843	29.351	28.089	30.678	27.469	30.079	30.421
TiO2	31.960	32.677	34.578	32.593	27.089	31.059	33.061	33.961	36.463	32.193	34.128	31.943	35.396
Al2O3	4.062	2.778	1.360	3.477	4.554	5.045	3.439	3.193	2.683	4.573	3.609	3.798	3.155
Sc2O3	-	-	-	-	-	0.429	-	-	-	-	-	0.383	-
V2O3	0.500	-	-	-	-	-	0.515	-	0.706	-	-	-	-
FeOt	-	0.618	0.695	1.145	5.378	1.171	0.926	0.527	3.229	0.618	7.462	4.155	-
MnO	-	-	-	-	-	-	-	-	-	-	0.581	-	-
MgO	-	0.265	-	0.348	1.260	-	-	-	0.282	-	0.514	0.713	-
CaO	27.228	26.878	27.214	26.920	24.318	27.410	27.144	27.648	25.213	28.599	23.632	25.717	28.501
Na2O	-	-	-	-	0.593	-	-	-	-	-	-	-	-
K2O	-	-	-	-	0.253	-	0.193	-	-	-	-	0.614	-
ZrO2	-	0.473	2.094	-	-	-	-	-	-	1.148	-	-	-
F	0.810	-	-	-	-	-	-	-	-	-	-	-	-
Cl	-	-	-	-	0.130	-	-	-	-	-	-	-	-
TOTAL	93.826	92.676	94.608	94.156	94.744	94.743	95.121	94.681	96.666	97.808	97.395	97.403	97.473
<i>Cations on the basis of (O) = 5</i>													
Si	1.019	1.019	0.999	1.024	1.080	1.016	1.021	1.009	0.957	1.022	0.944	1.017	1.013
Ti	0.837	0.864	0.906	0.846	0.706	0.801	0.851	0.878	0.934	0.806	0.882	0.812	0.886
Zr	-	0.008	0.036	-	-	-	-	-	-	0.019	-	-	-
Al	0.167	0.115	0.056	0.141	0.186	0.204	0.139	0.129	0.108	0.179	0.146	0.151	0.124
V	0.014	-	-	-	-	-	0.014	-	0.019	-	-	-	-
Sc	-	-	-	-	-	0.013	-	-	-	-	-	0.011	-
Fe	-	0.018	0.020	0.033	0.156	0.034	0.027	0.015	0.092	0.017	0.214	0.117	-
Mn	-	-	-	-	-	-	-	-	-	-	0.017	-	-
Mg	-	0.014	-	0.018	0.065	-	-	-	0.014	-	0.026	0.036	-
Ca	1.016	1.013	1.016	0.996	0.903	1.007	0.995	1.018	0.920	1.020	0.870	0.932	1.017
Na	-	-	-	-	0.040	-	-	-	-	-	-	-	-
K	-	-	-	-	0.011	-	0.008	-	-	-	-	0.026	-
sum	3.053	3.051	3.032	3.059	3.147	3.075	3.055	3.049	3.045	3.064	3.101	3.103	3.039
F	0.089	-	-	-	-	-	-	-	-	-	-	-	-
Cl	-	-	-	-	0.008	-	-	-	-	-	-	-	-
R012627/9/118-	titanite and impurities including probably albite and chlorite												
R012627/16/198-	titanite and impurities including probably Fe-chlorite												
R012627/16/199-	titanite and impurities including possibly biotite, Fe-chlorite and Ca-silicate												

Table 17. Apatite analyses														
Sample	R012627													C112167A
Site	6	6	9	9	9	13	13	14	14	14	15	16	19	6
Analysis	64	65	98	99	112	167	168	177	178	187	189	203	210	278
SiO ₂	0.449	0.406	-	-	0.685	0.364	-	0.449	0.300	0.385	-	0.428	-	0.428
FeO _t	-	-	-	0.489	0.862	-	-	-	-	-	-	-	-	0.553
ZnO	-	-	-	-	-	-	-	-	-	-	-	-	-	0.485
MgO	0.216	0.282	-	-	-	-	-	0.265	0.216	-	-	-	-	-
CaO	52.007	51.923	52.805	52.567	53.253	53.980	54.400	53.938	53.784	53.435	53.099	53.742	46.271	53.463
K ₂ O	-	-	-	-	-	-	-	-	-	-	-	-	-	0.169
P ₂ O ₅	42.115	41.657	42.826	42.757	43.055	43.605	43.926	42.986	43.307	43.169	43.582	43.376	40.076	42.619
F	2.500	2.310	2.070	2.390	2.650	2.540	2.610	2.720	2.020	2.210	2.370	2.660	3.110	2.400
Cl	0.300	0.390	0.330	0.370	0.300	0.340	0.350	0.350	0.350	0.290	0.250	0.350	0.300	0.220
TOTAL	97.588	96.969	98.031	98.573	100.804	100.829	101.285	100.709	99.976	99.489	99.301	100.556	90.964	99.130
<i>Cations of the base of O₁₂ (OH, F, Cl)</i>														
Si	0.038	0.035	-	-	0.057	0.030	-	0.037	0.025	0.032	-	0.036	-	0.036
Ca	4.768	4.795	4.804	4.782	4.746	4.792	4.817	4.814	4.796	4.790	4.769	4.791	4.579	4.827
Fe ^{II}	-	-	-	0.035	0.060	-	-	-	-	-	-	-	-	0.043
Zn	-	-	-	-	-	-	-	-	-	-	-	-	-	0.033
Mg	0.028	0.036	-	-	-	-	-	0.033	0.027	-	-	-	-	-
K	-	-	-	-	-	-	-	-	-	-	-	-	-	0.020
P	3.051	3.040	3.078	3.073	3.032	3.059	3.073	3.031	3.051	3.058	3.093	3.055	3.134	3.040
sum	7.885	7.906	7.882	7.890	7.895	7.881	7.890	7.916	7.898	7.881	7.861	7.882	7.809	7.903
F	0.677	0.630	0.556	0.642	0.697	0.666	0.682	0.717	0.532	0.585	0.628	0.700	0.909	0.640
Cl	0.044	0.057	0.047	0.053	0.042	0.048	0.049	0.049	0.049	0.041	0.036	0.049	0.047	0.031
OH	0.280	0.313	0.397	0.305	0.261	0.287	0.269	0.234	0.419	0.374	0.336	0.251	0.045	0.329

Table 18. Ilmenite analyses								
Sample	C112167A							
Site	4	4	4	4	7	7	7	7
Analysis	254	255	256	257	283	284	285	286
SiO ₂	-	-	-	-	-	0.300	-	-
TiO ₂	49.391	50.575	50.074	50.024	50.441	46.638	50.675	49.908
FeOt	43.779	44.795	44.988	45.143	45.503	41.849	44.808	44.319
MnO	3.486	3.306	3.344	3.318	3.112	3.021	3.783	3.538
TOTAL	96.656	98.676	98.407	98.486	99.056	91.809	99.267	97.765
<i>cations on the basis of Z=2, (O) =3</i>								
Si	-	-	-	-	-	excl	-	-
Ti	0.968	0.972	0.964	0.962	0.965	0.966	0.967	0.967
FeIII	0.063	0.057	0.072	0.075	0.070	0.068	0.065	0.065
FeII	0.891	0.900	0.892	0.890	0.898	0.895	0.886	0.890
Mn	0.077	0.072	0.073	0.072	0.067	0.070	0.081	0.077
<i>molar % end-members</i>								
FeTiO ₃	89.1	90.0	89.2	89.0	89.8	89.5	88.6	89.0
MnTiO ₃	7.7	7.2	7.3	7.2	6.7	7.0	8.1	7.7
Fe ₂ O ₃	3.2	2.8	3.6	3.8	3.5	3.4	3.3	3.3
Total	100.0	100.0	100.0	100.0	100.0	100.0	100.0	100.0

Table 19. Zircon analysis		
Sample	R012627	<i>Ideal</i>
Site	13	
Analysis	169	
SiO ₂	29.437	32.78
ZrO ₂	45.920	67.22
ThO ₂	1.070	
TiO ₂	0.267	
Al ₂ O ₃	3.420	
FeOt	5.506	
MgO	1.774	
CaO	0.504	
K ₂ O	0.530	
TOTAL	88.427	100.00
<i>probably ~80% zircon, 14% chlorite, 6% biotite</i>		
<i>Hf, P not detected</i>		

Table 20. Probable mixtures							
Sample	C112167A			R012627			
Site	1	3	7	6	8	10	19
Analysis	227	250	288	69	94	137	217
SiO2	48.648	35.213	55.644	33.373	22.099	46.231	37.459
Al2O3	32.782	25.016	21.748	19.783	8.389	24.960	23.033
FeOt	2.341	3.872	1.235	0.322	0.553	3.255	8.915
MgO	1.542	2.421	-	-	-	1.012	1.376
CaO	0.000	22.107	6.982	16.482	0.308	15.293	17.000
BaO	-	-	0.581	-	-	-	-
Na2O	1.887	0.849	0.000	0.000	1.631	3.518	1.334
K2O	8.577	0.337	10.805	-	1.831	-	0.735
SO3	-	-	-	-	0.699	-	-
Cl	-	0.220	-	-	-	-	-
Total	95.778	90.037	96.994	69.960	36.411	94.268	89.853
C112167A/1/227- possibly ~73% muscovite, ~16% albite, ~11% chlorite							
C112167A/3/250- probably pumpellyite with small amounts of alkali feldspar and possibly grossular							
C112167A/7/288- possibly ~70% alkali feldspar, ~30% prehnite							
R012627/6/69- possibly a mixture of clinozoisite, prehnite and a zeolite; note low total							
R012627/8/94- possibly a mixture including albite and sericite, note very low total							
R012627/10/137-probably ~68% pumpellyite, ~31% albite							
R012627/19/217-probably ~82% pumpellyite ± chlorite, ~18% alkali feldspar							

Table 21. Rare earth element (REE), Hf, Ta and Th analyses of the Cooe Dolerite								
Reg No	R016518	R016519	R016520	R016521	R016522	95220015	95220019	40412
Field No	ABS103	ABS104	ABS105	ABS106	ABS107			
method	INAA	INAA	INAA	INAA	INAA	ICPMS	ICPMS	XRF/IEX
La (ppm)	42.9	70.2	60.6	64.8	57.9	62.6	43.4	54.40
Ce	81.5	135.0	114.0	125.0	115.0	122.7	88.1	107.40
Pr						13.2	9.8	11.95
Nd	40.1	63.6	52.0	58.1	54.9	50.1	38.8	44.70
Sm	7.89	11.70	10.10	11.20	10.90	9.1	7.8	8.29
Eu	2.33	3.73	3.15	3.43	3.48	3.1	2.7	2.65
Gd						8.9	7.7	7.99
Tb	1.10	1.75	1.63	1.53	1.40	1.4	1.2	
Dy						7.4	6.4	7.10
Ho	1.30	2.10	1.60	1.40	1.50	1.6	1.4	
Er						4.6	3.8	4.25
Yb	2.57	3.67	3.48	3.67	3.17	3.7	3.1	3.54
Lu	0.40	0.51	0.49	0.58	0.45	0.6	0.5	
Hf	5.11	7.25	6.31	7.33	6.74	6.9	6.5	
Ta	4.51	7.77	6.57	7.56	5.78	7.1	4.9	
Th	6.38	10.60	9.03	9.88	8.00	8.8	6.1	

Table 22. Isotopic analyses from the Cooee Dolerite

Sample No.	93220001	95220019	93220002	95220015
$^{143}\text{Nd}/^{144}\text{Nd}$ (meas)	0.51256192	0.5125772	0.512516	0.512518
2 σ	34.1	68.4	37.2	26.3
ϵNd (measured)	-1.48	-1.19	-2.38	-2.33
Nd (ppm)	37.37	37.92	41.07	49.47
Sm (ppm)	7.25	7.59	7.79	9.09
Sm/Nd	0.1941	0.2001	0.1898	0.1837
$^{147}\text{Sm}/^{144}\text{Nd}$	0.1174	0.1211	0.1148	0.1111
$^{143}\text{Nd}/^{144}\text{Nd}$ at 734 Ma	0.511997	0.511995	0.511963	0.511984
ϵNd at 734 Ma*	5.97	5.93	5.31	5.71
$^{87}\text{Sr}/^{86}\text{Sr}$ (meas)	0.71665	0.71293	0.71745	0.72227
2 σ	11	11.2	13.2	15.2
Sr (ppm)	768	454	51	474
Rb (ppm)	71	67	5	16
Rb/Sr	0.0924	0.1476	0.0980	0.0338
$^{87}\text{Rb}/^{86}\text{Sr}$	0.268	0.427	0.284	0.098
$^{87}\text{Sr}/^{86}\text{Sr}$ at 734 Ma	0.713846	0.708456	0.714473	0.721250
$^{206}\text{Pb}/^{204}\text{Pb}$ (meas)	20.646	19.509	31.692	28.246
$^{207}\text{Pb}/^{204}\text{Pb}$ (meas)	15.712	15.641	16.371	16.139
$^{208}\text{Pb}/^{204}\text{Pb}$ (meas)	41.303	39.798	56.002	51.331
Pb (ppm)	6.0	6.0	3.0	1.5
U (ppm)	2.0	1.4	1.0	1.9
Th (ppm)	7.0	6.1	7.0	8.8
at. wt. Pb	207.2003	207.2035	207.1787	207.1835
$^{238}\text{U}/^{204}\text{Pb}$ (μ)	22.6602	15.3151	30.2631	105.8650
$^{235}\text{U}/^{204}\text{Pb}$	0.1643	0.1111	0.2195	0.7678
$^{232}\text{Th}/^{204}\text{Pb}$	81.9484	68.9493	218.8872	506.6300
$^{206}\text{Pb}/^{204}\text{Pb}$ at 734 Ma	17.9136	17.6624	28.0426	15.4795
$^{207}\text{Pb}/^{204}\text{Pb}$ at 734 Ma	15.5375	15.5228	16.1381	15.3253
$^{208}\text{Pb}/^{204}\text{Pb}$ at 734 Ma	38.2725	37.2474	47.9061	32.5930

*with $^{143}\text{Nd}/^{144}\text{Nd} = 0.512638$; $^{147}\text{Sm}/^{144}\text{Nd} = 0.1967$ for CHUR

Table 23. K/Ar results

Client ID		R012627/DBJ93	Standard
CSIRO ID		1737	HD-B1-107
K	%	1.120	7.956
Rad. ^{40}Ar	$\times 10^{-10}$ mol/g	11.566	3.3558
Rad. ^{40}Ar	%	97.14	91.61
Age*	Ma	514.52 \pm 10.4	24.16 \pm 0.36 *

Notes:

*Error to Hess & Lippolt (1994): -0.21%

$^{40}\text{Ar}/^{36}\text{Ar}$ reference value of air (Steiger & Jäger 1977)

ID AS103-AirS-1

$^{40}\text{Ar}/^{36}\text{Ar}$ 293.96 \pm 0.32

Table 24. ARGUSVI ⁴⁰Ar/³⁹Ar laser step-heating analytical results for BR1 biotite ^a

Sample ID	Step No	Laser Power (1 mm beam)	⁴⁰ Ar (fA) ±1σ	³⁹ Ar (fA) ^b ±1σ	³⁸ Ar (fA) ±1σ	³⁷ Ar (fA) ^b ±1σ	³⁶ Ar (fA) ±1σ	³⁹ Ar (x10 ⁻¹⁴ mol)	Ca/K ±1σ	% ⁴⁰ Ar ^c	⁴⁰ Ar/ ³⁹ Ar ±1σ	Cum. % ³⁹ Ar	Apparent Age (Ma) ^c ±1σ	Background Correction																		
														Blank no.	⁴⁰ Ar (fA) ±1σ	³⁹ Ar (fA) ±1σ	³⁸ Ar (fA) ±1σ	³⁷ Ar (fA) ±1σ	³⁶ Ar (fA) ±1σ													
Aliquot: BR1-2																																
Mineral: Biotite, 10 grains																																
BR1-2a	1	1.0%	371.772	0.112	13.410	0.012	0.0243	0.0001	0.86	0.61	0.1287	0.0005	0.0476	0.112	0.080	89.66	24.86	0.03	4.86	607.866	0.550	EXB#76	1.799	0.008	0.065	0.003	-0.078	0.007	-0.182	0.007	0.00890	0.00019
BR1-2b	2	1.5%	789.960	0.166	26.226	0.006	0.0074	0.0001	2.24	0.45	0.0394	0.0004	0.0931	0.150	0.030	98.51	29.67	0.01	14.37	705.159	0.201	EXB#76	1.799	0.008	0.065	0.003	-0.078	0.007	-0.182	0.007	0.00890	0.00019
BR1-2c	3	2.0%	1241.840	0.310	40.367	0.032	0.0047	0.0001	1.72	0.55	0.0247	0.0003	0.1433	0.075	0.024	99.40	30.58	0.03	29.01	722.945	0.502	EXB#76	1.799	0.008	0.065	0.003	-0.078	0.007	-0.182	0.007	0.00890	0.00019
BR1-2d	4	2.5%	1262.408	0.303	40.616	0.014	0.0025	0.0001	0.89	0.51	0.0131	0.0003	0.1442	0.038	0.022	99.69	30.99	0.01	43.74	730.796	0.260	EXB#77	1.995	0.011	0.056	0.010	-0.060	0.016	-0.173	0.003	0.00934	0.00021
BR1-2e	5	3.0%	1035.154	0.238	33.189	0.017	0.0019	0.0001	0.26	0.31	0.0103	0.0004	0.1178	0.014	0.016	99.70	31.10	0.02	55.78	732.946	0.344	EXB#77	1.995	0.011	0.056	0.010	-0.060	0.016	-0.173	0.003	0.00934	0.00021
BR1-2f	6	3.5%	739.427	0.096	23.670	0.022	0.0016	0.0001	0.05	0.09	0.0087	0.0005	0.0840	0.003	0.007	99.65	31.13	0.03	64.36	733.587	0.583	EXB#77	1.995	0.011	0.056	0.010	-0.060	0.016	-0.173	0.003	0.00934	0.00021
BR1-2g	7	4.0%	422.270	0.101	13.529	0.011	0.0007	0.0001	0.58	0.38	0.0036	0.0003	0.0480	0.075	0.050	99.75	31.13	0.03	69.27	733.671	0.516	EXB#78	1.995	0.016	0.047	0.006	-0.062	0.023	-0.195	0.006	0.01021	0.00017
BR1-2h	8	4.5%	459.287	0.064	14.737	0.015	0.0005	0.0001	0.58	0.44	0.0028	0.0003	0.0523	0.068	0.052	99.81	31.11	0.03	74.62	733.184	0.622	EXB#78	1.995	0.016	0.047	0.006	-0.062	0.023	-0.195	0.006	0.01021	0.00017
BR1-2i	9	5.0%	554.198	0.111	17.770	0.011	0.0010	0.0001	1.10	0.52	0.0054	0.0003	0.0631	0.108	0.052	99.71	31.10	0.02	81.06	732.937	0.394	EXB#78	1.995	0.016	0.047	0.006	-0.062	0.023	-0.195	0.006	0.01021	0.00017
BR1-2j	10	6.0%	397.514	0.099	12.731	0.013	0.0009	0.0001	1.48	0.54	0.0047	0.0004	0.0452	0.204	0.074	99.65	31.12	0.03	85.68	733.316	0.651	EXB#79	2.064	0.019	0.055	0.008	-0.063	0.008	-0.191	0.010	0.01010	0.00025
BR1-2k	11	8.0%	929.837	0.270	29.705	0.021	0.0025	0.0001	2.74	0.51	0.0135	0.0004	0.1055	0.162	0.030	99.56	31.17	0.02	96.45	734.304	0.466	EXB#79	2.064	0.019	0.055	0.008	-0.063	0.008	-0.191	0.010	0.01010	0.00025
BR1-2l	12	10.0%	306.716	0.055	9.788	0.016	0.0007	0.0001	0.78	0.63	0.0039	0.0004	0.0347	0.139	0.112	99.62	31.22	0.05	100.00	735.336	1.045	EXB#79	2.064	0.019	0.055	0.008	-0.063	0.008	-0.191	0.010	0.01010	0.00025
														Total gas age: 723.0 ± 0.9 Ma (2σ)																		
Aliquot: BR1-3																																
Mineral: Biotite, 10 grains																																
BR1-3a	1	1.0%	452.509	0.091	15.469	0.007	0.0228	0.0001	1.40	0.32	0.1211	0.0004	0.0549	0.158	0.036	92.01	26.92	0.02	5.46	650.119	0.307	EXB#80	1.953	0.007	0.056	0.004	-0.046	0.021	-0.195	0.006	0.00948	0.00022
BR1-3b	2	1.5%	914.205	0.146	30.348	0.014	0.0055	0.0001	2.62	0.40	0.0293	0.0004	0.1077	0.151	0.023	99.04	29.84	0.01	16.16	708.369	0.293	EXB#80	1.953	0.007	0.056	0.004	-0.046	0.021	-0.195	0.006	0.00948	0.00022
BR1-3c	3	2.0%	1294.684	0.272	41.868	0.020	0.0028	0.0000	0.75	0.45	0.0148	0.0003	0.1486	0.031	0.019	99.66	30.82	0.02	30.93	727.542	0.316	EXB#80	1.953	0.007	0.056	0.004	-0.046	0.021	-0.195	0.006	0.00948	0.00022
BR1-3d	4	2.5%	883.657	0.159	28.306	0.027	0.0019	0.0001	1.76	0.61	0.0098	0.0004	0.1005	0.109	0.038	99.67	31.11	0.03	40.91	733.301	0.583	EXB#81	2.267	0.012	0.055	0.006	-0.036	0.026	-0.206	0.010	0.01032	0.00030
BR1-3e	5	3.0%	1173.278	0.246	37.749	0.024	0.0025	0.0001	1.64	0.48	0.0134	0.0004	0.1340	0.076	0.022	99.66	30.97	0.02	54.22	730.592	0.410	EXB#82	1.574	0.014	0.057	0.009	-0.011	0.016	-0.192	0.006	0.00797	0.00019
BR1-3f	6	3.5%	684.307	0.151	21.940	0.013	0.0013	0.0001	0.35	0.43	0.0067	0.0005	0.0779	0.028	0.034	99.71	31.10	0.02	61.96	733.002	0.392	EXB#82	1.574	0.014	0.057	0.009	-0.011	0.016	-0.192	0.006	0.00797	0.00019
BR1-3g	7	4.0%	411.788	0.107	13.229	0.015	0.0005	0.0001	0.05	0.10	0.0029	0.0003	0.0470	0.006	0.013	99.79	31.06	0.04	66.63	732.288	0.714	EXB#83	1.799	0.010	0.039	0.008	-0.069	0.031	-0.178	0.004	0.00868	0.00027
BR1-3h	8	4.5%	393.603	0.091	12.606	0.014	0.0006	0.0001	0.30	0.74	0.0034	0.0005	0.0448	0.041	0.102	99.74	31.14	0.04	71.07	733.883	0.729	EXB#83	1.799	0.010	0.039	0.008	-0.069	0.031	-0.178	0.004	0.00868	0.00027
BR1-3i	9	5.0%	844.587	0.194	27.040	0.016	0.0013	0.0001	0.05	0.10	0.0071	0.0003	0.0960	0.003	0.006	99.75	31.16	0.02	80.61	734.123	0.383	EXB#83	1.799	0.010	0.039	0.008	-0.069	0.031	-0.178	0.004	0.00868	0.00027
BR1-3j	10	6.0%	389.483	0.109	12.483	0.017	0.0007	0.0001	0.12	0.65	0.0039	0.0004	0.0443	0.017	0.091	99.70	31.11	0.04	85.01	733.132	0.861	EXB#84	1.902	0.009	0.048	0.011	0.014	0.026	-0.188	0.010	0.00948	0.00026
BR1-3k	11	8.0%	981.570	0.245	31.417	0.025	0.0011	0.0001	0.26	0.67	0.0060	0.0005	0.1115	0.015	0.037	99.82	31.19	0.03	96.09	734.690	0.509	EXB#84	1.902	0.009	0.048	0.011	0.014	0.026	-0.188	0.010	0.00948	0.00026
BR1-3l	12	10.0%	346.624	0.066	11.085	0.016	0.0006	0.0001	0.05	0.10	0.0031	0.0003	0.0394	0.008	0.015	99.73	31.19	0.05	100.00	734.711	0.912	EXB#84	1.902	0.009	0.048	0.011	0.014	0.026	-0.188	0.010	0.00948	0.00026
														Total gas age: 725.2 ± 1.0 Ma (2σ)																		

^a Data are corrected for mass spectrometer backgrounds, discrimination, radioactive decay and interference corrections (see Table A.1 for values excluding the interference correction). Errors are one sigma uncertainties and exclude uncertainties in the J-value (propagating this error only has an effect in the third decimal place). Entries where ⁴⁰Ar signal <100 fA indicated in grey text are excluded from total gas age calculations.

^b Samples irradiated in Can UMR#83 (60 MWh, OSU TRIGA Reactor). Interference corrections: (³⁶Ar/³⁷Ar)_{ca} = (2.5798 ± 0.0027) × 10⁻⁴; (³⁹Ar/³⁷Ar)_{ca} = (6.564 ± 0.014) × 10⁻⁴; (⁴⁰Ar/³⁹Ar)_{ca} = (3.89 ± 0.21) × 10⁻⁴; (³⁸Ar/³⁹Ar)_{ca} = (1.1999 ± 0.0004) × 10⁻²

^c J values is 0.0161181 ± 0.0000039 (0.024%;1σ), calculated based on an age of 99.125 ± 0.039 Ma (1σ) for MD2 biotite (Phillips et al., 2017)

Table 24A. ⁴⁰Ar/³⁹Ar ARGUSVI data and blank values for laser step-heating analysis excluding interference corrections

Sample ID	Step No	Laser Power	⁴⁰ Ar ±1σ		³⁹ Ar ±1σ		³⁸ Ar ±1σ		³⁷ Ar ±1σ		³⁶ Ar ±1σ		Background Correction						Argus Sensitivity and Discrimination Corrections												
			(fA)		(fA)		(fA)		(fA)		(fA)		Blank no.	(fA)	(fA)	(fA)	(fA)	(fA)	H1/Ax [40]	H1/L1 [40]	H1/L2 [40]	AX (1amu)	L1 (1amu)	L2 (1amu)	H1/CDD ±1σ (%)						
Aliquot BR1-2																															
BR1-2a	1	0.01	371.777	0.112	13.411	0.012	0.243	0.027	0.857	0.611	0.1290	0.0005	EXB#76	1.799	0.008	0.065	0.003	-0.078	0.007	-0.182	0.007	0.00890	0.00019	1.00298	1.00517	1.00662	0.99362	0.99962	0.99383	310.469	0.076
BR1-2b	2	0.015	789.971	0.166	26.227	0.006	0.368	0.034	2.243	0.454	0.0400	0.0004	EXB#76	1.799	0.008	0.065	0.003	-0.078	0.007	-0.182	0.007	0.00890	0.00019	1.00298	1.00517	1.00662	0.99362	0.99962	0.99383	310.469	0.076
BR1-2c	3	0.02	1241.856	0.310	40.368	0.032	0.534	0.019	1.721	0.551	0.0252	0.0003	EXB#76	1.799	0.008	0.065	0.003	-0.078	0.007	-0.182	0.007	0.00890	0.00019	1.00298	1.00517	1.00662	0.99362	0.99962	0.99383	310.469	0.076
BR1-2d	4	0.025	1262.424	0.303	40.617	0.014	0.534	0.027	0.890	0.513	0.0133	0.0003	EXB#77	1.995	0.011	0.056	0.010	-0.060	0.016	-0.173	0.003	0.00934	0.00021	1.00298	1.00517	1.00662	0.99362	0.99962	0.99383	310.469	0.076
BR1-2e	5	0.03	1035.167	0.238	33.190	0.017	0.473	0.024	0.262	0.311	0.0104	0.0004	EXB#77	1.995	0.011	0.056	0.010	-0.060	0.016	-0.173	0.003	0.00934	0.00021	1.00298	1.00517	1.00662	0.99362	0.99962	0.99383	310.469	0.076
BR1-2f	6	0.035	739.436	0.096	23.670	0.022	0.300	0.019	0.047	0.094	0.0088	0.0005	EXB#77	1.995	0.011	0.056	0.010	-0.060	0.016	-0.173	0.003	0.00934	0.00021	1.00298	1.00517	1.00662	0.99362	0.99962	0.99383	310.469	0.076
BR1-2g	7	0.04	422.275	0.101	13.529	0.011	0.209	0.035	0.582	0.384	0.0037	0.0003	EXB#78	1.995	0.016	0.047	0.006	-0.062	0.023	-0.195	0.006	0.01021	0.00017	1.00298	1.00517	1.00662	0.99362	0.99962	0.99383	310.469	0.076
BR1-2h	8	0.045	459.292	0.064	14.737	0.015	0.206	0.029	0.577	0.437	0.0030	0.0003	EXB#78	1.995	0.016	0.047	0.006	-0.062	0.023	-0.195	0.006	0.01021	0.00017	1.00298	1.00517	1.00662	0.99362	0.99962	0.99383	310.469	0.076
BR1-2i	9	0.05	554.205	0.111	17.771	0.011	0.242	0.027	1.101	0.524	0.0051	0.0003	EXB#78	1.995	0.016	0.047	0.006	-0.062	0.023	-0.195	0.006	0.01021	0.00017	1.00298	1.00517	1.00662	0.99362	0.99962	0.99383	310.469	0.076
BR1-2j	10	0.06	397.519	0.099	12.732	0.013	0.138	0.022	1.485	0.540	0.0051	0.0004	EXB#79	2.064	0.019	0.055	0.008	-0.063	0.008	-0.191	0.010	0.01010	0.00025	1.00298	1.00517	1.00662	0.99362	0.99962	0.99383	310.469	0.076
BR1-2k	11	0.08	929.849	0.270	29.707	0.021	0.414	0.021	2.745	0.505	0.0142	0.0004	EXB#79	2.064	0.019	0.055	0.008	-0.063	0.008	-0.191	0.010	0.01010	0.00025	1.00298	1.00517	1.00662	0.99362	0.99962	0.99383	310.469	0.076
BR1-2l	12	0.1	306.720	0.055	9.788	0.016	0.088	0.067	0.775	0.629	0.0041	0.0003	EXB#79	2.064	0.019	0.055	0.008	-0.063	0.008	-0.191	0.010	0.01010	0.00025	1.00298	1.00517	1.00662	0.99362	0.99962	0.99383	310.469	0.076
Aliquot BR1-3																															
BR1-3a	1	0.01	452.515	0.091	15.470	0.007	0.244	0.035	1.397	0.316	0.1214	0.0004	EXB#80	1.953	0.007	0.056	0.004	-0.046	0.021	-0.195	0.006	0.00946	0.00022	1.00298	1.00517	1.00662	0.99362	0.99962	0.99383	310.469	0.076
BR1-3b	2	0.015	914.217	0.146	30.350	0.014	0.414	0.032	2.623	0.396	0.0300	0.0004	EXB#80	1.953	0.007	0.056	0.004	-0.046	0.021	-0.195	0.006	0.00946	0.00022	1.00298	1.00517	1.00662	0.99362	0.99962	0.99383	310.469	0.076
BR1-3c	3	0.02	1294.700	0.272	41.869	0.020	0.516	0.025	0.750	0.448	0.0150	0.0002	EXB#80	1.953	0.007	0.056	0.004	-0.046	0.021	-0.195	0.006	0.00946	0.00022	1.00298	1.00517	1.00662	0.99362	0.99962	0.99383	310.469	0.076
BR1-3d	4	0.025	883.668	0.159	28.307	0.027	0.408	0.029	1.759	0.615	0.0103	0.0004	EXB#81	2.267	0.012	0.055	0.006	-0.036	0.026	-0.206	0.010	0.01032	0.00030	1.00298	1.00517	1.00662	0.99362	0.99962	0.99383	310.469	0.076
BR1-3e	5	0.03	1173.292	0.246	37.750	0.024	0.458	0.023	1.638	0.475	0.0139	0.0004	EXB#82	1.574	0.014	0.057	0.009	-0.011	0.016	-0.192	0.006	0.00797	0.00019	1.00298	1.00517	1.00662	0.99362	0.99962	0.99383	310.469	0.076
BR1-3f	6	0.035	684.315	0.151	21.940	0.013	0.300	0.020	0.349	0.430	0.0068	0.0004	EXB#82	1.574	0.014	0.057	0.009	-0.011	0.016	-0.192	0.006	0.00797	0.00019	1.00298	1.00517	1.00662	0.99362	0.99962	0.99383	310.469	0.076
BR1-3g	7	0.04	411.793	0.107	13.229	0.015	0.184	0.040	0.048	0.096	0.0029	0.0003	EXB#83	1.799	0.010	0.039	0.008	-0.069	0.031	-0.178	0.004	0.00868	0.00027	1.00298	1.00517	1.00662	0.99362	0.99962	0.99383	310.469	0.076
BR1-3h	8	0.045	393.608	0.091	12.606	0.014	0.172	0.033	0.296	0.738	0.0034	0.0004	EXB#83	1.799	0.010	0.039	0.008	-0.069	0.031	-0.178	0.004	0.00868	0.00027	1.00298	1.00517	1.00662	0.99362	0.99962	0.99383	310.469	0.076
BR1-3i	9	0.05	844.597	0.194	27.040	0.016	0.380	0.039	0.048	0.096	0.0071	0.0003	EXB#83	1.799	0.010	0.039	0.008	-0.069	0.031	-0.178	0.004	0.00868	0.00027	1.00298	1.00517	1.00662	0.99362	0.99962	0.99383	310.469	0.076
BR1-3j	10	0.06	389.488	0.109	12.483	0.017	0.123	0.034	0.123	0.647	0.0040	0.0003	EXB#84	1.902	0.009	0.048	0.011	0.014	0.026	-0.188	0.010	0.00948	0.00026	1.00298	1.00517	1.00662	0.99362	0.99962	0.99383	310.469	0.076
BR1-3k	11	0.08	981.582	0.245	31.417	0.025	0.329	0.036	0.264	0.669	0.0060	0.0005	EXB#84	1.902	0.009	0.048	0.011	0.014	0.026	-0.188	0.010	0.00948	0.00026	1.00298	1.00517	1.00662	0.99362	0.99962	0.99383	310.469	0.076
BR1-3l	12	0.1	346.628	0.066	11.085	0.016	0.136	0.027	0.048	0.096	0.0031	0.0003	EXB#84	1.902	0.009	0.048	0.011	0.014	0.026	-0.188	0.010	0.00948	0.00026	1.00298	1.00517	1.00662	0.99362	0.99962	0.99383	310.469	0.076



Tasmanian
Government

Mineral Resources Tasmania

PO Box 56 Rosny Park

Tasmania Australia 7018

Ph: +61 3 6165 4800

info@mrt.tas.gov.au www.mrt.tas.gov.au